F I N A L   R E P O R T

Toward Development of a Steel Bridge System - Simple for Dead Load and Continuous for Live Load

Atorod Azizinamini, Ph.D., P.E.
Nick J. Lampe
Aaron J. Yakel

National Bridge Research Organization (NaBRO)
(http://www.NaBRO.unl.edu)
Department of Civil Engineering
College of Engineering and Technology

W150 Nebraska Hall
Lincoln, Nebraska 68588-0531
Telephone (402) 472-5106
FAX (402) 472-6658

Sponsored By

Nebraska Department of Roads

October, 2003

Table of Contents

List of Figures

CHAPTER 7
Test Results 77

CHAPTER 8

List of Tables

Acknowledgement

Abstract

A detailed market analysis was carried out to investigate trends in bridge construction in the mid-west region of the country. Results from this study show a decline in the use of steel bridges in the medium to short span ranges. An investigation, sponsored by the Nebraska Department of Roads, was implemented to develop a steel girder system that would offer better economy in these span ranges. Placing steel girders to behave as simple beams for non-composite dead loads and as continuous beams for composite dead and live loads can introduce some economy into steel girder bridges. The focus of this research was placed on the design of the continuity connection over the interior pier support. The analysis and design of the continuity connection over the interior support was completed using finite element analysis and engineering principles. A full-scale model of the connection was constructed and evaluated at various stages of the design life. A material cost comparison between conventional steel bridges systems and the proposed concept resulted in substantial cost savings with the proposed system.

Executive Summary

The use of steel girder bridges has declined since the introduction of more economical materials and methods of construction. Through a market analysis of several mid-western states, it was determined that spans 80 to 110 ft in length have accounted for the largest declines. Several factors can be attributed to the loss of economy in these medium to short span bridges. In a series of discussions with fabricators, designers, and contractors, the recommendation was to eliminate the bolted field splices and simplify the interior pier bearing details.

The concept investigated consists of placing two simple span girders over the abutment and pier and casting the deck slab. At the pier location, the girder ends are cast in a concrete diaphragm. Compressive force from negative bending would be transferred through bearing of the steel section on the concrete diaphragm. The tensile force is carried by additional reinforcing steel in the deck slab. The system then becomes continuous only after the concrete has cured, thus providing continuity for live load and superimposed dead loads only.

The dead load deflections of the proposed system are greater than the fully continuous counterpart. This characteristic reduces the applicability of this concept for projects utilizing phased construction.

Trial designs were carried out to compare the proposed concept to conventional design practice. On average, the proposed concept required 4 to 5% more steel than fully continuous design. Review of the trial designs prompted recommendations to focus on spans near 100 ft in length and to utilizing rolled I-shaped girders. The Military Road bridge in Omaha, NE was chosen as the model for the prototype bridge. The spans were 95 ft long, and the bridge had recently been reconstructed. Therefore, this bridge would provide up-to-date cost information for comparisons between the conventional construction and proposed systems.

Results of the cost comparison for the Military Road bridge demonstrated material and girder fabrication cost savings of 4 to 8% over the conventional continuous girder design.

Design of the continuity connection over the pier focused on the transfer of the large compressive force in the bottom flange to the concrete diaphragm without crushing the concrete. Results of numerical analyses indicated that a mechanism was required to transfer the compressive stress, thereby reducing the stress in the concrete. The connection detail selected consisted of extending the girder bottom flange through the diaphragm. The extended bottom flanges would be partial penetration welded after placement. End bearing plates flush with the end of the girder web and top flange aid in distributing the remaining force into the concrete.

The connection detail tested provides an economical and efficient means of transferring the forces at the pier, and reducing the stress carried by the concrete.

When the connection detail was subjected to 75 years of simulated truck traffic, the connection experienced no appreciable loss in rigidity. The mode of failure of the connection detail was yielding of the tension reinforcement in the slab. The yielding of the reinforcement resulted in a ductile failure mechanism. The connection was subjected to a large level of

displacement after the reinforcement had yielded without a significant decrease in load.

The performance of this connection detail was judged a success. The connection is durable, reliable, and inexpensive to fabricate. Further investigation into the simplification the connection detail is necessary. The level of concrete confinement of the diaphragm between the girders may prevent crushing if the end bearing plates were omitted.

Introduction

1.1 PROBLEM STATEMENT

The latter half of the twentieth century has seen many changes in the design of bridges. One of the most significant changes has come from the introduction of alternative materials for use in the construction of bridges. Prestressed concrete has become increasingly popular since its introduction in the 1950's [1]. The increase in the use of prestressed concrete has caused a decline in steel usage in short to medium span bridges. The diminishing competitiveness of steel bridges in the bridge market can be attributed to the following:

- A relatively lower degree of research and introduction of innovative ideas to steel bridge design and construction.

- When using bolted field splices, estimates for the average cost of material, installation and inspection of one bolt can be as high as $20.00. In addition, ambiguity in available design provisions for

the design of bolted field splices have resulted in misinterpretation of these provisions. It is not uncommon to see drastically different numbers of bolts in the web and flange splices for similar splices.

- A belief on the part of some who contend that putting more costly details in steel bridges will translate to more income. Prior to the introduction of prestressed concrete concepts to bridge applications this might have been true. The use of costly details in steel bridge construction is the primary reason for the diminishing competitiveness in the bridge market.

- Steel bridge design includes more complex procedures and provisions when compared to prestressed concrete design. This is especially true, considering the fact that there are very reliable computer programs to design complete prestressed concrete bridges.

- Construction provisions governing steel bridges are effectively developed for long span bridges; however, the majority of steel bridges constructed do not need to follow such rigorous construction provisions.

- Failure to take advantage of the fact that steel bridge superstructures are lighter than prestressed concrete alternatives. As a result, in some cases the same substructure system is used for both steel and concrete alternatives for a given bridge.

- Bearing devices at the pier locations, though many states have stopped using pot bearings, many still use expensive details that could be simplified.

1.2 RESEARCH OBJECTIVES

The objective of this research is to develop a steel girder system that is more economical and suited for continuous span bridges.

1.3 REPORT CONTENT

This report summarizes the results from tests completed on rolled I-shaped girders representing the interior pier (negative flexure) region of a 2-span bridge. The goal of this examination is to economize the use of steel in bridges commonly designed and constructed in the U.S. This report

documents the details of the connection analysis and design, test setup, laboratory and field testing, and test results.

Chapter 2 summarizes the market analysis carried out to obtain the span range(s) for which steel bridges have become less competitive. Identification of the new bridge system is outlined in Chapter 3. Chapter 4 contains a summary of trial designs completed within the span range determined from the market analysis. The trial designs were completed according to AASHTO LRFD Bridge Design Specifications [2]. Chapter 5 describes the analysis and design of the connection detail over the interior support.

A complete description of the test setup is contained in Chapter 6. This description includes both loading and support geometry, instrumentation types and locations, materials testing and properties, and specimen construction and erection. Discussion of the test results is given in Chapter 7. A summary of the research findings and conclusions is given in Chapter 8 along with suggestions for future research.

The support information leading to the final result is contained in the appendices. These include trial design sample calculations and the raw data obtained from the experimental investigation.

Market Analysis 2

A detailed market analysis was carried out to investigate trends in bridge construction in the mid-west region of the country. This chapter presents an overview of the analysis of National Bridge Inventory (NBI) data obtained from the Federal Highway Administration (FHWA) for seven mid-western states. The data was separated into categories based on the material of construction. The objective of this analysis is to identify trends in the use of bridge materials in Nebraska and the surrounding region.

2.1 GENERAL DESCRIPTION

Bridge inventory data is included from the following states; Colorado, Iowa, Kansas, Nebraska, Oklahoma, South Dakota, and Wyoming. The inclusion of several states was intended to reduce the overall effect of one state's tendency to favor the use of one particular material over another. The National Bridge Inspection Standards (NBIS) [3] mandate an inspection of

each bridge at regular intervals and not to exceed 2 years unless a Federal Highway Administrator approves a proposal stating otherwise. Data from the inspection reports are sent in a standard format from the states to the Federal Highway Administration.

2.2 DATA REDUCTION

Bridges were categorized based on their construction material (NBI Item 43A). Only bridges built of reinforced concrete, prestressed concrete, steel and timber were included in the analysis. The material of the superstructure for the main span determined the classification. For each state, the different construction material categories were compared to each other on the basis of total numbers by the year built and by the maximum span length. Particular attention has been given to the comparison between prestressed concrete and steel bridges in each of the states.

The time period examined (NBI Item 027) was the 88-year span from 1911 through 1998, with particular attention paid to bridges built during the last two decades. The overall time period was divided into eight groups of ten years each, with the exception of the oldest group, 1911-1930, and the most recent time period, 1991-1998. The maximum span lengths (NBI Item 048) were divided into thirty-three groups. The first set includes bridges with maximum span lengths less than 25 ft. The next twenty-seven groups have 5-ft span increments, including bridges from 26 ft through 160 ft. The next four groups have 10-ft span increments, with the final set including bridges from 201 ft through 550 ft.

The performance of the bridges in Nebraska was based on the condition ratings submitted to the FHWA (NBI Items 058 and 059). The ratings of existing physical conditions of the deck and superstructure elements determined the overall deterioration measurement. Bridges classified as "structurally deficient" are those with ratings in the poor, serious, critical

and failure categories, 4 or less on the condition ratings scale. A condition rating of 4 is described as "poor condition - advanced section loss, deterioration, spalling or scour." A rating equal or less than the limit given above for one or more components indicates a potentially critical structural problem and the bridge receives the classification of "structurally deficient."

2.3 ANALYSIS RESULTS

Based on the data from the inspection reports compiled in the NBI, the characteristics by state can be generalized in the following manner.

2.3.1 NEBRASKA

Timber bridges were not considered in the evaluation and comparison of the Nebraska data. Reinforced concrete (RC) has been used as a dominant material for bridge construction in the 60 ft or less span ranges over the historical period studied (68% RC, 15% Prestressed Concrete (PC), 17% steel). Over the last two decades, in the 60 ft - 100 ft maximum span group, PC had a marginally higher percentage of bridges over steel (RC 3%, PC 52%, steel 45%). Considering all span lengths during 1980-1998, distribution of bridge materials was fairly even with RC at 29%, PC at 37% and steel at 34%. From 1991-1998, however, the shift has been toward more concrete with RC at 34%, PC at 40%, and steel at only 26%. As a trend, PC had peaks over steel in the number of bridges reported in the early 1990's. In comparing materials across the span lengths, RC was dominant in the 60 ft and under lengths, PC showed solid numbers in the 100 ft and under lengths with a definitive peak in the 66 ft - 70 ft group, and steel was distributed throughout the span lengths. The comparison of PC with steel over the last two decades indicates an increase in length and number of PC bridges, particularly in the 130 ft and less span lengths.

The measure of performance of the bridges in Nebraska comes from the condition ratings of the existing deck and superstructure elements. If the

bridge is having or has the potential to have serious structural problems, it is classified as structurally deficient. The number of bridges classified as deficient compared to the number of bridges in service gives the percent deficiency. As could be predicted, there were no deficient bridges in either reinforced concrete, prestressed concrete or steel from 1981-1998. Concentrating on the time period from 1961 to 1980, each material has a representative number of bridges built (259 RC, 292 Steel, 243 PC). Considering all three materials, the total number of structurally deficient bridges is low with only 34 out of 794 bridges receiving that classification. This equates to only 4.282% of the total number of bridges built during that 20-year time period. The percentage of structurally deficient bridges does not vary significantly by material as RC contributes 3.5%, steel 4.8% and PC 4.5%. Maximum span length also appears to have little effect on the performance level of the materials. As expected, there is an increase in the deficiency percentage with age for all three materials. Figure 2-1 illustrates the trends in the number of bridges vs. span length vs. year built for steel and prestressed concrete.

2.3.2 KANSAS

Approximately 87% of all the timber bridges in Kansas have been constructed for span lengths of 25 ft or less, with only 4% of the timber bridges being built in the last three decades. PC bridges constitute only 5% of the total number of bridges, with their peak span length in the 36 ft - 40 ft group. From 1991-1998, RC and steel almost equally have controlled the span lengths of 65 ft - 70 ft and less (RC 46%, PC 5%, steel 47%, timber 2%). Over all time periods, more bridges have been built of steel than RC in all span lengths except the 35 ft - 65 ft. Figure 2-2 illustrates the trends in the number of bridges vs. span length vs. year built for both steel and prestressed concrete bridges.
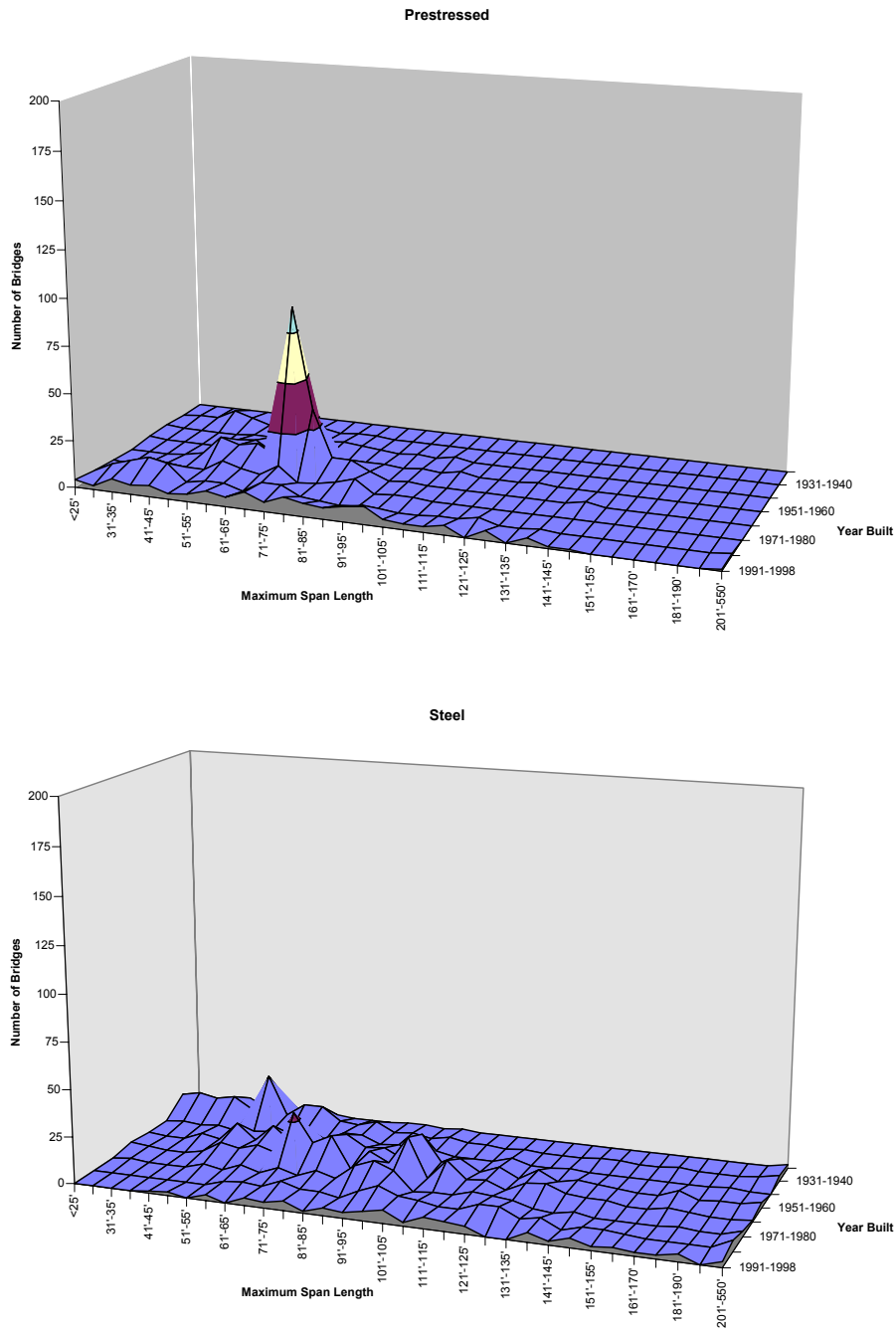
Prestressed

Steel

Figure 2-1: Steel and Prestessed Concrete Bridges in Nebraska

2.3.3 OKLAHOMA

There has been very little bridge construction activity in Oklahoma over the last three decades. Of the bridges constructed, a significant number have been PC in the 45 ft - 100 ft span lengths. In the 71 ft - 100 ft range, PC has 85% of the bridges while steel represents 15% (49 PC to 9 steel). Steel has a
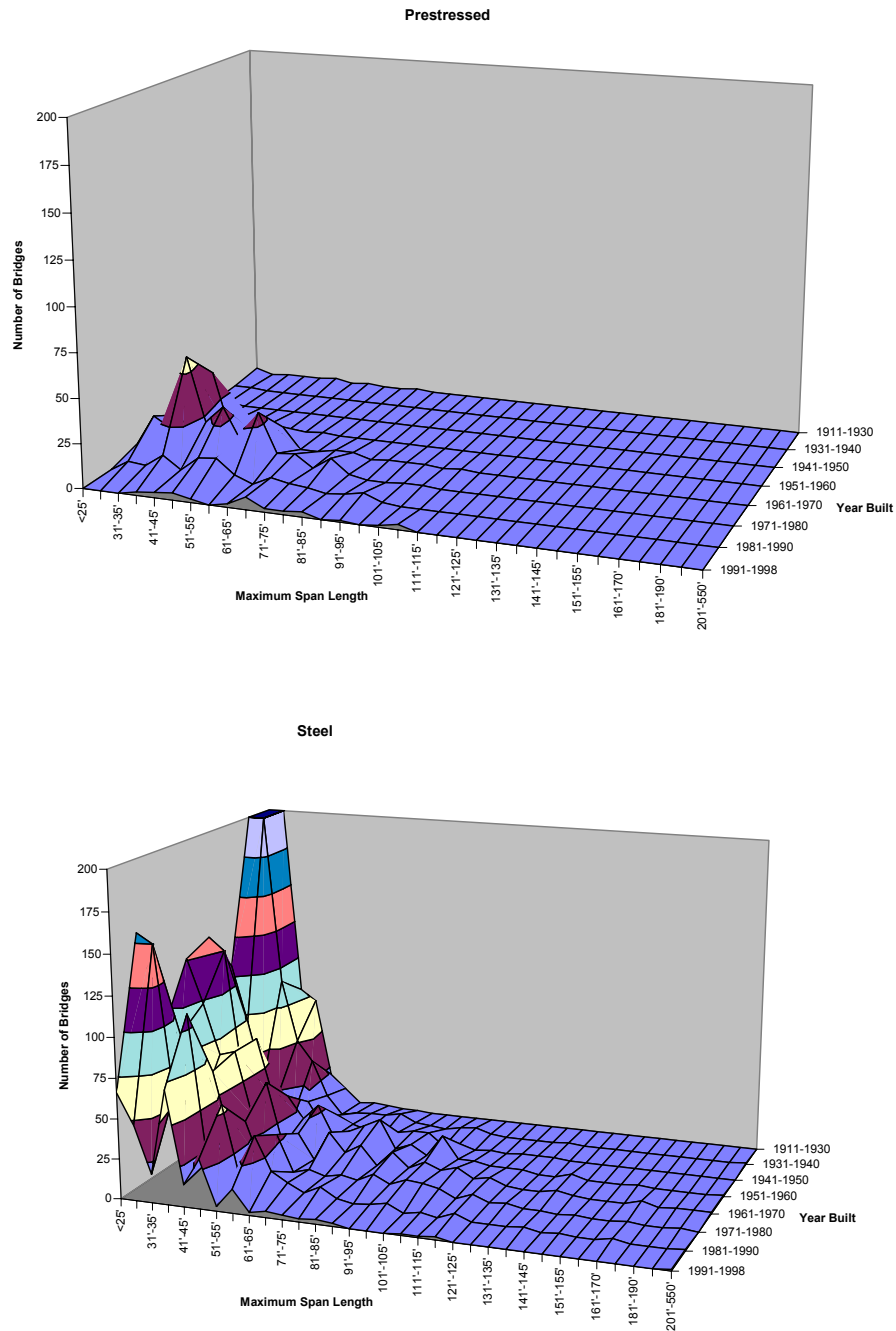
Figure 2-2: Steel and Prestessed Concrete Bridges in Kansas

significantly higher percentage than PC in the span lengths 60 ft and below. Figure 2-3 illustrates the trends in the number of bridges vs. span length vs. year built for both steel and prestressed concrete bridges.
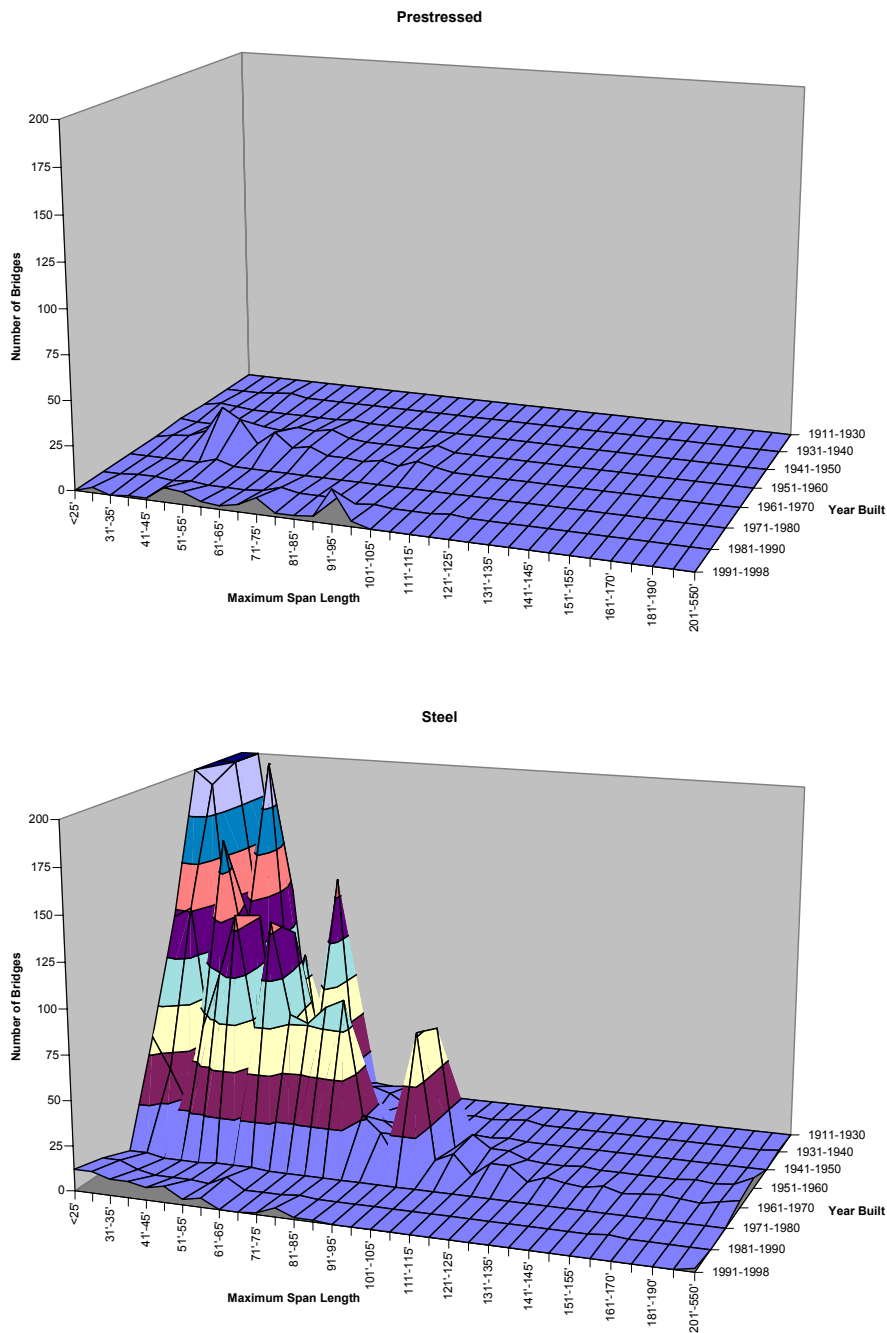
Prestressed

Steel

Figure 2-3: Steel and Prestessed Concrete Bridges in Oklahoma

2.3.4 IOWA

Timber bridges in Iowa have basically been limited to maximum span lengths of 35 ft or less. Approximately 51% of the RC bridges have been built in the last three decades, 26% in the last two decades, and the majority of the RC bridges, 96%, have been constructed at span lengths of 55 ft or

less. Over the last two decades, steel bridges have had maximum span lengths primarily in the 70 ft or less groups. From 1991-1998, 73% of the bridges have been constructed of concrete, both reinforced and pre-stressed (RC 34%, PC 39%, steel 16%, timber 11%). PC has had a prominent impact at almost all span lengths up to 115 ft, dominating specifically at the longer length spans from 50 ft - 115 ft. Figure 2-4 illustrates the trends in the number of bridges vs. span length vs. year built for both steel and prestressed concrete bridges.

2.3.5 COLORADO

The majority of the timber bridges (81%) were built between 1930-1960, with over half of those in the 1930's alone. Approximately 66% had maximum span lengths between 50 ft and 70 ft. Very few timber bridges have been constructed in Colorado in the last three decades. Reinforced concrete also has not generally been selected as a bridge construction material for most span ranges over that time period. More recently, PC and steel have both been selected as construction materials in basically all span lengths. In the 90 ft - 115 ft range, PC has claimed more than three times as many bridges as steel (66 PC compared to 19 steel). In the 90 ft - 150 ft range, PC has almost doubled the number of bridges made of steel (117 PC to 64 steel). Steel dominates the numbers in the span ranges up to 90 ft. Figure 2-5 illustrates the trends in the number of bridges vs. span length vs. year built for both steel and prestressed concrete bridges.

2.3.6 SOUTH DAKOTA

Data from South Dakota reflects the impact the state-owned cement plants have on the choice of bridge material. From 1991-1998, PC accounts for 59% of the bridges, with RC next at 26%, steel with 13% and timber with only 2%. Only 5% of all the timber bridges have been built in the last three decades. The majority (93%) of the timber bridges have maximum span lengths of 30 ft or less. Although in the past, steel has been chosen for the longer span ranges, 90 ft - 150 ft, the last two decades show an increased
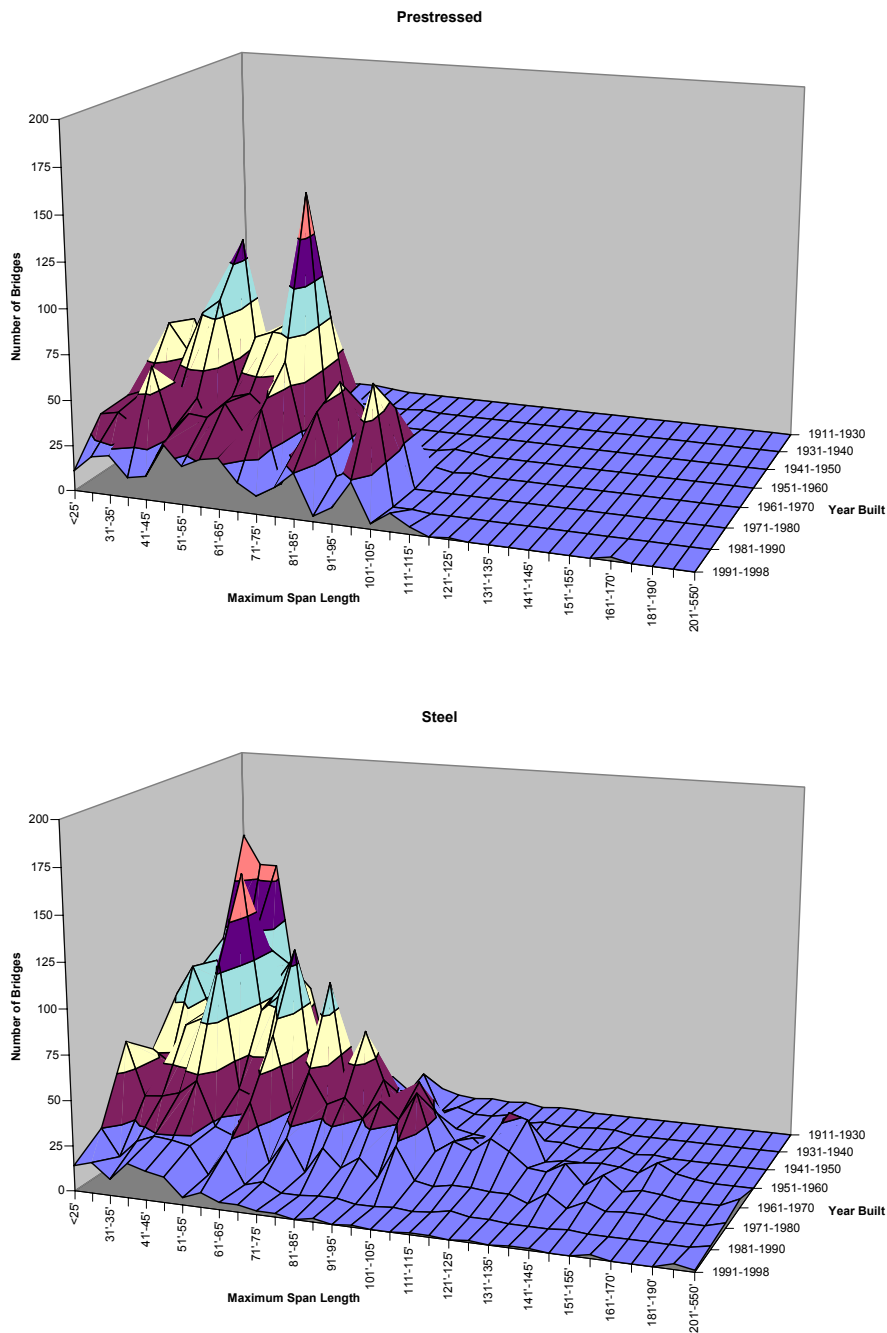
Figure 2-4: Steel and Prestessed Concrete Bridges in Iowa

usage of PC in these span lengths. RC has concentrated in the 50 ft or less span range, but PC has fairly steady numbers across all span ranges up to 135 ft, with peaks in the 35 ft - 65 ft ranges. Figure 2-6 illustrates the trends in the number of bridges vs. span length vs. year built for both steel and prestressed concrete bridges.
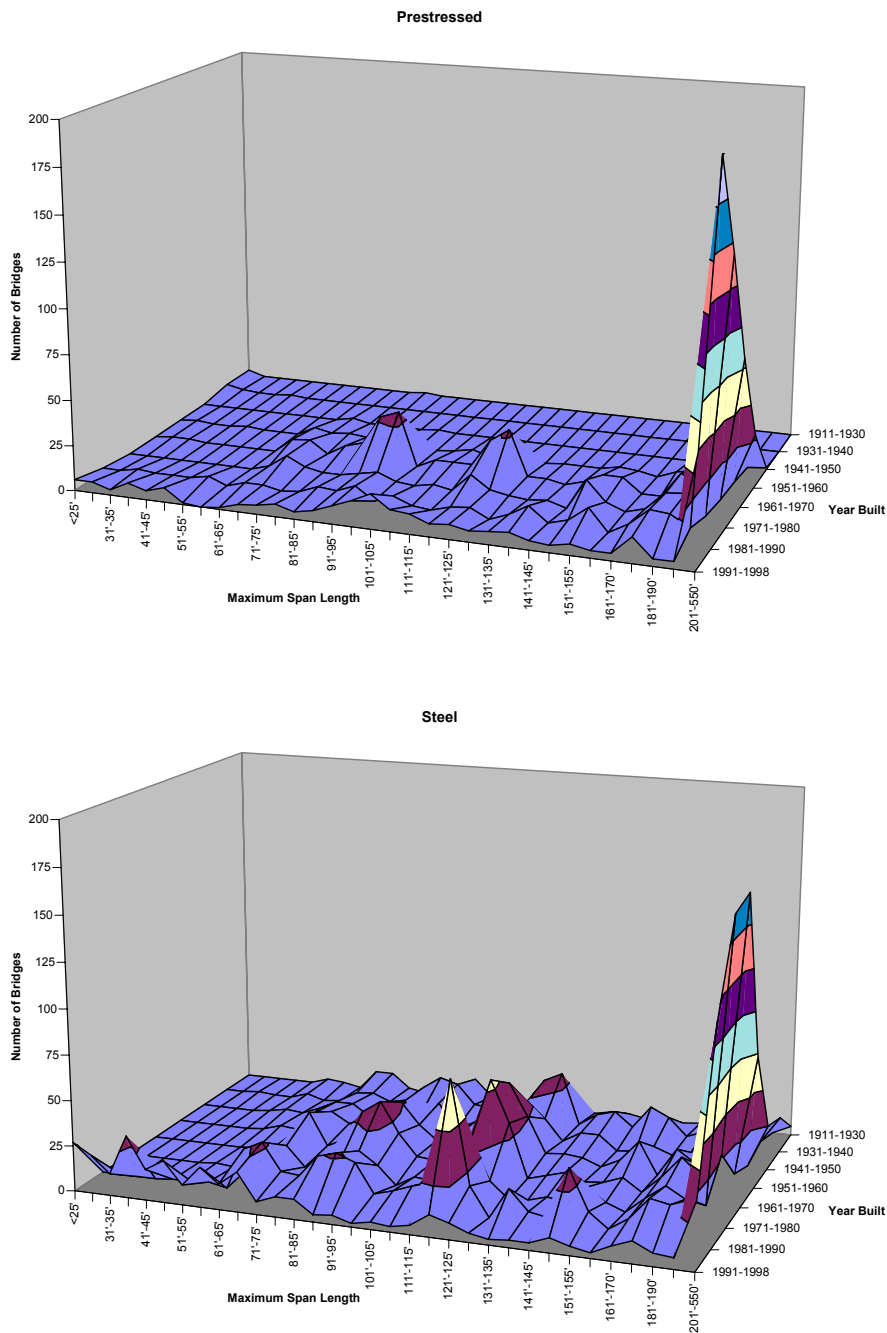
Prestressed

Figure 2-5: Steel and Prestessed Concrete Bridges in Colorado

2.3.7 WYOMING

Over the last two decades, steel has dominated all span ranges, with 72% of the total number of bridges (RC 12%, PC 13%, timber 3%). Steel had high concentrations of numbers in the 100 ft or less span lengths and was the material of choice in most span lengths over 100 ft. PC was used rather
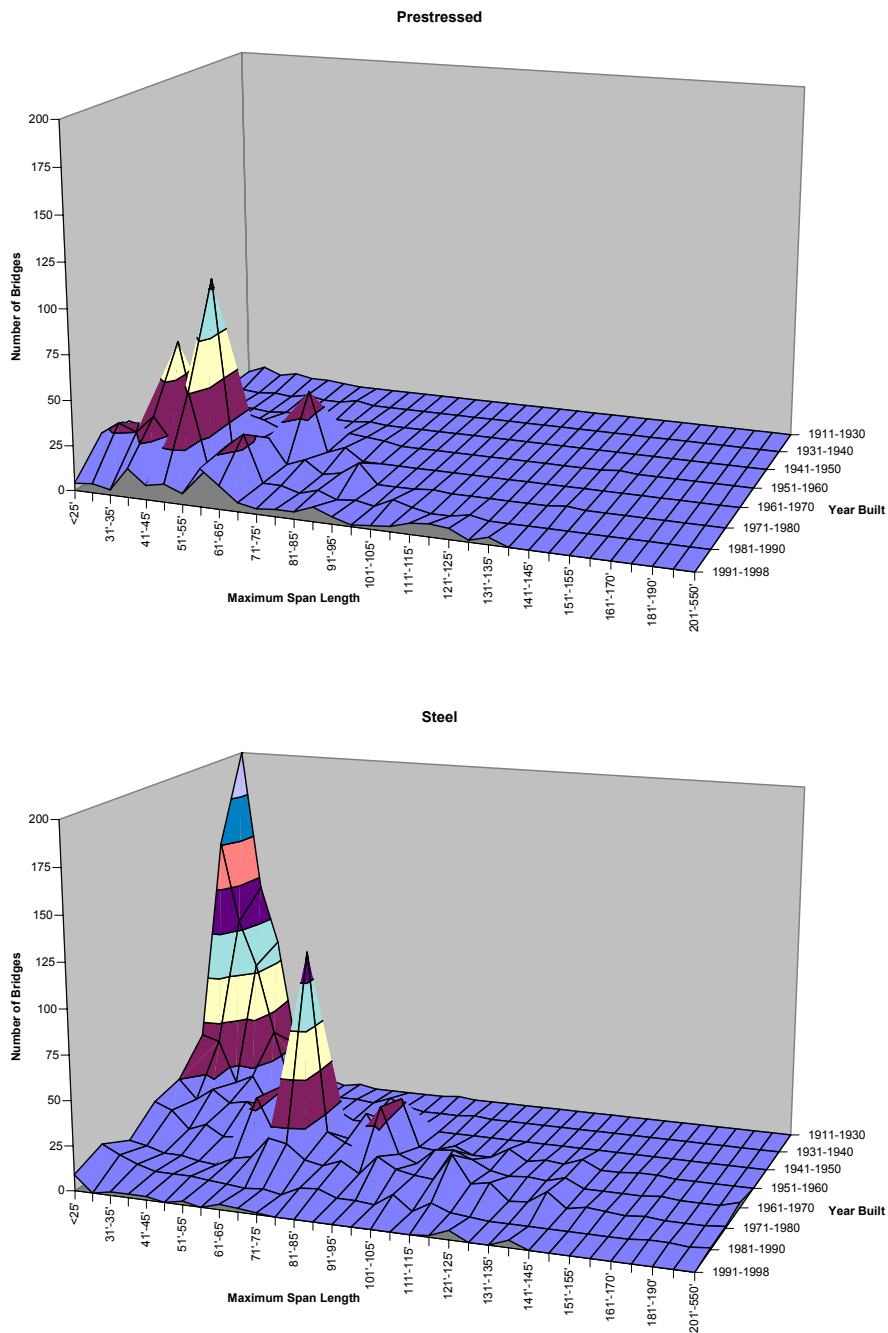
Prestressed

Steel

Figure 2-6: Steel and Prestessed Concrete Bridges in South Dakota

evenly in the 115 ft and below range, with particular usage in the 40 ft - 80 ft range from 1991-1998, the 110 ft or less range from 1981-1990, and the 75 ft or less group from 1971-1980. Only 6 % (18/288) of the timber bridges have been built during the last 20 years. Figure 2-7 illustrates the trends in

the number of bridges vs. span length vs. year built for steel and pre-
stressed concrete bridges.
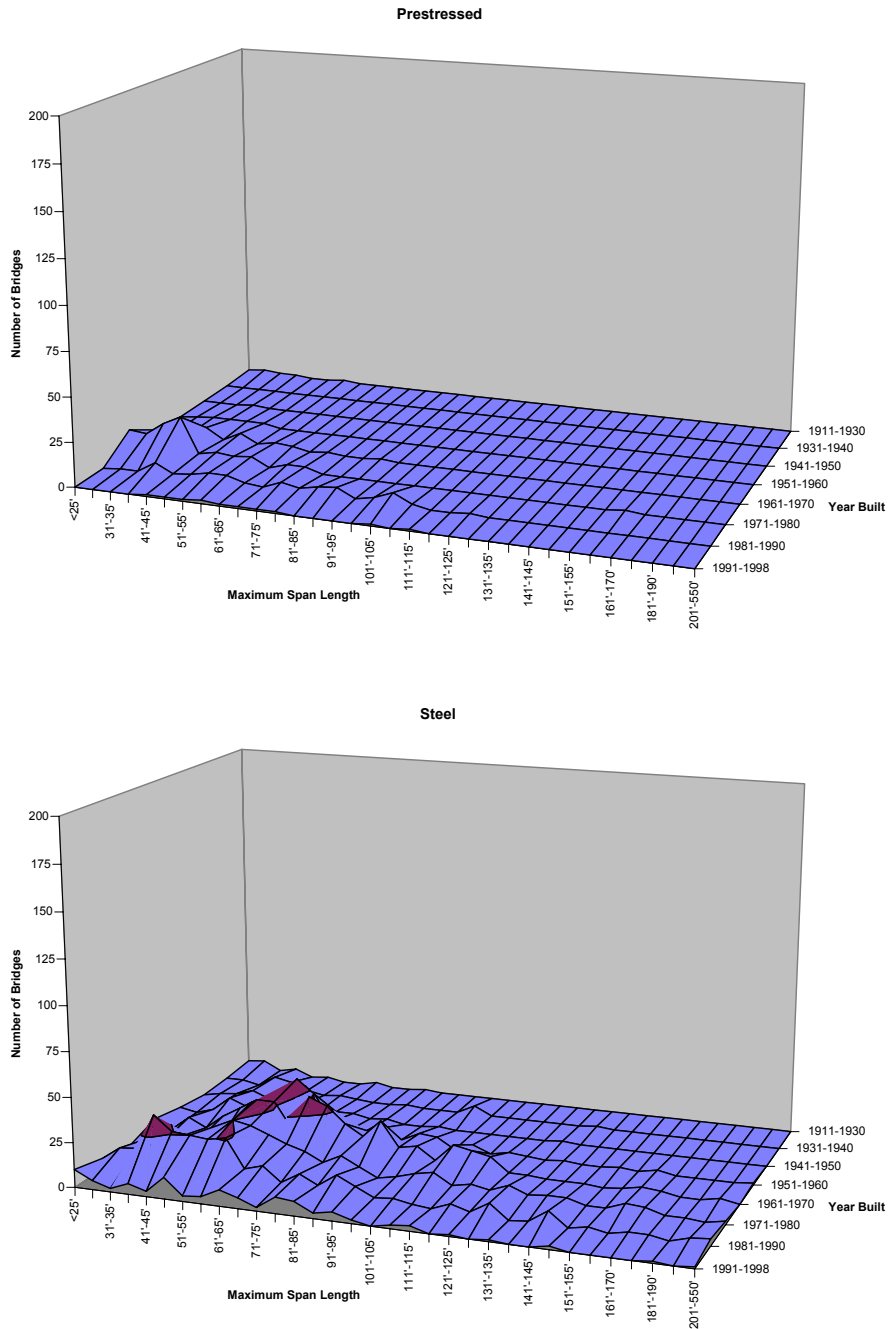
Figure 2-7: Steel and Prestessed Concrete Bridges in Wyoming

2.4 CONCLUSIONS

Based on these trends identified through the market analysis, the primary conclusions are as follows:

1. The use of timber as a bridge construction material, although basically limited to lower span lengths, has significantly decreased over the time period examined.

2. In most states studied, reinforced concrete has remained a fairly consistent choice for span lengths of 50 ft or less.

3. Prestressed concrete construction captured a large share of the market in the 60 ft - 100 ft span ranges in the 1960's and 1970's. The current trends indicate that prestressed concrete has extended its presence as a construction material choice across all span lengths. In the last two decades, steel bridge construction in all span lengths has remained steady or decreased in number. However, there has been an increase in the number of prestressed concrete bridges built in the longer span lengths.

4. In the short span ranges (80 - 110 ft), prestressed concrete girder bridges have become the dominant bridge type.

Identification of the Concept System

Before developing a new steel bridge system, it was deemed necessary to evaluate the factors that add to the cost of constructing steel bridges and issues that could enhance steel bridge economy. This chapter outlines the identification and selection of the proposed concept.

3.1 BACKGROUND

Currently, multi-span steel bridges are constructed as continuous beams providing continuity for both non-composite dead and superimposed dead and live loads. Figure 3-1 shows a conventional two-span continuous steel bridge girder. The construction sequence consists of placing the middle segment and connecting the two end sections using a bolted or welded field splice. This type of construction usually requires two cranes on site with a possible interruption to traffic. In a series of discussions held with

designers, fabricators, and contractors, two factors were identified to be essential in developing a new system:
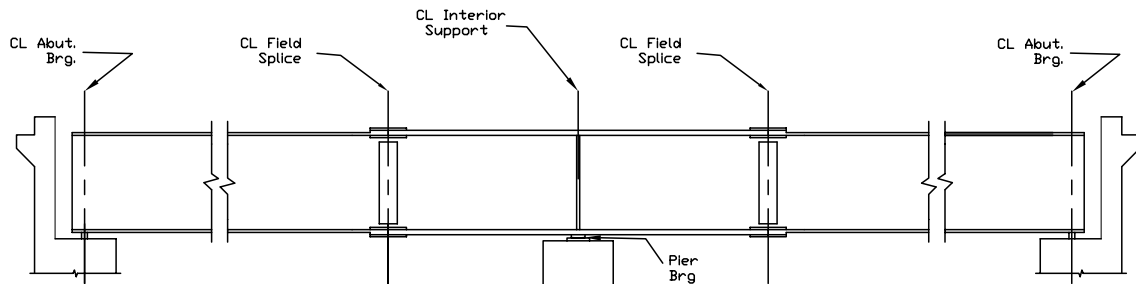
Figure 3-1: Conventional Two-Span Continuous Steel Girder

- elimination of field splices,

- simplify the type of details currently used at the pier location, which in general consists of a combination of anchor bolts, sole plate, and some type of bearing.

3.2 PARAMETRIC STUDY

A parametric study was conducted to investigate the effects of the system modifications outlined in the previous section. The study was carried out on bridges of two equal spans with lengths of 100, 120, and 150 ft subjected to HL-93 live load. In addition to the variable span length, the support geometry was also a parameter. There were four scenarios that were evaluated. These include:

Case #1   Girders acting as simple span for non-composite dead loads
          Girders acting continuous for composite dead and live loads
          Superstructure not connected to pier (non-integral pier system)

Case #2   Girders acting as continuous for all dead loads
          Girders acting continuous for all live loads
          Superstructure not connected to pier (non-integral pier system)

Case #3   Girders acting as simple span for non-composite dead load
          Girders acting continuous for composite dead and live loads
          Superstructure connected to pier (integral pier system)

Case #4   Girders acting as continuous for all dead load
          Girders acting continuous for all live loads
          Superstructure connected to pier (integral pier system)

In Cases 1 and 2, the superstructure is not connected to the pier. In Cases 3 and 4, the superstructure and substructure are integrated.

In Cases 1 and 3, the girders are assumed to act as simple spans for non-composite dead load (concrete slab portion of the dead load), and continuous for composite dead and live loads. This is similar to the practice used to construct prestressed concrete bridges. In Cases 2 and 4, the girders are assumed to act as continuous for both dead and live loads.

Additional parameters included the variation of the relative rigidity of the girder to pier column rigidity, or EI_B/EI_C. This ratio was varied between 0.1 and 8.

Results from this analysis indicated the most desirable situation was a support condition in which the girders act as simple spans for non-composite dead loads and continuous for composite dead and live loads. Figure 3-2 shows the relationship between the proposed concept and the conventional (fully continuous) construction for maximum negative moments at the interior support. In this figure, EI_B/EI_C was specified as 2. Similar results are shown in Figure 3-3 comparing the maximum positive moments at mid-span for an EI_B/EI_C ratio of 2. In each plot, the solid lines indicate the conventional continuous case, while the dashed line indicates the simple support for dead loads condition. In both Figures 3-2 and 3-3, the red lines correspond to the integral pier and the black lines indicate the non-integral pier condition. By inspection of the plots, it can be shown that there is a significant reduction in negative moment at the interior support with smaller increases in positive moment at mid-span. The effects of the integral pier were negligible in the short spans with more dramatic effects in the long spans. Similar results are shown in Figure 3-4 for maximum negative moments with EI_B/EI_C of 0.5. Maximum positive moments for EI_B/EI_C of 0.5 are shown in Figure 3-5. Figures 3-6 and 3-7 provide maximum negative and positive moments respectively for EI_B/EI_C of 8.
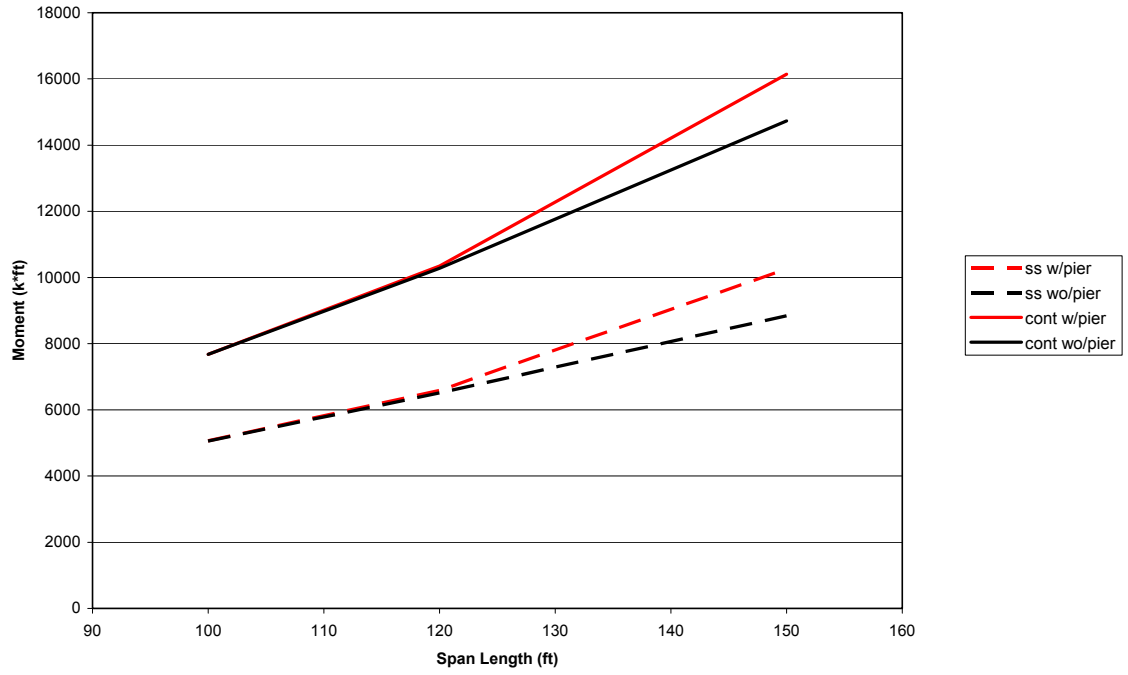
Figure 3-2: Negative Moment Comparison for EI_B/EI_C of 2
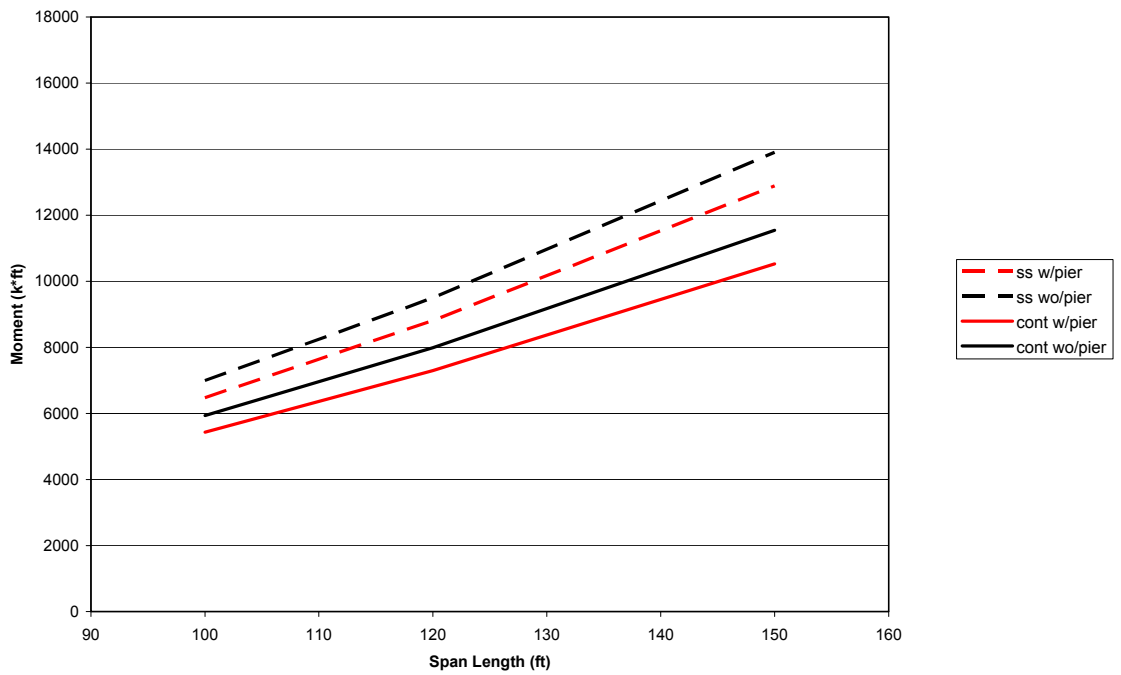
Figure 3-3: Positive Moment Comparison for EI_B/EI_C of 2
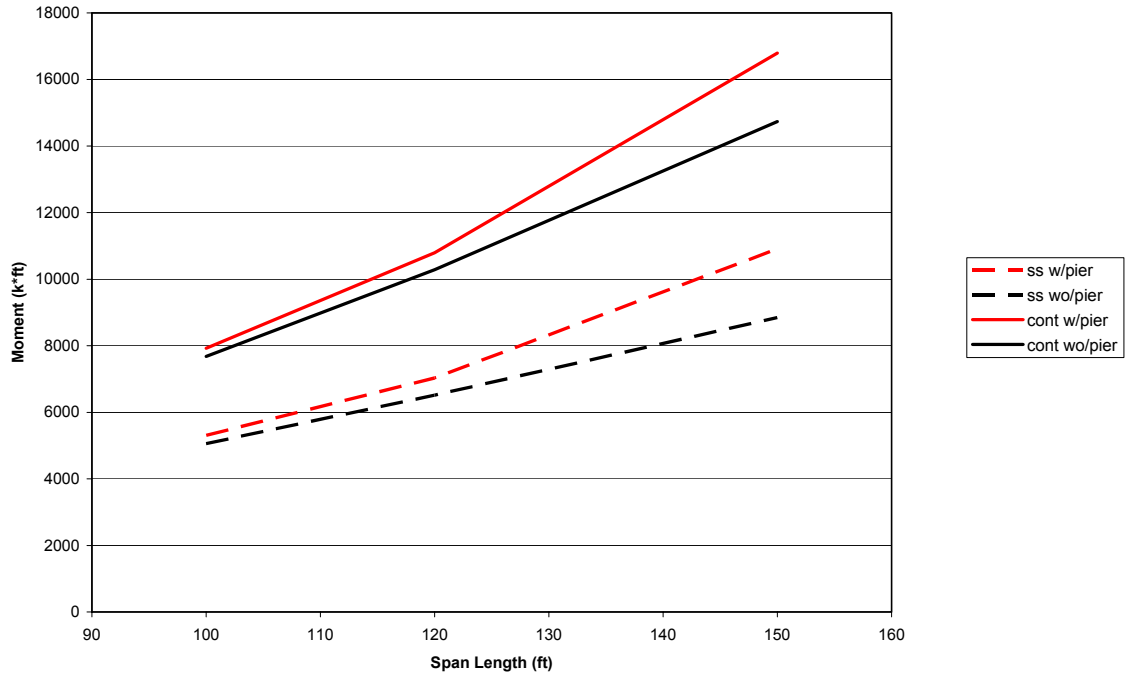
Figure 3-4: Negative Moment Comparison for EI_B/EI_C of 0.5
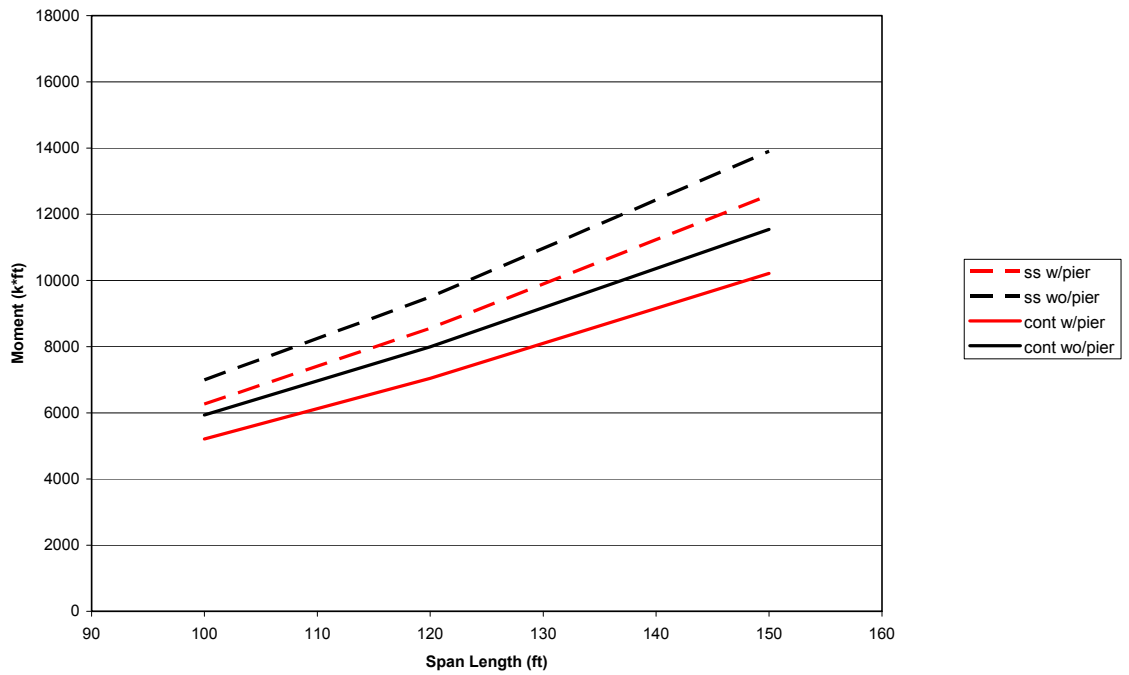
Figure 3-5: Positive Moment Comparison for EI_B/EI_C of 0.5
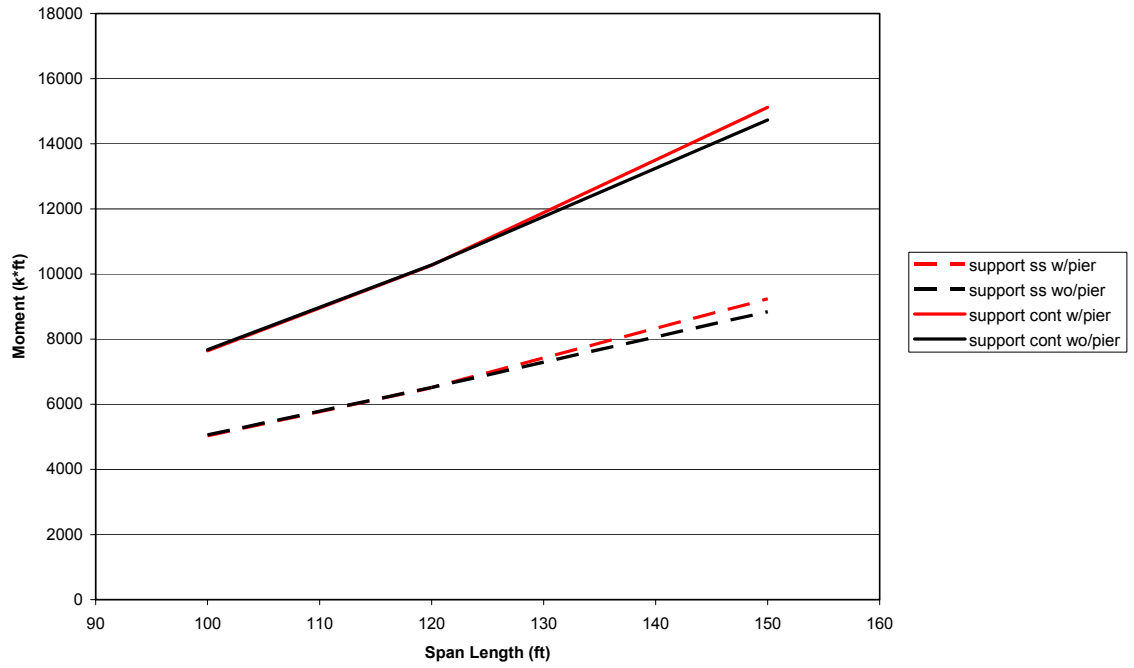
Figure 3-6: Negative Moment Comparison for EI_B/EI_C of 8
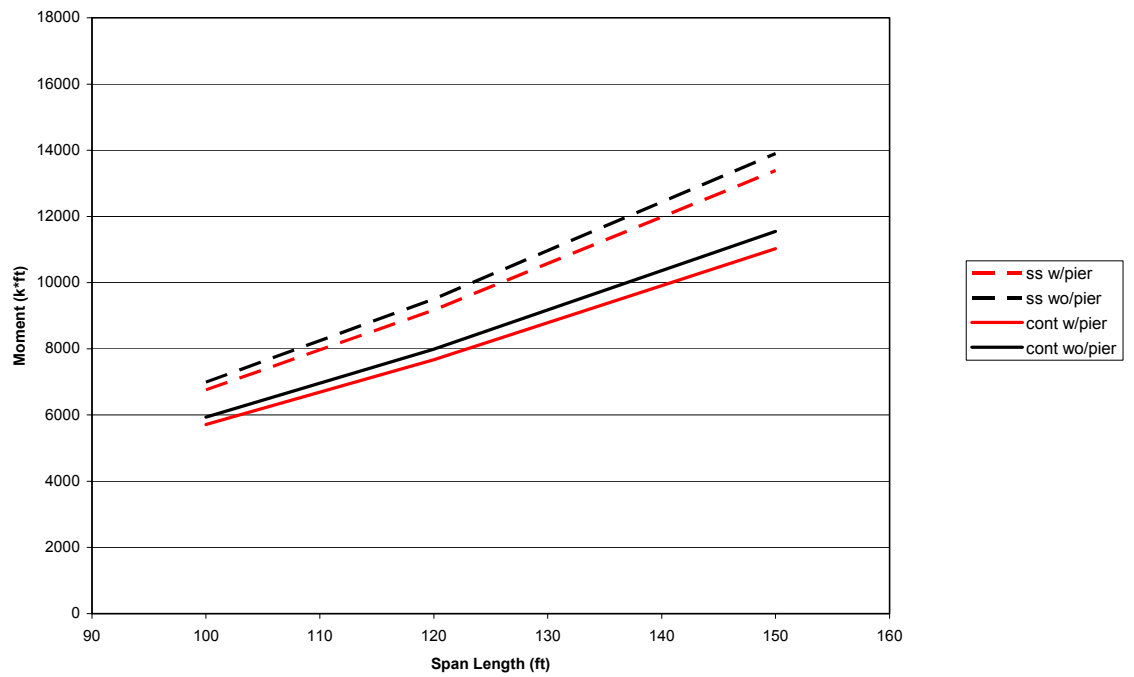
Figure 3-7: Positive Moment Comparison for EI_B/EI_C of 8

3.3 PARAMETRIC STUDY CONCLUSIONS

The effects of the integral pier are negligible in the shorter span lengths for both support conditions.

The proposed system has many advantages, some of which are as follows:

- The need for expensive field bolted or welded splices are completely eliminated for spans of up to approximately 150 ft (as controlled by transportations considerations).

- The contractors will only need one crane. Girders can be placed over the support without significant interruption to traffic. Elimination of the need for more cranes has another advantage. This allows smaller contractors to bid for jobs which usually results in better economy as well as being adaptable for rural areas.

- The resulting moments in the positive and negative regions are such that one could utilize the same cross section for an entire span. In the case of fabricated plate girders, this eliminates the need for changing the plate thickness for the flanges and reduces the fabrication cost.

- The reduction in negative moment over the pier, in most cases, results in reducing the number of cross frames.

Based on the results of this analysis, it was decided to further investigate the simply supported for non-composite dead loads concept, and abandon the integral pier. With the concept identified, the objective becomes quantifying the economic benefit.

Trial Designs 4

From the previous chapters two conclusions have been made. First, the simple support for non-composite dead loads/continuous for live loads concept exhibited definite advantages in load reduction and simplified fabrication. Second, the span range in which steel bridges have become less competitive is approximately 80 - 110 ft. Thus, a benefit-cost analysis was required to determine the economic validity of the proposed concept. To this end, designs were completed for two equal span bridges within the range of 90 - 130 ft span length.

4.1 DESIGN CONSIDERATIONS

The trial designs were completed in accordance with the 1997 American Association of State Highway and Transportation Officials (AASHTO) Load and Resistance Factor Design Specifications (LRFD) [2,4]. Generation of the live load envelopes was done in part using the software package

QCon-Bridge [5]. Additional guidelines observed in the trial designs were taken from the Nebraska Department of Roads (NDOR) BOPP Manual [6]. These guidelines include minimum width and thickness of the top flanges, and minimum web thickness. The top flanges are to be not less than 3/4 in. thick and not less than 12 in. wide. Minimum thickness for webs was set at 3/8 in. thick. In order to facilitate the designs, optimization was done with respect to weight of the steel. The length to depth ratio (L/d) was set at approximately 28. Designs for each span length were completed for both the conventional continuous support condition and the proposed concept allowing for a representative weight comparison.

4.2 BRIDGE DESCRIPTION

The same superstructure geometry was used for both the 90 and 130 ft span bridges. The cast-in-place deck thickness was 8.5 in. with ½-in. integral wearing surface. Support for the deck was provided by 4 lines of girders spaced at 10 ft center to center. Figure 4-1 shows the typical superstructure cross-section. The clear roadway dimension was 34 ft with 1.5-ft wide barriers on either side. Exterior girder overhang was 3.5 ft from the center of the exterior girder to the edge of deck.

4.3 DESIGN SUMMARY

It was determined that the exterior girders controlled the design for flexure, and the interior girders governed shear design at the strength limit state. This was true for both the fully continuous support geometry and the proposed concept. For the proposed concept, the live load distribution factors were the same for both the positive and negative flexure regions for both the interior and exterior girders. Tables 4-1 and 4-2 contain summaries of the live load distribution factors for the 90 and 130 ft span bridges, respectively. The governing shear and bending moments are shown in Tables 4-3 and 4-4. Note the reduction in negative moment was due to no
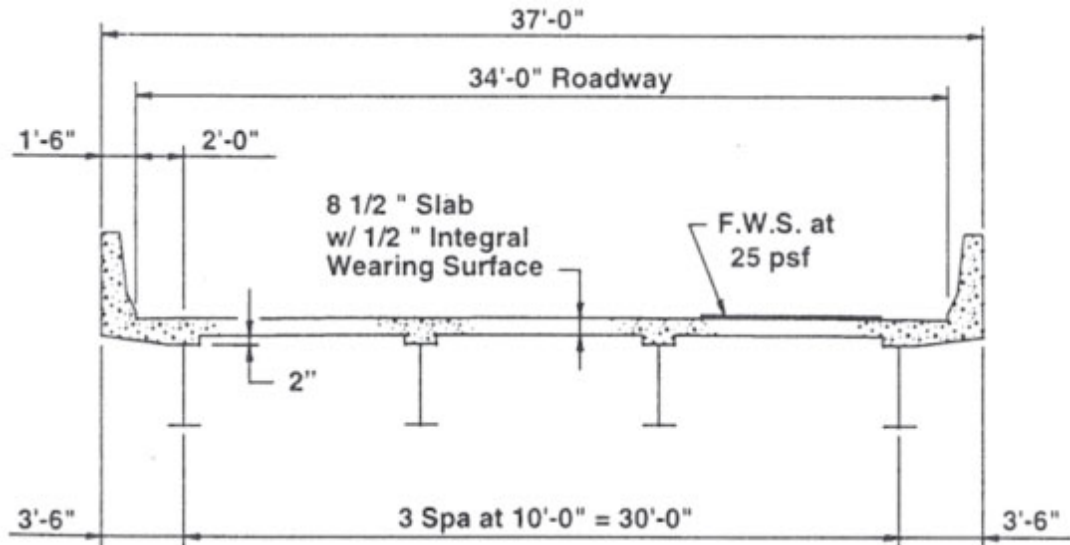
Figure 4-1: Geometry for 90 and 130 ft Designs

contribution from the non-composite dead loads for the proposed concept. AASHTO LRFD (6.10.4.4) allows an optional 10% reduction in negative moment from moment redistribution for compact sections [3]. This allowance was used only for the conventional continuous design.

		Simple Dead Continuous Live		Continuous Dead Continuous Live	
		Positive	Negative	Positive	Negative
Exterior	Moment	0.865	0.865	0.865	0.865
	Shear	0.865	0.865	0.865	0.865
Interior	Moment	0.712	0.712	0.700	0.732
	Shear	0.965	0.965	0.966	0.966

Table 4-1: Distribution Factor Summary for the 90-ft Span

		Simple Dead Continuous Live		Continuous Dead Continuous Live	
		Positive	Negative	Positive	Negative
Exterior	Moment	0.865	0.865	0.865	0.865
	Shear	0.865	0.865	0.865	0.865
Interior	Moment	0.703	0.703	0.693	0.728
	Shear	0.965	0.965	0.966	0.966

Table 4-2: Distribution Factor Summary for the 130-ft Span

		Simple Dead Continuous Live	Continuous Dead Continuous Live
Moment (k·ft)	Positive	4430	4212
	Negative	3699	5269
Shear (kip)	Positive	287	267
	Negative	329	348

Table 4-3: Maximum Design Moments for the 90-ft Span

		Simple Dead Continuous Live	Continuous Dead Continuous Live
Moment (k·ft)	Positive	9003	7374
	Negative	7248	11319
Shear (kip)	Positive	347	314
	Negative	404	437

Table 4-4: Maximum Design Moment for the 130-ft Span

The 90 ft span bridge was designed as both a welded plate girder and a rolled I-shape girder. A summary of the designs is shown in Table 4-5. The values in the table are presented as ratios in the form of demand/resistance. Recall that the designs were optimized in terms of steel weight only, resulting in a weight increase of approximately 4%.

Similar to the 90 ft span summary, Tables 4-6 and 4-7 contain the summaries for the 130 ft span designs. The first set of designs utilized a 48 in web, and the second set used a 54 in web in an attempt to decrease the dead load deflection. The 48 and 54 in webs resulted in an L/d ratios of 32.5 and 28.9, respectively. The increase in steel weight was 5% for the 48 in web and 2% for the 54 in web.

The results of these designs were presented to the members of the advisory panel. From this meeting, the following conclusions were made:

1. The cost of the additional steel would easily be offset by the elimination of the bolted field splices, and

2. The magnitude of the dead load deflection reduces the applicability of this concept to phase construction projects.

			Simple for Dead Loads		Continuous for Dead Loads		Rolled (W40x199)	
			Positive	Negative	Positive	Negative	Positive	Negative
Section Properties	Dimensions	Top Flng	$\frac{7}{8} \times 13\frac{1}{2}$		$\frac{3}{4} \times 14$	1×16	$1\frac{1}{16} \times 15\frac{3}{4}$	
		Web	$\frac{1}{2} \times 36$		$\frac{7}{16} \times 36$	$\frac{1}{2} \times 36$	$\frac{5}{8} \times 36\frac{9}{16}$	
		Bot Flng	$1\frac{1}{4} \times 15$		$1\frac{1}{8} \times 16$	$1\frac{1}{2} \times 16$	$1\frac{1}{16} \times 15\frac{3}{4}$	
	Weight	Area	48.6		44.25	59.5	58.4	
		Length	90		63	27	90	
		Wt (lb)	14884		9486	5466	17910	
		Tot Wt	14884		14952		17910	
Service	Perm Defl	Comp	51%	85%	49%	93%	42%	85%
		Tension	93%	78%	97%	94%	92%	64%
	LL Defl	(in)	1.297		1.276		1.246	
Strength	Flexure	Compact Section	91%	94%	97%	99%	88%	86%
	Shear		Stiffeners not Required		Stiffeners not Required		Stiffeners not Required	
DL Defl @ Midspan		(in)	5.9		3.4		4.8	

Table 4-5: 90-ft Span Design Summary

			Simple for Dead Loads		Cont. for Dead Loads	
			Positive	Negative	Positive	Negative
Section Properties	Dimension	Top Flng	$1\frac{3}{8} \times 18$	Same	$\frac{3}{4} \times 12$	$2\frac{1}{8} \times 22$
		Web	$\frac{7}{16} \times 48$	Same	$\frac{3}{8} \times 48$	$\frac{1}{2} \times 48$
		Bot Flng	$1\frac{1}{2} \times 21$	Same	$1\frac{1}{4} \times 19\frac{1}{2}$	$2\frac{1}{2} \times 22$
	Weight	Area	77.25		51.375	125.75
		Length	130		91	39
		Wt (lb)	34172		15908	16688
		Tot Wt	34172		32596	
Service	Perm Defl	Comp	67.5%	77.6%	77.2%	76.7%
		Tension	96.1%	67.4%	99.3%	76.8%
	LL Defl	(in)	1.714		1.841	
Strength	Flexure	Compact Section	96.9%	Comp 99.5% / Tens 86.4%	98.9%	Comp 95.5% / Tens 95.4%
	Shear		Requires Stiffeners		Requires Stiffeners	
DL Defl @ Midspan		(in)	8.2		5.6	

Table 4-6: Design Summary for 130 ft Span, 48 in Web

			Simple for Dead Loads		Cont. for Dead Loads	
			Positive	Negative	Positive	Negative
Section Properties	Dimension	Top Flng	$1\frac{1}{4} \times 16$	Same	$\frac{3}{4} \times 12$	2×20
		Web	$\frac{7}{16} \times 54$	Same	$\frac{3}{8} \times 54$	$\frac{1}{2} \times 54$
		Bot Flng	$1\frac{1}{2} \times 18$	Same	$1\frac{1}{8} \times 18$	$2\frac{1}{4} \times 21\frac{1}{2}$
	Weights	Area	70.625		49.5	115.375
		Length	130		91	39
		Wt (lb)	31242		15328	15311
		Tot Wt	31242		30639	
Service	Perm Defl	Comp	68.8%	78.0%	77.2%	76.7%
		Tension	96.6%	67.6%	99.3%	76.8%
	LL Defl	(in)	1.51		1.65	
Strength	Flexure	Compact Section	98.9%	Comp 100% / Tens 86.6%	96.2%	Comp 94.7% / Tens 95.5%
	Shear		Requires Stiffeners		Requires Stiffeners	
	DL Defl @ Midspan	(in)	7.5		5.1	

Table 4-7: Design Summary for 130 ft Span, 54 in Web

Based on the second recommendation, the decision was made to focus primarily on spans of approximately 100 ft in length and to utilize rolled beams. The Military Avenue project was selected for two reasons. First the 95-ft spans represent a common 2-span bridge constructed in Nebraska. Second, the project was recently designed and erected and would provide current cost estimates for economic comparisons between current practice and the proposed concept.

4.4 MILITARY ROAD PROJECT

The Military Road structure consisted of two 95 ft spans, and a 5 girder cross-section. The girder spacing was 8'-4" and supported a 30 ft clear roadway and a pedestrian sidewalk. This superstructure geometry is shown in Figure 4-2. To simplify the design procedure, the sidewalk was removed and the number of girders reduced from 5 to 4. This altered geometry is shown in Figure 4-3. The designs for this structure were car-

ried out using the simple support for non-composite dead loads/continuous for composite dead and live loads concept and rolled I-shape girders. Designs for span lengths of 100 and 105 ft were also completed using the geometry defined in Figure 4-3. The summaries for these designs are shown in Table 4-8.
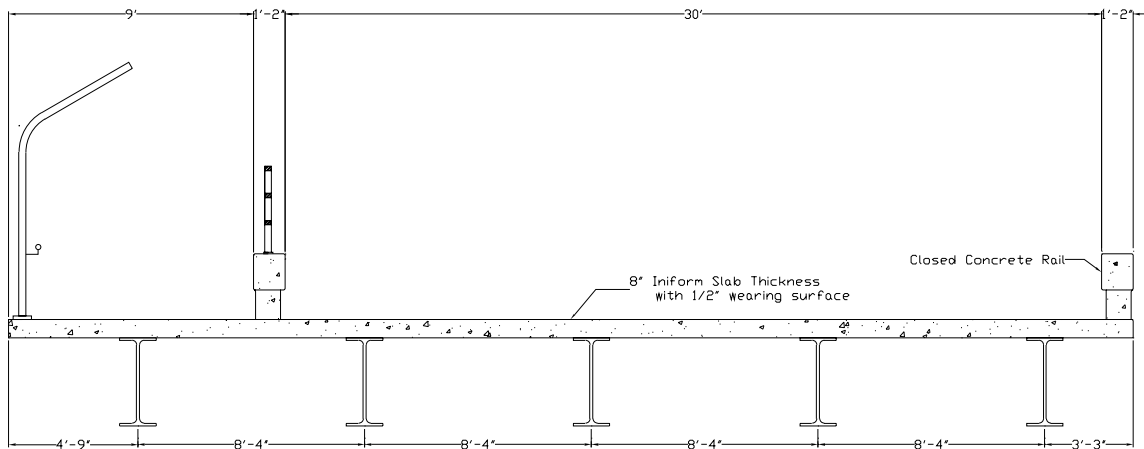
Figure 4-2: Military Road Bridge Typical Cross-Section
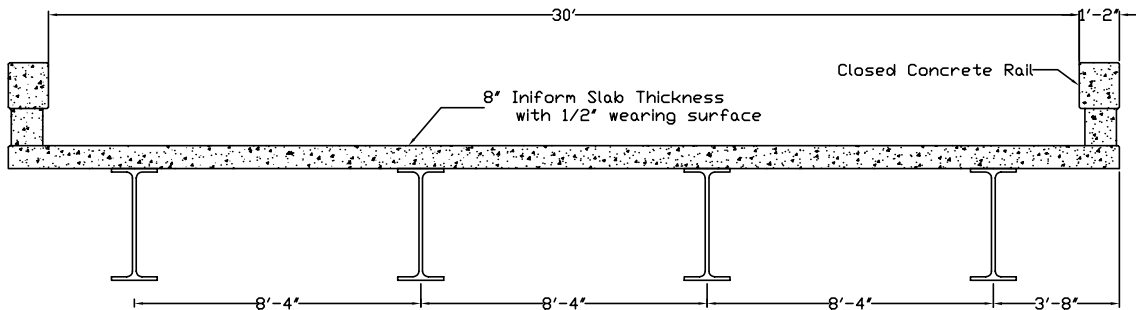
Figure 4-3: Modified Military Avenue Cross-Section

		Span Length (Feet)				
		95		100		105
Section		W40×215		W40×249		W40×277
DL Deflection (int/ext)		4.4/4.2		4.7/4.5		5.3/5.1
LL Deflection		99.4		95.9		98.8
Flexural Strength	Pos	92.6		88.8		88.5
	Neg	83.0		78.2		78.3
Permanent Deflection	Pos	96.5	48.1	91.8	48.3	92.0	50.7
	Neg	62.6	80.9	60.5	75.7	82.5	75.2

Table 4-8: Military Road Design Summary

From the results in the table, increases in span length from 95 ft result in decreases in beam demand/beam capacity ratios. Thus, the designs become less optimized as the span length increases. In addition, the magnitude of the dead load deflection may warrant cambering of the girders, reducing the economic benefit.

The 95 ft span was selected as the model for the experimental investigation, primarily to see the cost comparison to the actual project constructed.

Complete details of the design process including sample calculations can be found in Appendix A.

Connection Detail Analysis and Design

<div style="text-align: right; font-size: 3em;">5</div>

The final design of the pier connection detail was the product of recommendations from NDOR, fabricators, and contractors, combined with results from finite element analysis. This chapter outlines the analysis and modeling issues for the design of the pier connection detail.

5.1 BACKGROUND

The proposed system consists of placing two simple span girders over the abutment and pier, casting the deck slab, and providing the continuity for live load and superimposed dead loads only. Figure 5-1 shows a schematic of such a system. This is similar to the practice that has been used for years by the prestressed concrete industry. In the case of prestressed girders, continuity for live and superimposed dead load is accomplished by placing reinforcing bars over the pier and casting the concrete diaphragms over the

pier [2,7,8]. In such situations, the bottom portion of the concrete diaphragms in the vicinity of the girders is subjected to compressive force transferred from adjacent girders. In the case of prestressed girders, the bottom flanges of the girders generally have large areas and are able to distribute the compressive force and prevent crushing of the concrete. In developing an equivalent system for steel bridges, the presence of a large compressive force at the bottom of the concrete diaphragms presents a challenge. The bottom flanges of steel girders usually have smaller cross sectional areas compared to prestressed girders and, therefore, there is a possibility of crushing the concrete under negative moment created by live loads and superimposed dead loads. To investigate the stresses in the concrete diaphragm, a series of finite element analyses was carried out to evaluate the behavior of the concrete in the vicinity of the compression flange.
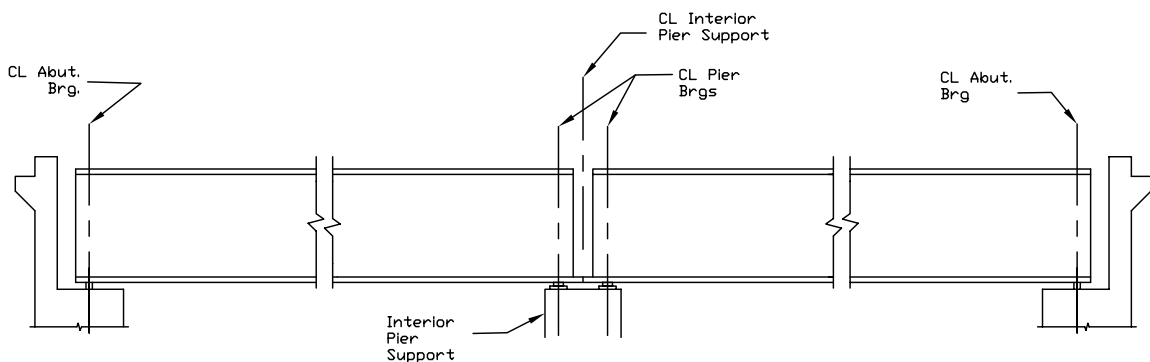
Figure 5-1: Illustration of Proposed Concept

5.2 FINITE ELEMENT MODELING

Several finite element models were analyzed using the finite element software SAP2000® [9] to investigate the behavior of the proposed system. Shell elements were used to generate the steel members and solid elements were used to model the concrete. The steel girder in the model had the cross-sectional dimensions of a W 40 x 215 I-shape. The model consisted of the steel section in bearing against the solid elements. Load information for the model was taken directly from the 95 ft span design. The elasto-

meric bearing pad is modeled using springs under the girder flange nodes, with stiffness K_e, where the value of K_e is defined using the stiffness equation shown in Equation 5-1.

$$K_e = \frac{AE}{L}$$ (5-1)

Where

A = tributary area of corresponding node (in^2)

E = elastic modulus of elastomeric pad (ksi)

L = depth of elastomeric pad (in)

Four configurations were analyzed to determine the effect that different details would have on the resulting concrete stress. These configurations include:

1. The steel girder section bearing against the concrete diaphragm,

2. The steel girder with end bearing plates equal to the girder flange width,

3. The steel girder with the bottom flange continuous, and

4. The steel girder with both the end bearing plates and the bottom flange continuous.

These analyses were carried out assuming linear elastic behavior and are therefore subject limitations in their applicability. However, the results can be quite useful in following the system response under loads which are less than ultimate to determine the critical regions and elastic response of the system. The results of this study are shown in Table 5-1. From these results, the option which produces the lowest stresses is the option with both the continuous bottom flange and the end bearing plates.

The thickness of the end bearing plates was also determined using a finite element study. The model defined in case (2) from above was used with the end bearing plate thickness as a variable. From this study, thick plates, in excess of 3 in., were required to dramatically reduce the stress in the con-

	Stress (ksi)	
	w/ Bearing Plate	w/o Bearing Plate
w/o Flange Connection	25.5	45.3
w/ Flange Connection	5.9	8.2

Table 5-1: Concrete Compressive Stress

crete. Thinner plates lacked the flexural rigidity to efficiently distribute the compressive force. Thick plates are less readily available or as economical as the thinner plates. For this reason, several finite models were utilized to investigate the effects of braced thinner plates. Bracing of a thinner plate within the concrete compression zone results in lower, more even stresses in the concrete diaphragm.

5.3 FINITE MODELING FOR DEAD LOADS

Results from the previous analysis indicate a mechanism is necessary to transfer the compressive force through the concrete diaphragm. The simplest mechanism is extending the bottom flange through the diaphragm. The concept under investigation consists of extending the bottom flanges from each span half the gap dimension, and connecting by use of a partial penetration weld. One concern arose from this concept. Would connecting the bottom flanges prior to girder deflection cause substantial rotational restraint? Restraint would correspond to initial stresses in the continuous flange. The finite element model used in the previous studies was subjected to the non-composite distributed loads. The end rotation values from this model were compared to those obtained using Equation 5-2. The end rotation of a simply supported beam subjected to a uniform distributed load can be calculated using Equation 5-2.

$$\phi = \frac{wL^3}{24EI}$$

(5-2)

Where

w = distributed load (kip/in)

L = span length (in)

E = elastic modulus (ksi)

I = moment of inertia (in^4)

A possible reduction in the end rotation could be attributed to the bottom flange connection and support from the elastomeric bearing pad. As expected, the rotation of a simple supported 95-ft long W40 x 215 beam subjected to distributed load of 1.15 k/ft is 0.0121 radians. and the average value of rotation from the finite element analysis was 0.0092 radians. The average rotation was calculated from rotations of the end nodes from the finite element model.

From elementary mechanics, the elastic bending moment is related to stress σ in Equation 5-3 shown below.

$$\sigma = \frac{M\,c}{I} = \frac{M}{S} \tag{5-3}$$

Where

M = moment (kp·in)

c = distance from neutral axis to outermost fiber (in)

I = moment of inertia (in^4)

S = section modulus (in^3)

From the finite element model the maximum moment in the continuous bottom flange produced a corresponding stress equal to 34 ksi. The thought is that the connection plate should not reach yield under non-composite dead loads. From the analysis, the maximum bending stress is below yield.

From the analysis completed to this point, the thickness of the end bearing plates and the gap between girders over the pier have been sized.

5.4 DETAIL DESCRIPTION

The remaining detailing issues were similar to standard NDOR details used in the design of prestressed concrete girder bridges including the transverse reinforcement in the diaphragm. Figure 5-2 shows the girder portion of the pier detail as a final concept for fabrication and testing. The bottom flanges extend 4 in beyond the edges of the top flange and web. Bearing stiffeners were attached flush at this web edge with gusset plate stiffeners within the compression zone. Holes are drilled (preferred) or flame cut in the web for the diaphragm transverse reinforcement. Figure 5-3 shows elevation and plan views of the diaphragm reinforcement. The stirrups are closed hoops with one located 6 in from the outer edge of the bearing stiffeners and the remaining placed on 12 in centers within the remaining space between adjacent girders. See the plan view in Figure 5-3 for an illustration.

Typically, empirical deck design is used in design of the composite slab by NDOR, as outlined in AASHTO LRFD Design Specifications [2,6]. Empirical deck design for longitudinal steel includes #4 bars at 12-in. on centers in the top layer and #5 bars at 12-in. on centers in the bottom layer. For transverse steel, reinforcement consists of #5 bars at 12-in. on centers in the bottom layer and #4 bars at 12-in. on centers in the top layer.

In addtion to the longitudinal reiforcing required by the empirical design method, the detail being investigated will require additonal continuity reiforcment to transfer the tensile component of moment over the pier. The total area of required longitudinal reinforcement is calculated as a reinforced concrete beam with compression steel. Calculation of the tension steel area is calculated based on Strength I limit state design moments generated for the prototype bridge. Figure 5-4 shows the free-body diagram and the strain profile for the reinforcement calculation. The strain profile

Figure 5-2: Pier Connection Detail

2 Sp. @ 12"

Diaphragm
Hoops

Girder

6"

Diaphragm

Plan View

#8 BARS

#5 BARS

Elevation

Figure 5-3: Pier Diaphram Transverse Reinforcement

in Figure 5-4 is based on the assumption that both the tension and compression steels have reached yield where:

M_u = 3911 kp·ft (Strength I limit state design moment)

b = 15.75 in (width of the bottom flange)

f'_c = 4 ksi (concrete compressive strength)

d = 41.51 in
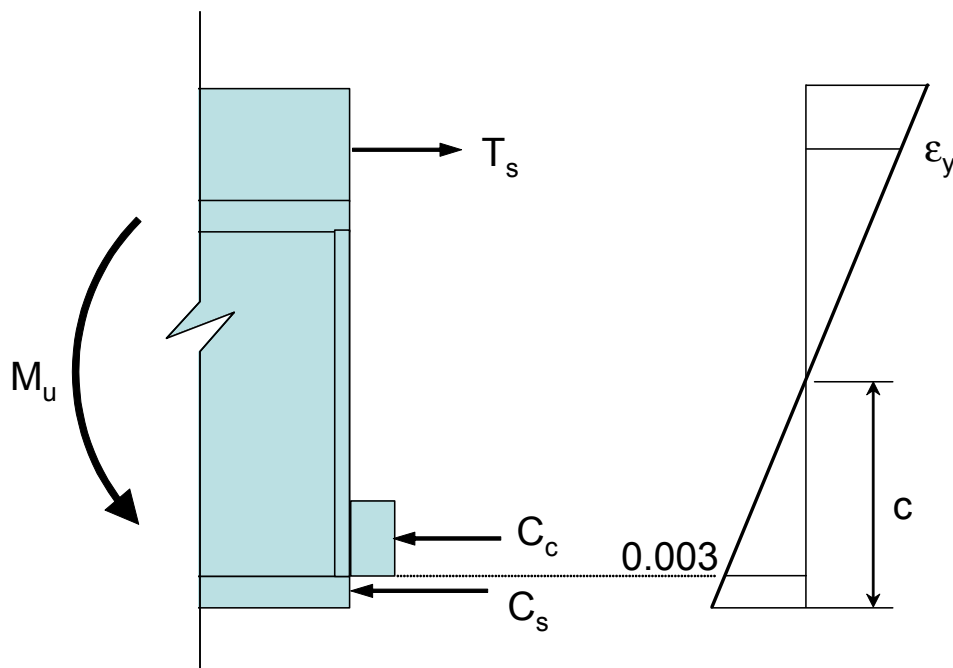
Figure 5-4: Force Diagram for Reinforcement Design

Assuming that the tension and compression steel both yield, the force equilibrium equation is expressed in Equation 5-4.

$$T_s - C_c - C_s = 0$$
$$A_s f_s - 0.85 f'_c(ab) - A'_s f'_s = 0$$

(5-4)

Where

T_s = tensile force in the reinforcing (kips)

C_c = resultant compressive force in the concrete (kips)

C_s = compressive force in the bottom flange (kips)

A_s = area of tension reinforcement (in²)

f_s = theoretical reinforcement yield stress (ksi)

a = depth of the concrete compressive stress block (in.)

b = width of the bottom flange (in.)

Similar to Equation 5-4, the moment equilibrium equation is expressed as shown in Equation 5-5 as shown.

$$A_s f_s (d) - C_c \left(\frac{a}{2} \right) - M_u = 0 \qquad (5\text{-}5)$$

Solving Equations 5-3 and 5-4 simultaneously results in an A_s required for the specified design moment of 18.96 in^2. Substituting A_s into Equation 5-4 as a check of the yield condition assumption produces Equation 5-6:

$$C_c + C_s = T_s$$
$$0.85 f_c' (ab) + 960.75 = 18.96 (60) \qquad (5\text{-}6)$$
$$a = 3.30\, in$$

Where

c = a/b = 3.3/0.85 = 3.885 in

the yield assumption is valid

For the test specimen, the additional reinforcement required in the top layer is comprised of 2 - #8 bars centered between adjacent #4 bars. Similarly, 1 - #7 bar is centered between adjacent #5 bars in the bottom longitudinal layer. This follows the typical 2/3 of the reinforcing steel in the top layer and 1/3 of the total area in the bottom layer. The effective flange width is calculated as 93 in. by 7.5 in. in thickness, for the test specimen, and no haunch was included.

6

Experimental Program

Based on the analysis results and guidance from the advisory panel, the pier connection detail was chosen for full-scale testing. An experimental investigation was carried out to check assumptions made during the design process, check validity of the FEM model, and to examine the performance of the pier connection detail under field conditions.

6.1 GENERAL TEST DESCRIPTION

The geometry of the test specimen was selected to represent an interior pier section of a 2-span bridge subjected to construction and service loads. Figure 6-1 shows the conceptual test specimen geometry. The double cantilever system provides an effective means of simulating loading of the structure in the field. In this loading system, the shear/moment ratio can be accurately modeled.
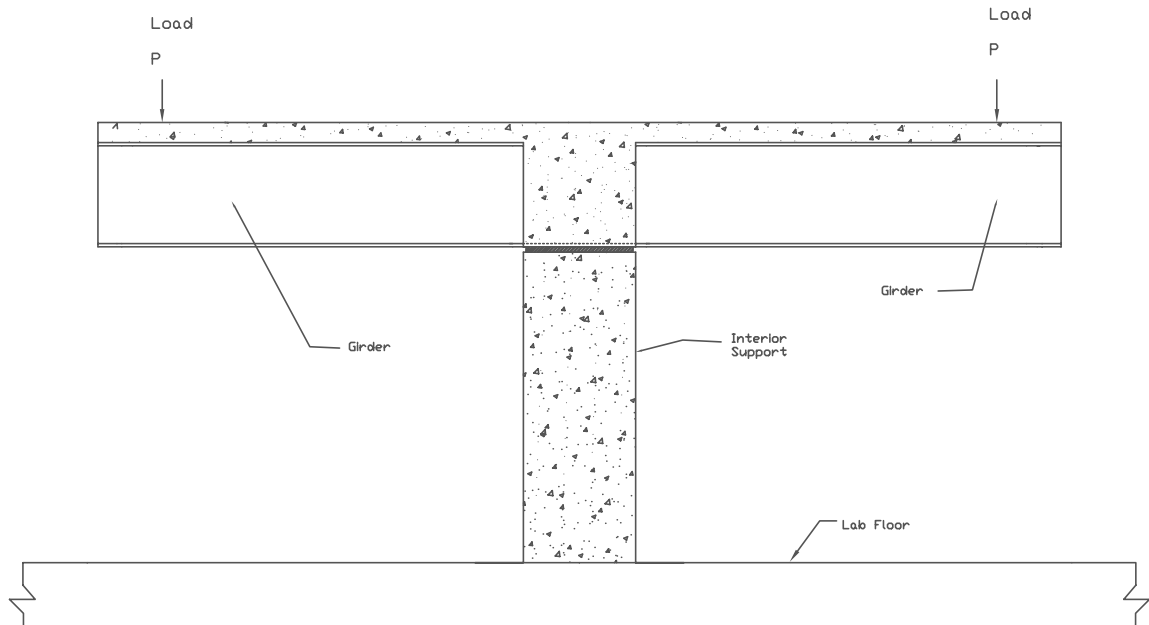
Figure 6-1: Conceptual Test Configuration

The test specimen was designed according to the AASHTO LRFD Specifications for Highway Bridges [2]. The strength portion of the design, as outlined in Appendix A, is taken further to include fatigue and shear resistance. The objective was to obtain experimental data to compare with the results of the FEM analysis. In order to accurately represent the loads the structure would encounter, 3 load stages were identified. These are as follows:

1. The application of the non-composite dead loads (casting of wet concrete deck), which causes rotation of the girder ends,

2. The cyclic fatigue loading which is based on a fatigue load from analysis and the detail fatigue category, and

3. The ultimate distributed moment based on the governing strength limit state.

In order to obtain data from these load stages, several types of data collection hardware were employed.

6.2 INSTRUMENTATION

As discussed in the previous section, 3 main load stages were identified. Within each load stage exists a distinct load pattern warranting slight variations in instrumentation configurations. Monitoring of the specimen was done using potentiometers, bonded electrical and vibrating wire strain gauges. Collection of data was done through the use of a Megadac Data Acquisition System by Optim Electronics. The data acquisition system is shown in Figures 6-2 and 6-3. This acquisition system collected data from all instruments except the vibrating wire gages. Readings from the vibrating wire gages were taken manually. To aid in record keeping, the instruments were assigned a designation according to instrument type.

The strain gage designation is as follows:

SG - steel surface electrical strain gages,

EG - concrete embedment vibrating wire strain gages,

VW - steel surface vibrating wire gages,

CG - concrete surface electrical strain gages, and

Pots - potentiometers (linear transducers).

Gages SG1 through SG7 were located on the top surface of the bottom flange over the pier, as shown in the plan view of Figure 6-4. Figure 6-5 illustrates the locations of gages SG8 through SG14 located across the thickness of the bottom flange near the transverse centerline of the structure. Electronic instrumentation attached to the reinforcing bars and the deck surface is shown in Figure 6-6. Gages SG15 through SG30 were attached to select reinforcing bars placed within the deck slab, as illustrated in Section A-A of Figure 6-6. Gages with a CG designation were attached to the top surface of the concrete deck slab, with gages CG1 through CG4 located at the specimen centerline. As Figure 6-6 indicates, gages CG1 through CG4 are paired with corresponding reinforcement instrumentation. Gage CG1 was paired with SG16, CG2 with SG18, CG3 with
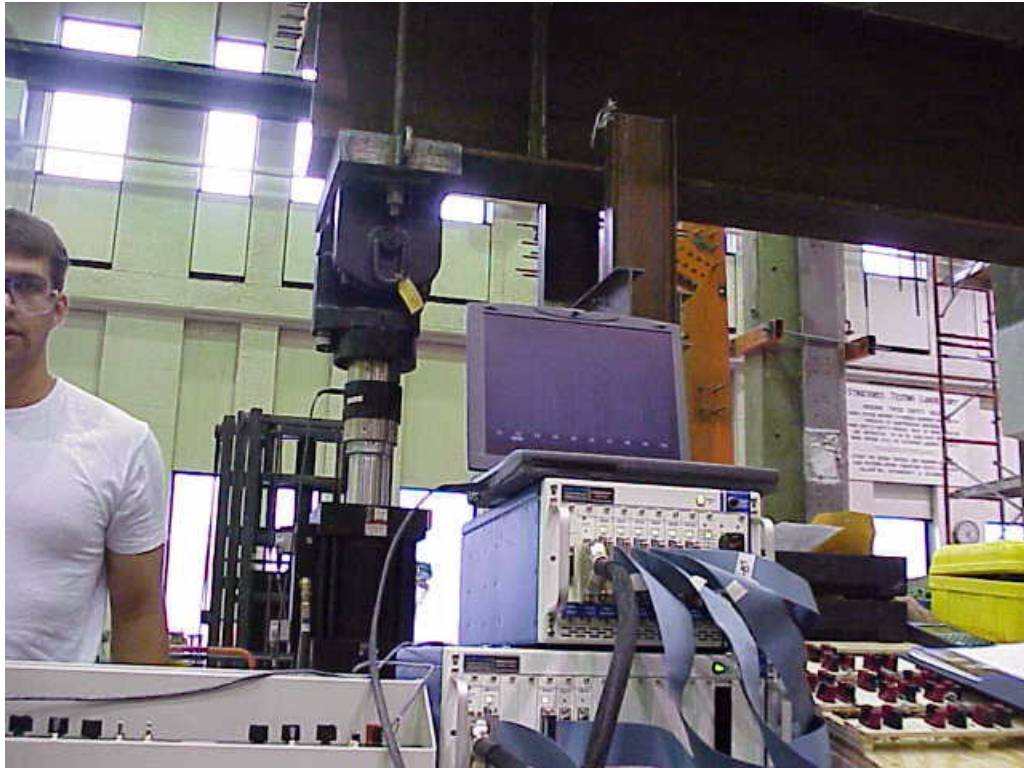
Figure 6-2: Data Acquisition System by Optim Electronics

Figure 6-3: Data Acquisition and Load Control Systems

SG20, and CG4 with SG22. Gages CG5 through CG9 were located 21.5 in. east of centerline over the diaphragm edge, and gages CG10 through CG12 were located over the west edge of the diaphragm. As shown in Figure 6-6, two linear transducers were located across the diaphragm edges, each with a 10-in. gage length.
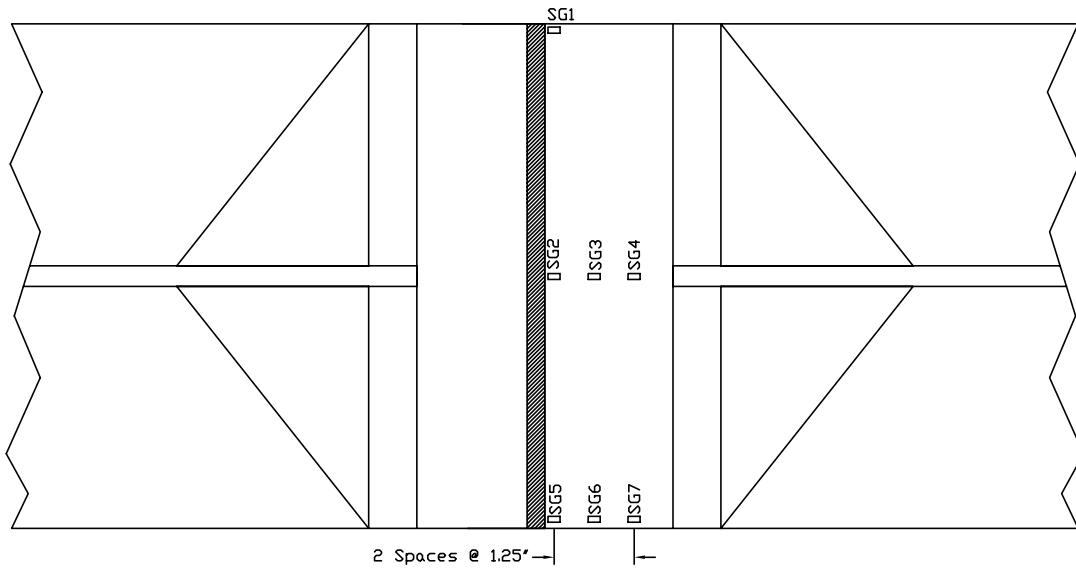
Figure 6-4: Gages SG1 through SG7
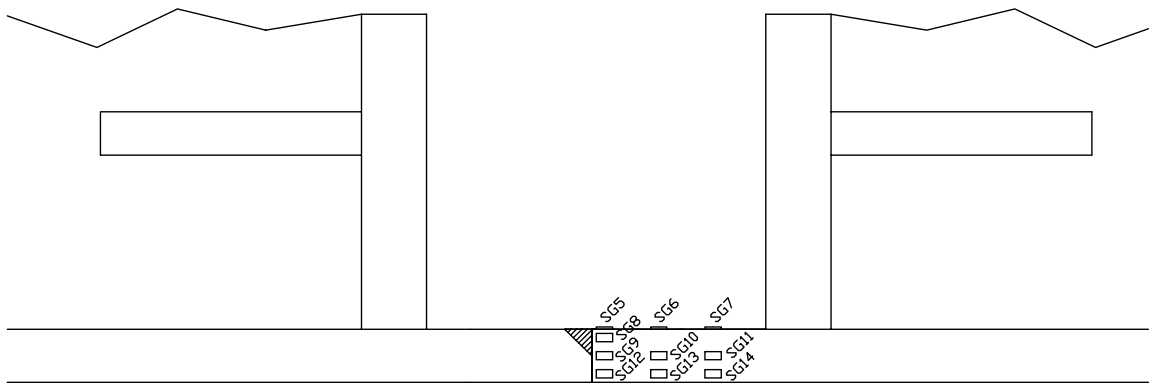
Figure 6-5: Gages Across the Thickness of the Bottom Flange

Additional instrumentation attached to the steel girders is shown in Figure 6-7. Gages SG31 through SG37 were located within the limits of the concrete diaphragm at the locations shown in Figure 6-7. Gages VW1, VW2,
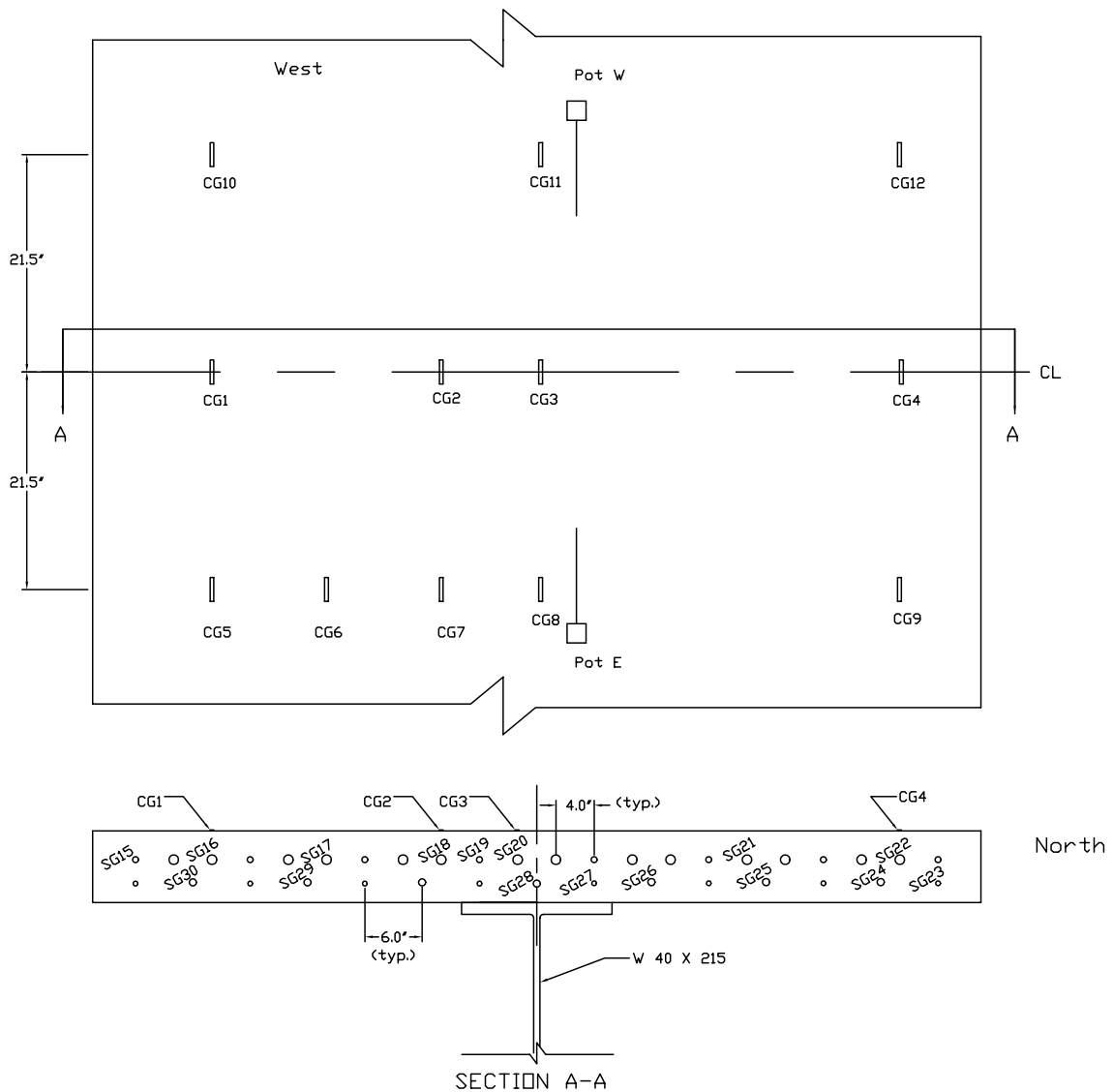
Figure 6-6: Deck and Reinforcing Steel Instrumentation Layout

and VW5 were attached to the girder web immediately outside the diaphragm. Instrumentation of the bottom flange outside the diaphragm consisted of both VW and SG gages, while the VW gages were centered within the width of the flange and the SG gages were placed at the flange width quarter points.

Embedment gages, designated EG, were used to monitor strains in the concrete diaphragm and deck at several locations. Embedment gages were placed at 3 locations along the length of the specimen. The three locations

Figure 6-7: Additional Girder Instrumentation

A, B, and C are illustrated in Figure 6-8. Location A corresponds to the specimen centerline, where EG gages were placed both in the diaphragm and deck. Location B is 6 in. inside the diaphragm and where the EG gages were placed only in the diaphragm. Location C is at the edge of diaphragm and where gages were placed only in the deck. In the transverse direction, EG gages were grouped in vertical planes at predetermined locations. Figure 6-9a illustrates the transverse groups at location A (specimen CL), divided into groups 1 through 5 as shown. Similarly, Figure 6-9b shows embedment gage groupings at locations B and C.
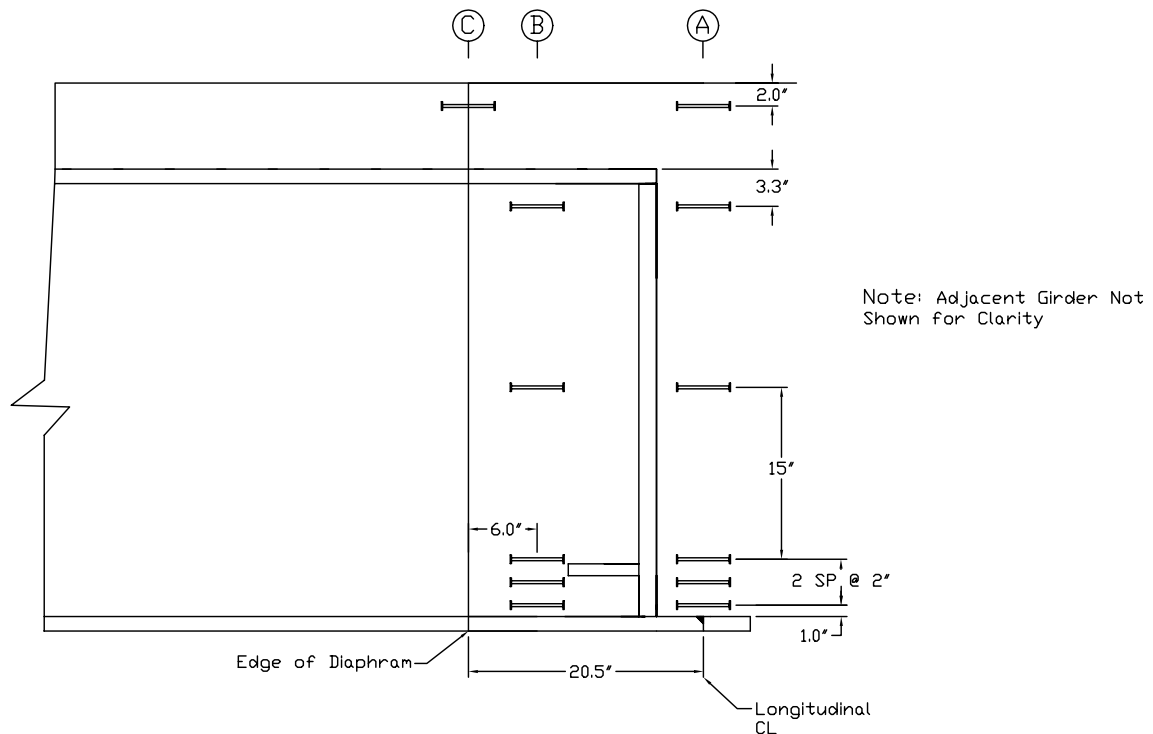
Figure 6-8: Embedment Longitudinal Location Groupings
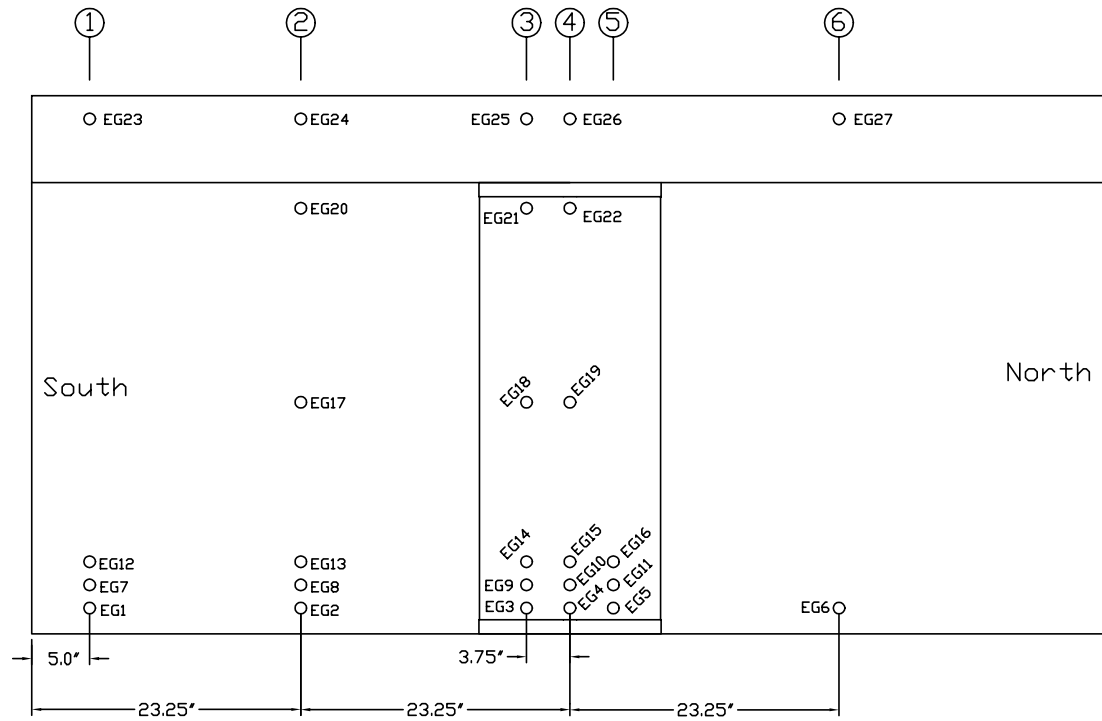
(a)
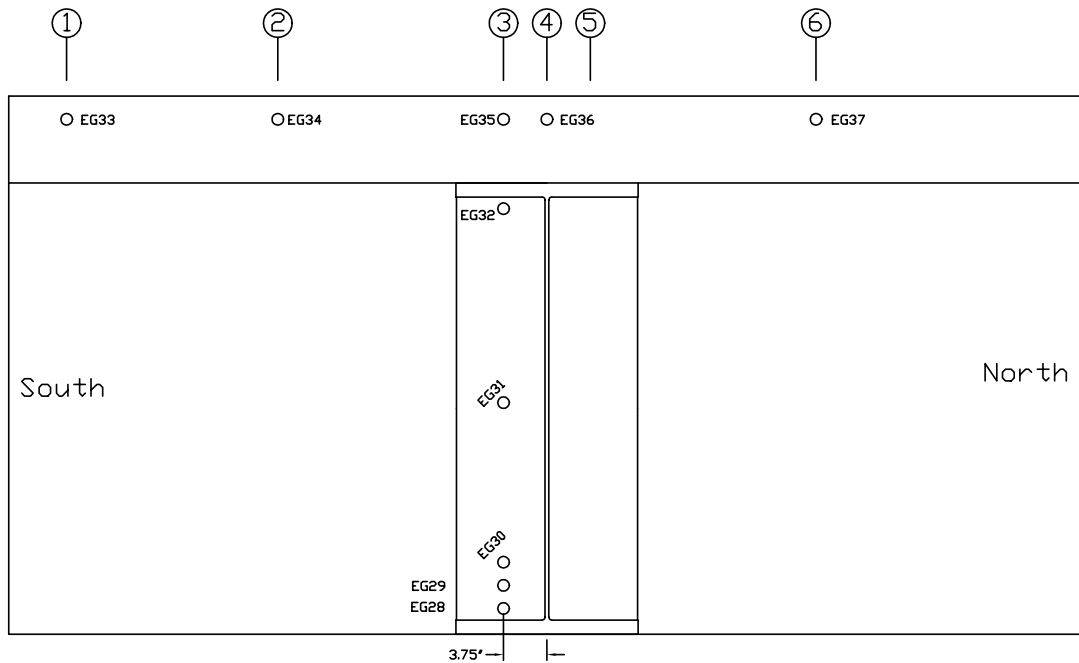
(b)

Figure 6-9: Embedment Transverse Location Diagrams

Additional potentiometers were positioned at each point of load application in order to measure total deflection. The potentiometers were designated according to placement on either the east and west girder.

6.3 CONSTRUCTION AND ERECTION

Construction of the test specimen was completed in the structures lab at the University of Nebraska-Lincoln. Support for the cantilever system was achieved by designing and casting a concrete pier similar to those used by NDOR. A drawing of the pier is shown in Figure 6-10. The dimensions of the pier were based on the height requirements of the MTS® hydraulic actuators and the attachment hardware required for the fatigue test. For safety and stability reasons, the pier was post-tensioned to the lab floor through PVC ducts at the pier centerline. Figure 6-11 shows the completed pier form-work prior to casting, and Figure 6-12 shows casting of the pier concrete. After curing for 7 days, the forms were removed and the pier rotated upright into position and post tensioned to the laboratory floor.

As mentioned previously, the steel girder sections were obtained from the Lincoln Steel Corporation. Some grinding was done in the lab prior to girder placement to insure that no protrusions extended beyond the face of the end bearing plates. Bearing stiffeners were welded onto the girders at 11'-6" from the face of the end bearing plate. This corresponds to the loading point for the ultimate strength test. Figure 6-13 shows the girders after fabrication. Subsequently, measurements of all lengths, widths, and thicknesses of the steel girders were taken before girder placement. Measured dimensions are discussed later in Chapter 7.

The elastomeric bearing pad, known commercially as "Fiberlast", was obtained from Voss Engineering. Design of this pad was completed by Voss Engineering through the use of in house software. The dimensions of this pad were 15.75 in. wide by 36 in. long by 1 in. thick. This pad was centered
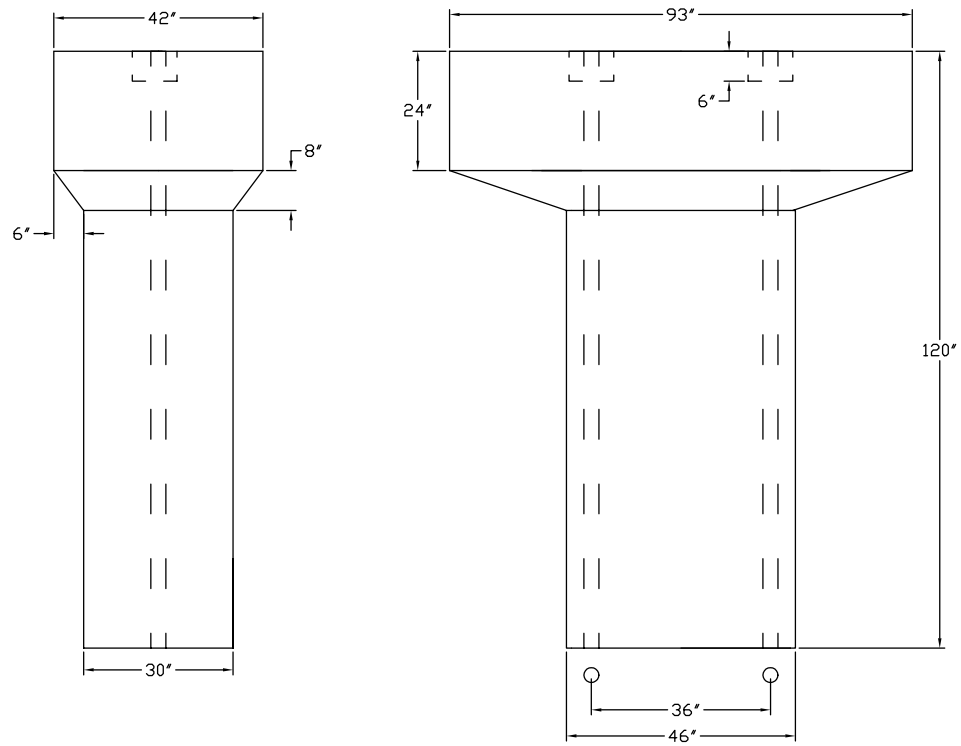
Figure 6-10: Pier Elevation and Dimensions

Figure 6-11: Pier Form Work Prior to Casting

Figure 6-12: Casting of Pier Concrete
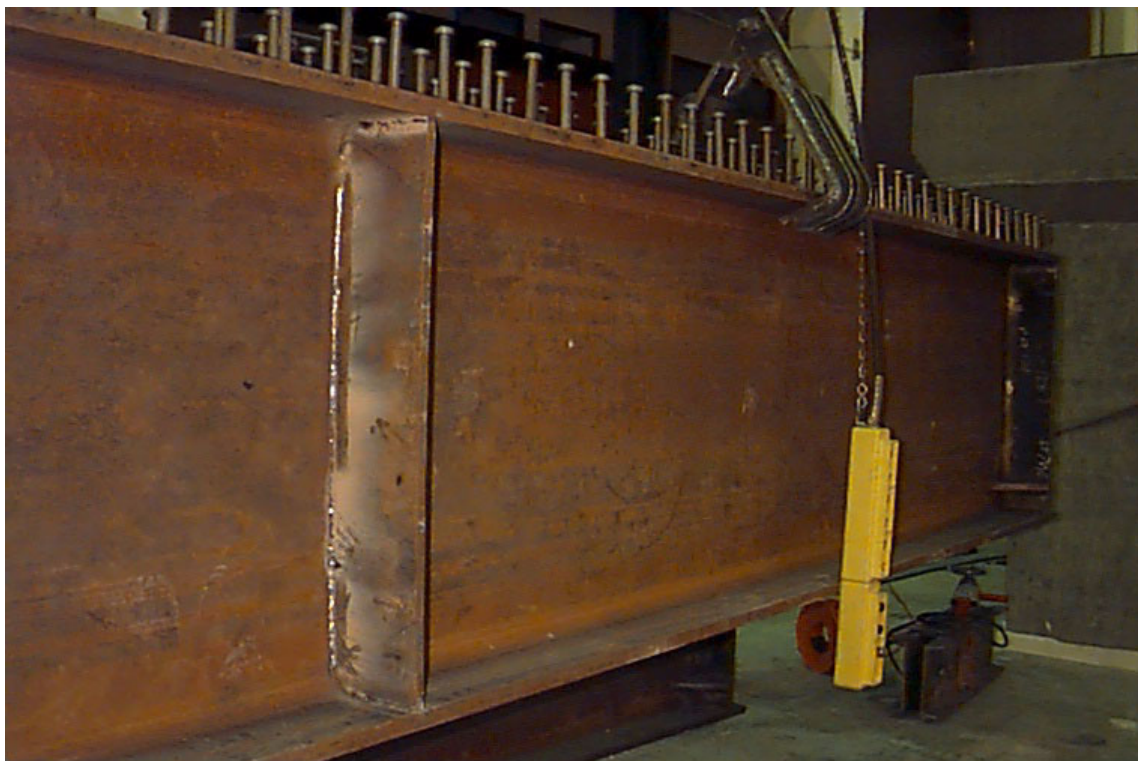
Figure 6-13: Girders After Fabrication

on the pier, and definite markings were made to insure detection of any movement in the pad during construction. Figure 6-14 shows the bearing pad location prior to girder placement. Figures 6-15 and 6-16 show placement of the first girder. The polished areas indicate locations in which protrusions beyond the end bearing plates were removed by grinding. After both girders were placed, the bottom flanges joined utilizing a partial penetration weld. Figure 6-17 illustrates the alignment of the two girders prior to welding. Lincoln Steel Corp. was responsible for welding of the girders. Figure 6-18 illustrates the specimen after completion of the welding process. Although there was concern that heat from welding could cause damage to the elastomeric bearing pad, no detectable damage was observed after the specimen was welded, as shown in Figure 6-19.

Figure 6-14: Bearing Pad Placement

In this double cantilever system, the test specimen is unstable until composite action is acquired, thus, temporary supports were necessary at the outer ends of each cantilever during erection and casting of the specimen.

Figure 6-15: Placement of First Girder and Additional Grinding

Figure 6-16: Placement of First Girder on Bearing Pad

Figure 6-17: Girder Alignment Prior to Welding

Figure 6-18: Flange Weld After Completion

Figure 6-19: Bearing Pad After Welding

These temporary supports are shown in Figure 6-20. In addition, the hydraulic ram is used for positioning of the girder and allowing deflection for simulation of non-composite dead loads (casting of the deck). During construction, safety cables for attaching the stiffeners to the temporary supports were added.

Supports for the deck slab forms were supplied by Capital Contractors of Lincoln. These supports are similar to those used in the field. Form-work for the deck and diaphragm was added after the diaphragm reinforcing steel was placed, as shown in Figure 6-21. One-inch thick polystyrene was placed at the base of the diaphragm in order to prevent bonding between the pier and concrete diaphragm. Completed form-work for the deck and diaphragm is shown in Figures 6-22 and 6-23. It should be noted that not

Figure 6-20: Temporary Supports

all of the longitudinal reinforcing was in place at the time of the partial diaphragm pour in order to allow for the most efficient use of time and labor.

It was suggested by NDOR that a 3-in. transition be formed into the diaphragm deck interface to reduce the effects of stress concentrations associated with abrupt changes in the cross-section. Casting of the slab and diaphragm was to be completed in two stages. The first stage consisted of casting the diaphragm to half the total depth. The second stage consisted of the remainder of the diaphragm and deck slab. This is done to add stability to the specimen during deck casting and allowed the construction process to follow procedures used in field. Figure 6-24 and 6-25 show casting of the diaphragm to partial fill. The remainder of the diaphragm and deck was cast a day later. Figure 6-26 shows the casting of the deck. Capital Contractors provided the finishing expertise and some additional man-

power for the slab casting. The deck was then covered with burlap and plastic and moist cured, as shown in Figure 6-27. Also, the temperature and strains were monitored during the curing phase.

Figure 6-21: Diaphragm Reinforcing Layout

6.4 MATERIAL PROPERTIES

The laboratory test specimen was constructed using representative materials utilized in actual bridge construction. The deck slab and diaphragm were constructed with 47-BD concrete. The 28-day design compressive strength of 47-BD was 4500 psi. The pier concrete was designed to attain a 28-day compressive strength of 5000 psi. Only grade 60 reinforcing steel was used in the construction of the test specimen. The bridge girders were fabricated from W40 X 215 rolled I-girders conforming to ASTM A709-50W
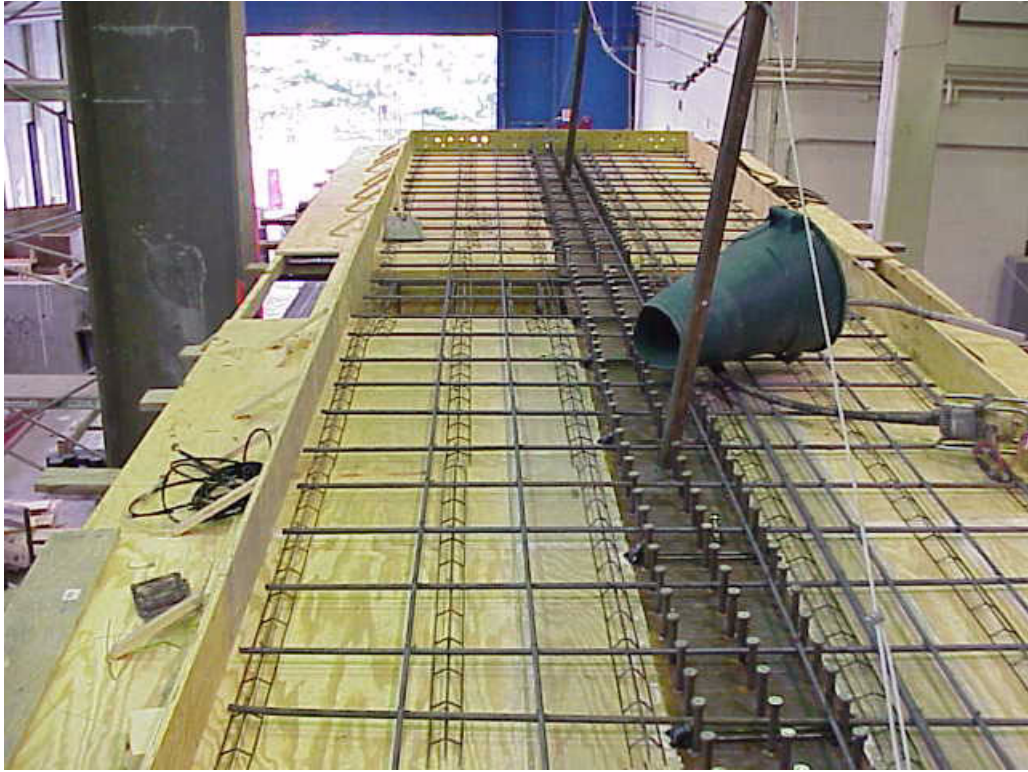
Figure 6-22: Completed Deck Forms

Figure 6-23: Completed Diaphragm Forming

Figure 6-24: Partial Casting of the Diaphragm

Figure 6-25: Completed Partial Diaphragm Casting

Figure 6-26: Casting of Deck Slab

Figure 6-27: Casting of Deck Slab (Completed)

specifications. In order to insure that the bridge components complied with the material specifications, several component tests were performed.

For the concrete materials, several 6-in. diameter by 12-in. long concrete cylinders were sampled during the casting of each component. Two concrete cylinders were tested from the deck and diaphragm components after curing for ten days. Similarly, four were tested after 28 days of curing. Two from both pours were tested at 49 days, this day coincided with the ultimate strength test. Results of the concrete compressive tests for the diaphragm concrete are shown in Figure 6-28. The 28-day compressive strength of the diaphragm concrete was 5190 psi. Similarly, the 28-day compressive strength of deck slab concrete was 4860 psi. Figure 6-29 shows the concrete compressive strength for the deck slab. The pier concrete compressive strength was tested after seven days only. The compressive strength at this time was approximately 4250 psi. Pier concrete material properties were not required for data reduction, therefore further compressive tests were not necessary.

For the steel reinforcing materials, three samples of each deck reinforcing bar size were submitted to IFR Engineering for mechanical testing. Each sample was tested as a full section according to ASTM A370 Specifications. Results of the tensile tests are shown in Table 6-1. The average reinforcing bar yield stress was approximately 65 ksi.

For the steel bridge girders, two samples were tested one from the girder web and the other from the tension flange. Both samples were taken from regions which were subjected to low flexural stresses during the testing sequence. Both of these samples were tested as full sections according to ASTM A370 Specifications. The average yield strength of the girder steel was determined to be 57 ksi. Figure 6-30 shows the results of the girder steel tensile tests. The stress/strain data is based on engineering strain.
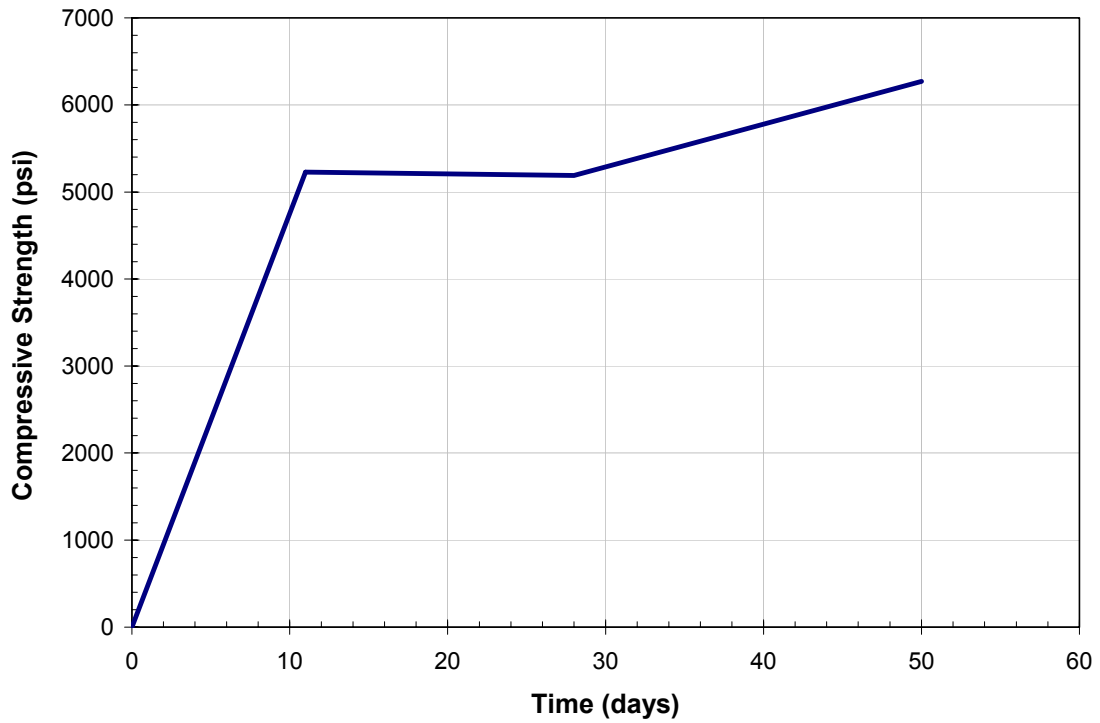
Figure 6-28: Diaphragm Concrete Compressive Strength
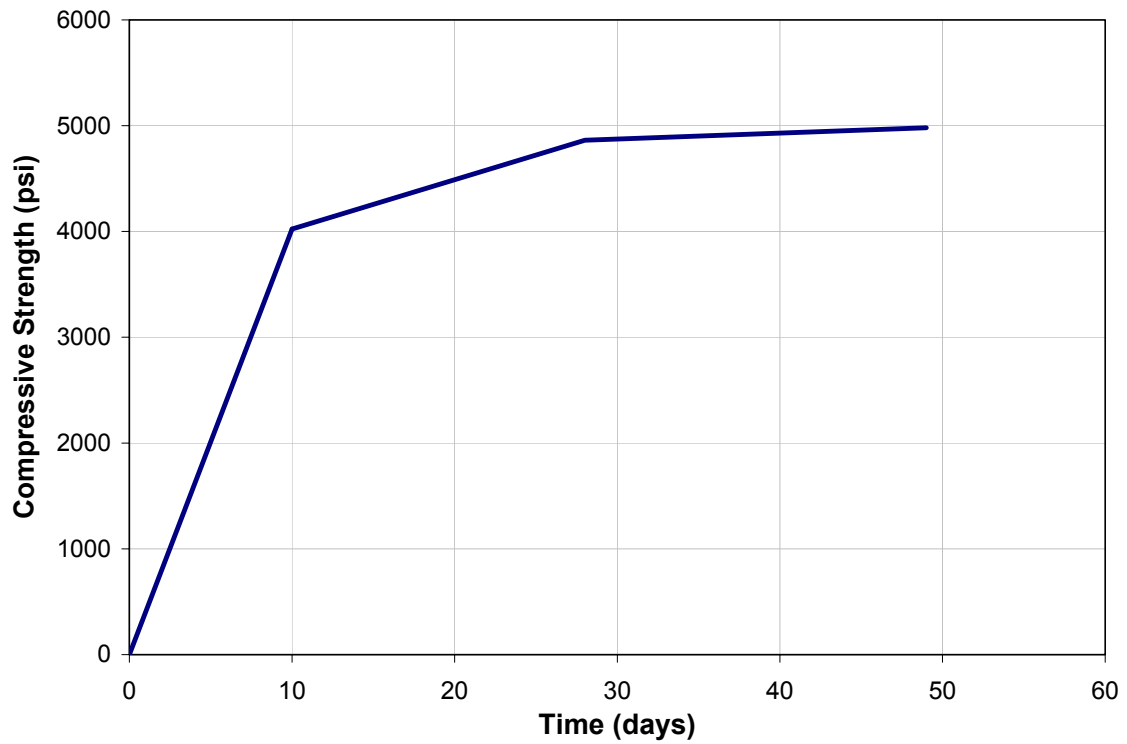
Figure 6-29: Deck Concrete Compressive Strength

Bar Size	Area (In²)	Yield Load (lb)	Yield Strength (psi)	Ultimate Load (lb)	Ultimate Strength (psi)	Elongation (% in 2")
4	0.2	12,500	62,500	20,184	101,000	15
4	0.2	13,000	65,000	20,124	101,000	18
4	0.2	13,000	65,000	20,281	101,000	20
5	0.31	19,800	63,900	31,320	101,000	15
5	0.31	19,500	62,900	31,351	101,000	20
5	0.31	20,100	64,800	31,316	101,000	18
7	0.6	41,800	69,700	60,780	101,000	15
7	0.6	41,200	68,700	60,441	101,000	16
7	0.6	39,800	66,300	60,083	101,000	15
8	0.79	52,160	66,030	82,803	104,810	15
8	0.79	51,040	64,610	83,291	105,430	15
8	0.79	52,000	65,820	83,868	106,160	15

Table 6-1: Tensile Test Results
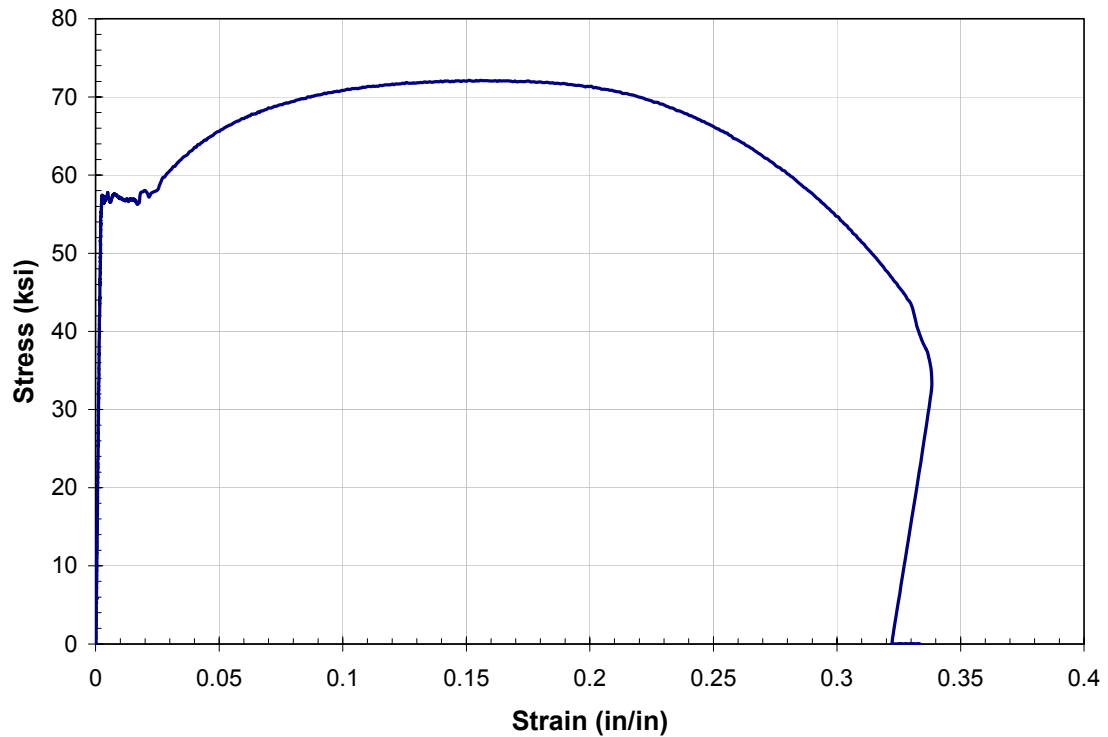
Figure 6-30: Girder Material Property Test Results
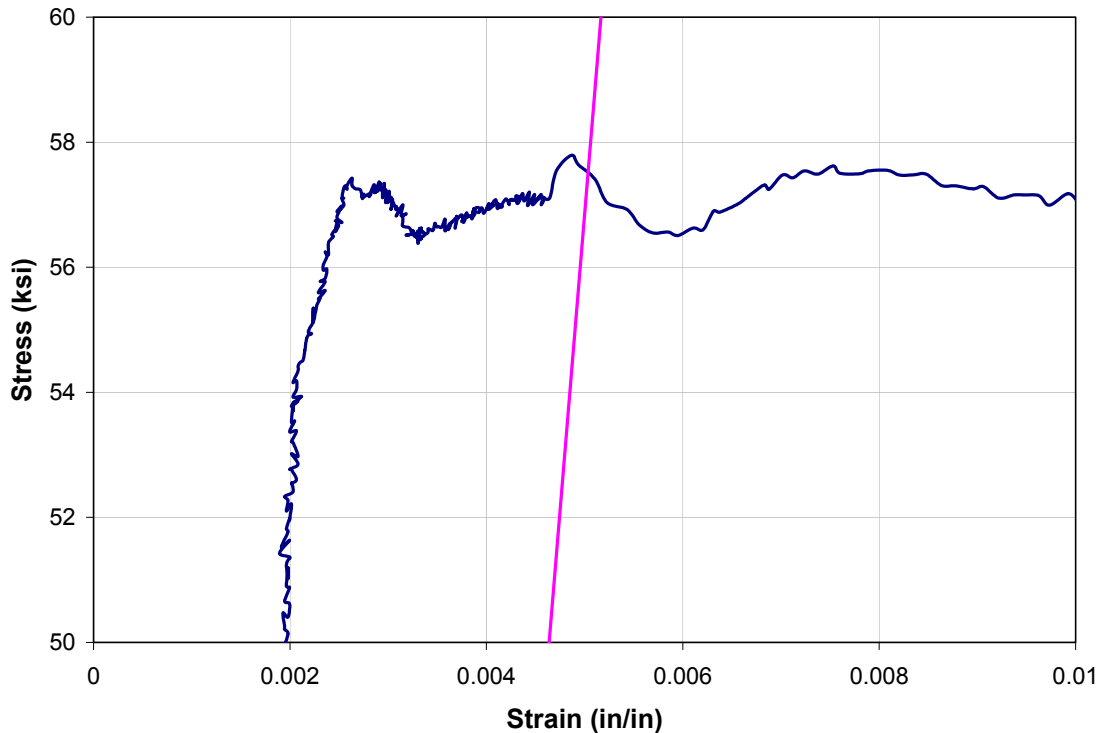
Figure 6-31: Girder Material Property Test Results (Detail at Yield)

6.5 SIMULATION OF DEAD LOADS

Wet concrete applied to simply supported girders causes a parabolic deflected shape and rotation of the girder ends. This rotation produces bending of the bottom flange at the center-line of the pier. In the cantilever model, the supports on the outer end of the beams were released slowly until the rotation at the girder ends matched those of the full-span girder. Hydraulic rams placed under each cantilever allowed for the control of beam deflection at various stages of construction. As mentioned previously, gages SG1 through SG14 were monitored during the rotation of the interior pier section. Four potentiometers were attached between the bearing surfaces of the girders. The upper-most pot was located at the centroid of the top flange with 10 in. separating each adjacent pot, as shown in Figures 6-32 and 6-33.
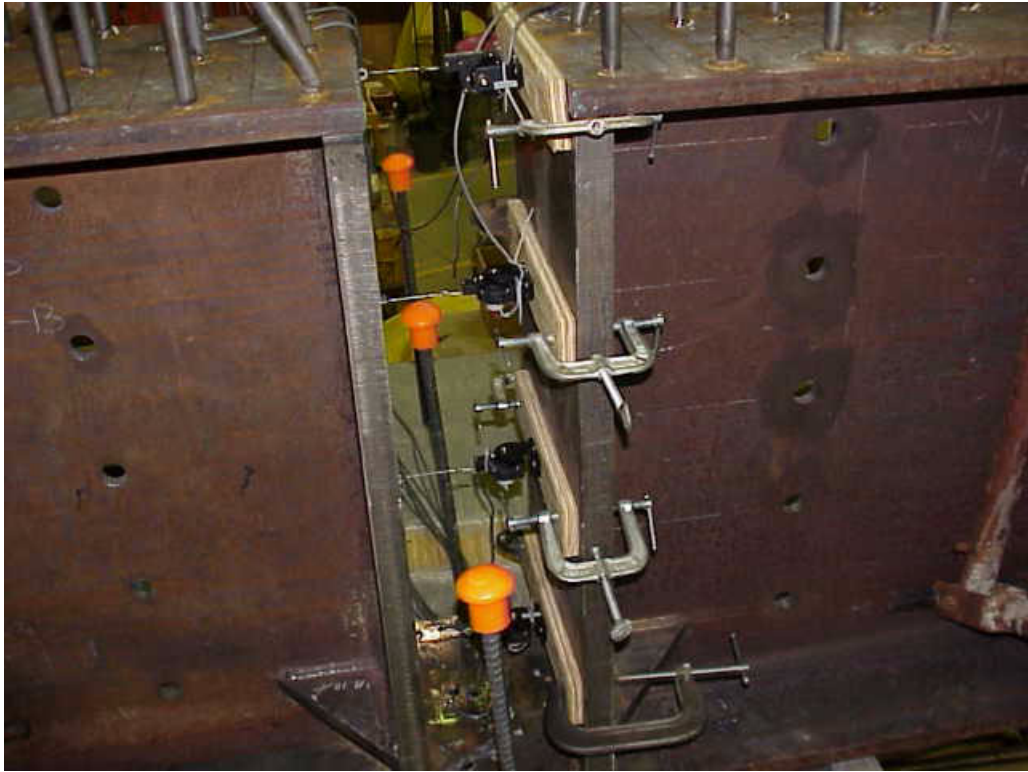
Figure 6-32: Dead Load Potentiometers
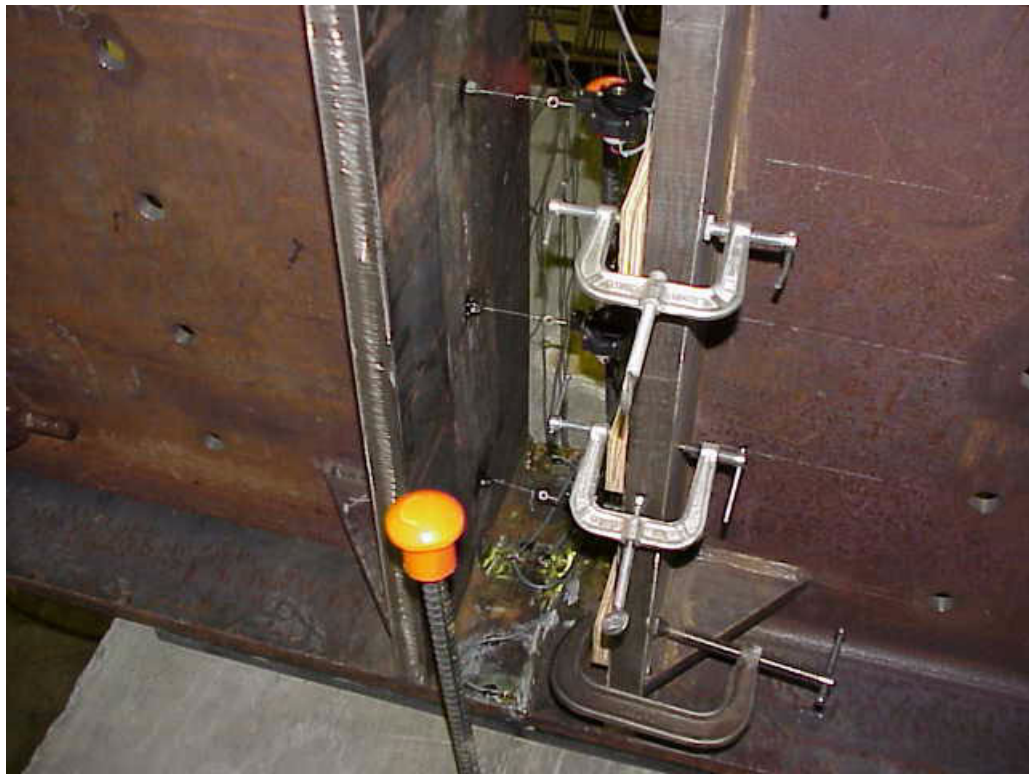
Figure 6-33: Dead Load Potentiometers (Alternate View)

6.6 FATIGUE (CYCLIC LOADING)

Fatigue shear and moment envelopes were generated with the design live load analysis. The loads generated correspond to a very high number of cycles. To conserve time, the number of cycles was reduced. The load required at the reduced number of cycles was based on the general S-N curve equation. The shape of a general S-N curve is defined by Equation 6-1.

$$(\Delta F)_N = \left| \frac{A}{N} \right|^{\frac{1}{3}} \geq \frac{1}{2}(\Delta F)_{TH} \qquad (6\text{-}1)$$

Where

$(\Delta F)_N$ = nominal fatigue resistance (ksi)

A = constant based on the fatigue category

n = number of stress range cycles per truck passage

$(\Delta F)_{TH}$ = fatigue threshold value based on fatigue category

N = $(365)(75)n(ADTT)_{SL}$

$(ADTT)_{SL}$ = single lane average daily truck traffic

For any given detail, $(\Delta F)_N$ can be related to the fatigue moment by multiplying both sides of Equation 6-1 by the section modulus, S results in Equation 6-2. Here S depends on the location of the detail.

$$S(\Delta F)_N = S \left| \frac{A}{N} \right|^{\frac{1}{3}} \qquad (6\text{-}2)$$

$$M = S \left| \frac{A}{N} \right|^{\frac{1}{3}} \qquad (6\text{-}3)$$

For the same detail subjected to different moments, Equation 6-3 takes the following form. Moment M_1 corresponds to a number of cycles N_1 as shown in Equation 6-4. A similar expression for moment M_2 and N_2 is shown in Equation 6-5 shown below.

$$M_1 = S \left| \frac{A}{N_1} \right|^{\frac{1}{3}}$$

(6-4)

$$M_2 = S \left| \frac{A}{N_2} \right|^{\frac{1}{3}}$$

(6-5)

Dividing Equation 6-4 by Equation 6-5 yields the following result. The S terms cancel out and Equation 6-6 remains. Simplifying the expression, the constant A drops out as well, leaving Equation 6-7. Since the number of cycles will always be positive, the absolute value can be omitted.

$$\frac{M_1}{M_2} = \left(\frac{S \left| A/N_1 \right|}{S \left| A/N_2 \right|} \right)^{\frac{1}{3}}$$

(6-6)

$$\frac{M_1}{M_2} = \left(\frac{N_2}{N_1} \right)^{\frac{1}{3}}$$

(6-7)

From analysis the governing fatigue moment was found to be 352 kip·ft. With M_1 and N_1 known and requiring that N_2 = 2,000,000 cycles,

Equation 6-7 was used to solve for M_2. Substituting M_1, N_1, and N_2 into Equation 6-7 results in the following relationship.

$$\frac{352}{M_2} = \left(\frac{2,000,000}{135,000,000} \right)^{\frac{1}{3}} \tag{6-8}$$

Solving Equation 6-8 for M_2 = 1433 kip·ft or an applied load P of 102 kips, located at 14 ft from the specimen centerline. In a bridge of two equal spans, at no time will the bottom flange experience tension. In order to insure this trend and that the target load would be reached, the cyclic load range was shifted from 0 to 102 kips to 2 to 106 kips.

The cyclic loading portion of the testing sequence began on July 28, 2000. The cyclic load was applied using 220-kip MTS actuators, as shown in Figures 6-34 and 6-35. Displacement control was used throughout the course of the fatigue investigation. The specimen was loaded slowly to peak load, and the cracks in the deck slab were mapped. The displacement needed to achieve the target peak load was approximately 0.31in., as determined from the finite element analysis. The experimental displacement required to attain the 106 kip load was 0.3083 in. The maximum displacement was adjusted at approximately 7400 cycles from 0.3083 in. to 0.3115 in. This adjustment was made because the maximum displacement was not producing the 106-kip load. This was the only adjustment to the displacement that was required in the 2,000,000 cycles of loading. The cyclic loading was continuous except for short pauses for vibrating wire gage readings, to be taken once every 24 hours. Cracking of the deck slab was mapped at 1 million cycles, 1.5 million, and 2 million cycles. Fatigue loading was completed on August 8, at which time the loading system was altered for the ultimate strength test.

Figure 6-34: Fatigue Loading System

Figure 6-35: Fatigue Loading System (Alternate View)

6.7 ULTIMATE STRENGTH TESTING

For the ultimate strength test, load was increased slowly in 10 to 25-kip increments. At the end of each load stage, both the load data and electrical instrument data was collected. The time required to collect data from the vibrating wire gages was approximately 30 minutes. In order to conserve time, data from the vibrating wire instruments was collected after every other load step.

The loading system was changed for the ultimate strength test. The MTS equipment was replaced with four 300-kip actuators. Two actuators were placed at each end of the cantilever specimen. The point of load application was moved toward the center-line, reducing the moment arm from 14 ft to 12 ft in length to accomodate the geometry of the laboratories strong floor. The loading system is shown in Figures 6-37 and 6-36.

Figure 6-36: Ultimate Capacity Loading System (Side View)

Figure 6-37: Ultimate Capacity Loading System (End View)

The instrumentation used for the ultimate capacity test was the same as that used in previous tests except for those which were contained within the MTS system. Loading for the ultimate capacity test took place on Friday, August 18, 2000.

7

Test Results

The test sequence was developed to model the actual structure in the field. The first load stage was completed while the specimen was under construction. After the deck had cured 28-days, the remaining testing sequence commenced. This chapter outlines the experimental observations and data at various stages in the investigation.

7.1 SPECIMEN BEHAVIOR

As discussed in Chapter 6, the experimental investigation consisted of three distinct load stages. Non-composite dead loads, cyclic (fatigue) loading, and ultimate strength loading.

7.1.1 NON-COMPOSITE LOADING

Simulation of non-composite dead loads was produced by the initiation of vertical displacement at the temporary support locations. The displace-

ments at the temporary support locations have been converted to rotation from data collected from the potentiometers. The displacement was initiated in stages, with data sets collected at each stage of displacement. Figure 7-1 shows the girder end separation relative to support displacement for the 4 potentiometers. A graphical representation of the girder end rotation over the support displacement interval is shown in Figure 7-2. The gap between the end bearing plates (also top flanges and webs) was set to insure that the continuous bottom flange would not reach yield when subject to the theoretical rotation. The purpose of this load stage was to monitor and record stresses generated in the flange due to the application of non-composite dead loads. Gages SG1, SG2, and SG5 were located adjacent to the flange weld at the centerline of the girders. Gage SG1 was monitored manually as the support displacement was applied. Figure 7-3 contains a plot of stress-rotation data collected from gages SG2 and SG5. The maximum stress at the outer-most fiber reached 47 ksi, or approximately 80% of the yield stress. Figure 7-4 shows the stress distribution across the thickness of the flange near the specimen center-line from gages SG8, SG9, and SG12. Figure 7-5 contains a plot of stress vs. rotation data at the girder center-line for gages SG2, 3, and 4. As expected, the highest stresses remain below yield and occur at the specimen centerline.
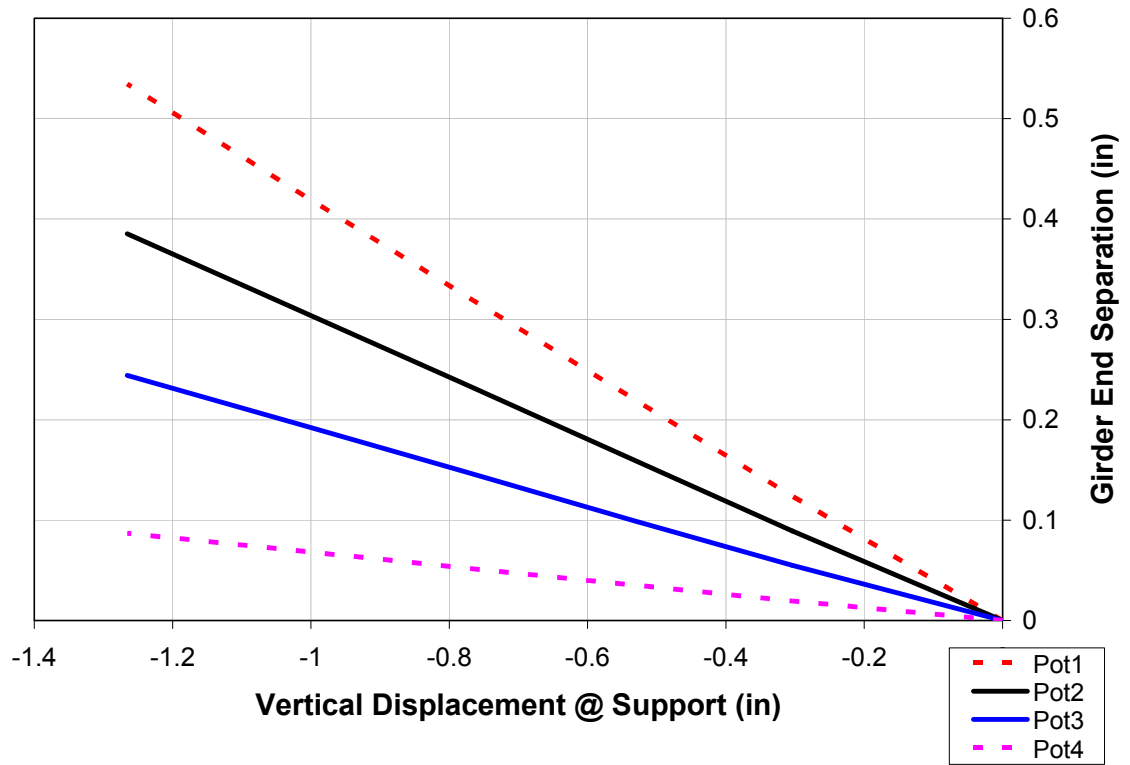
Figure 7-1: Girder End Separation Under Simulated Dead Loads
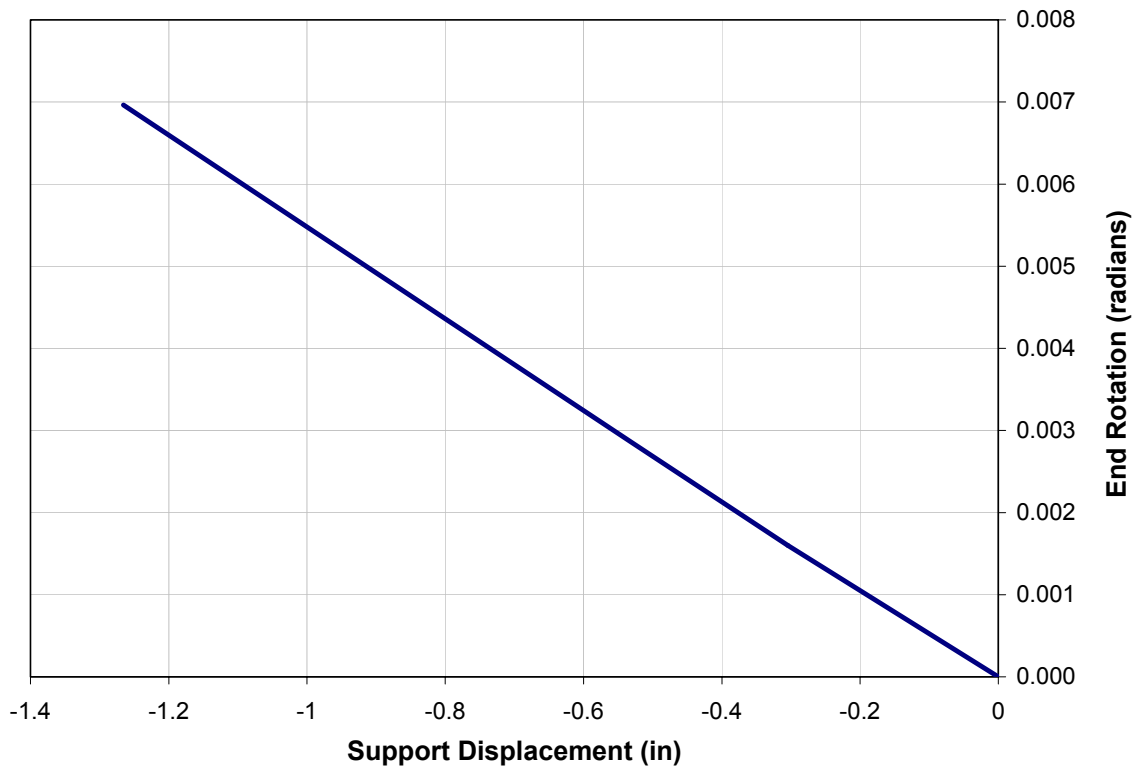
Figure 7-2: Girder Rotation Under Simulated Dead Loads
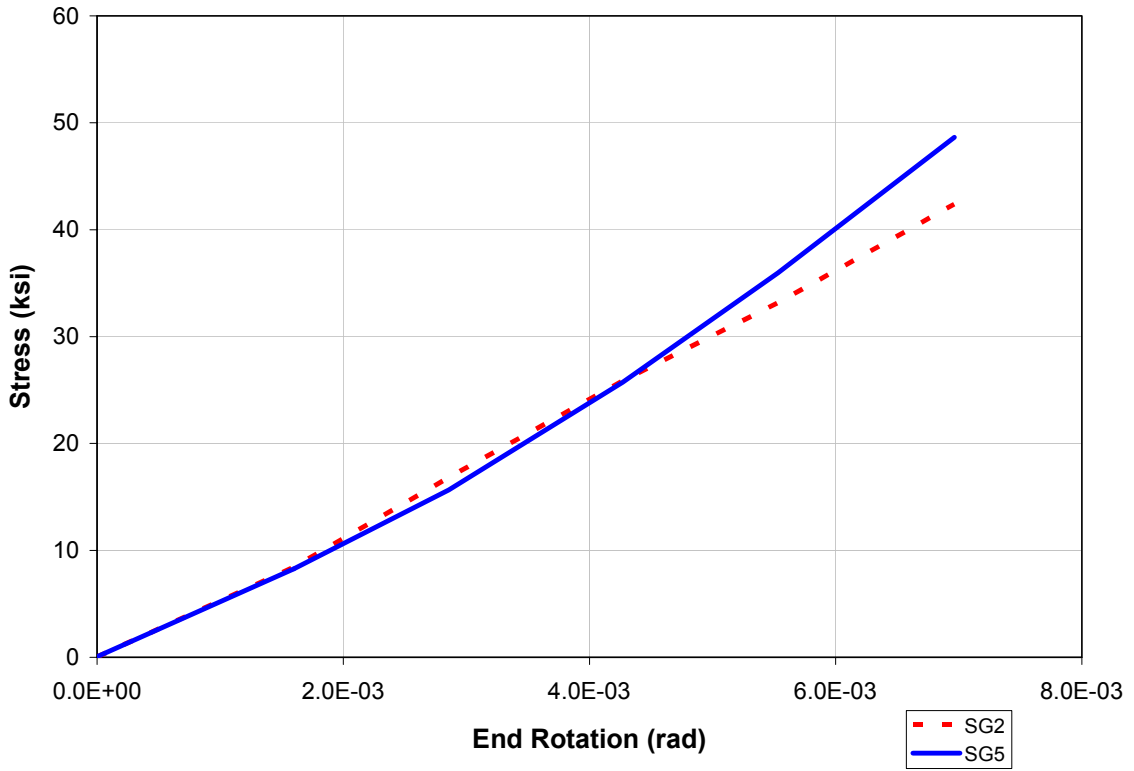
Figure 7-3: Stress Rotation Relationship for SG2 and SG5
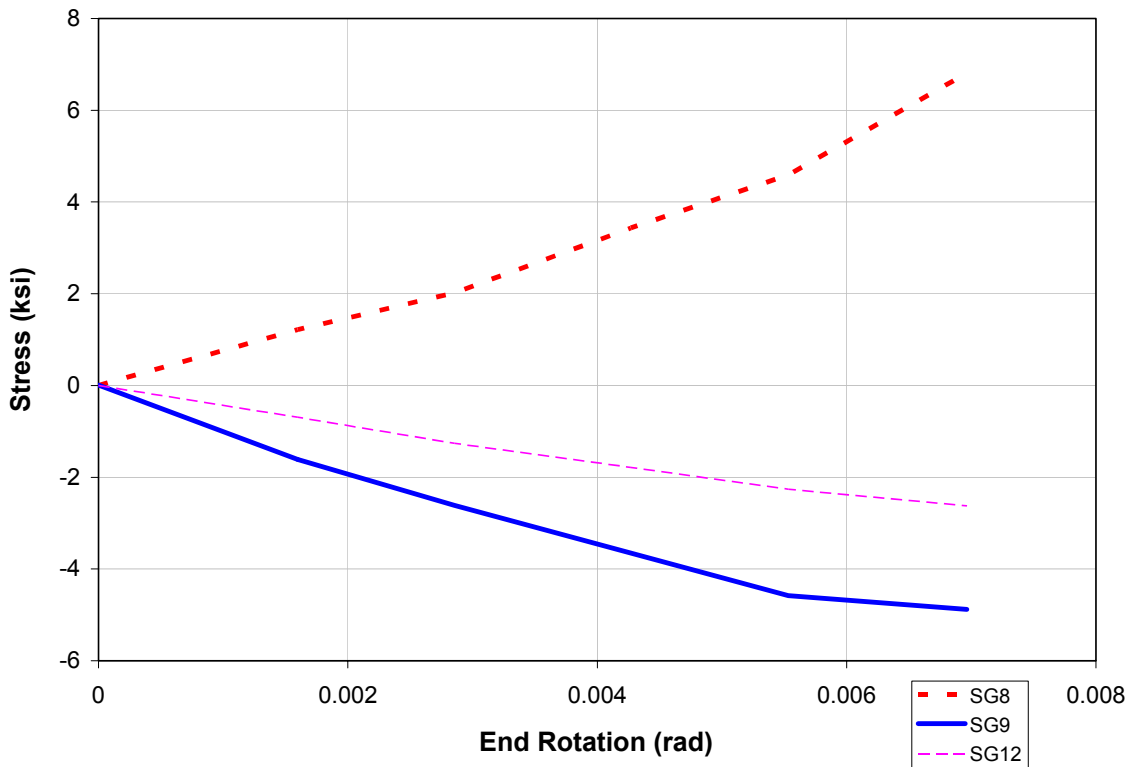
Figure 7-4: Stress Rotation Relationship for SG8, SG9, and SG12
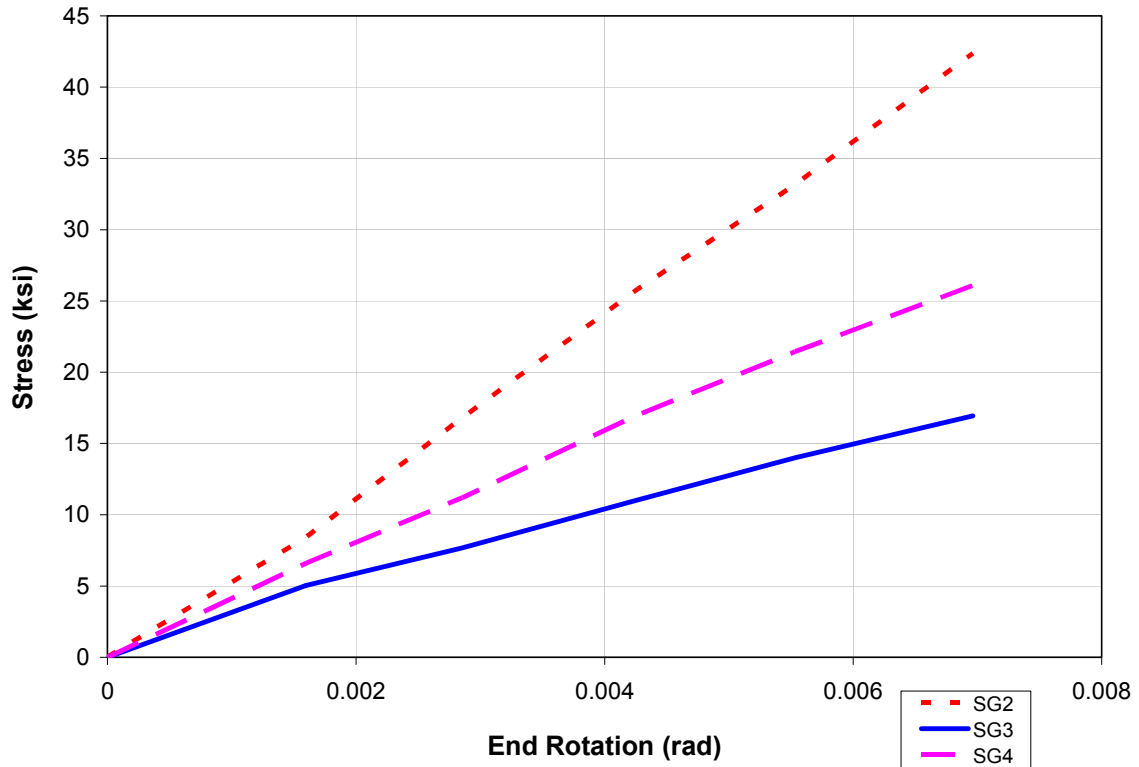
Figure 7-5: Stress Rotation Relationship for SG2, SG3, and SG4

7.1.2 FATIGUE LOAD PHASE

The amplitude and frequency of cyclic loading was outlined in Chapter 6. The initial ramp to 106 kips was applied incrementally with pauses for the collection of data sets. A plot of the load-deflection curve is shown in Figure 7-6. The breaks in the plot are at the pauses for data collection, where deflection was held constant and the load relaxed through force redistribution in the deck reinforcement.

Several gages attached to the surface of the concrete deck slab were lost due to the concrete cracking. The cracks on the surface of the deck slab were documented prior to application of fatigue cycles. Figures 7-7 and 7-8 show mapping of the cracks at 106 kips load. In the foreground of Figure 7-8, some of the cracks are visible. For location reference, the instrumentation is located directly above the diaphragm. Figure 7-9 contains a crack map at maximum load prior to any cycling. The majority of cracking occurred near the edge of the diaphragm. At this location there is an abrupt
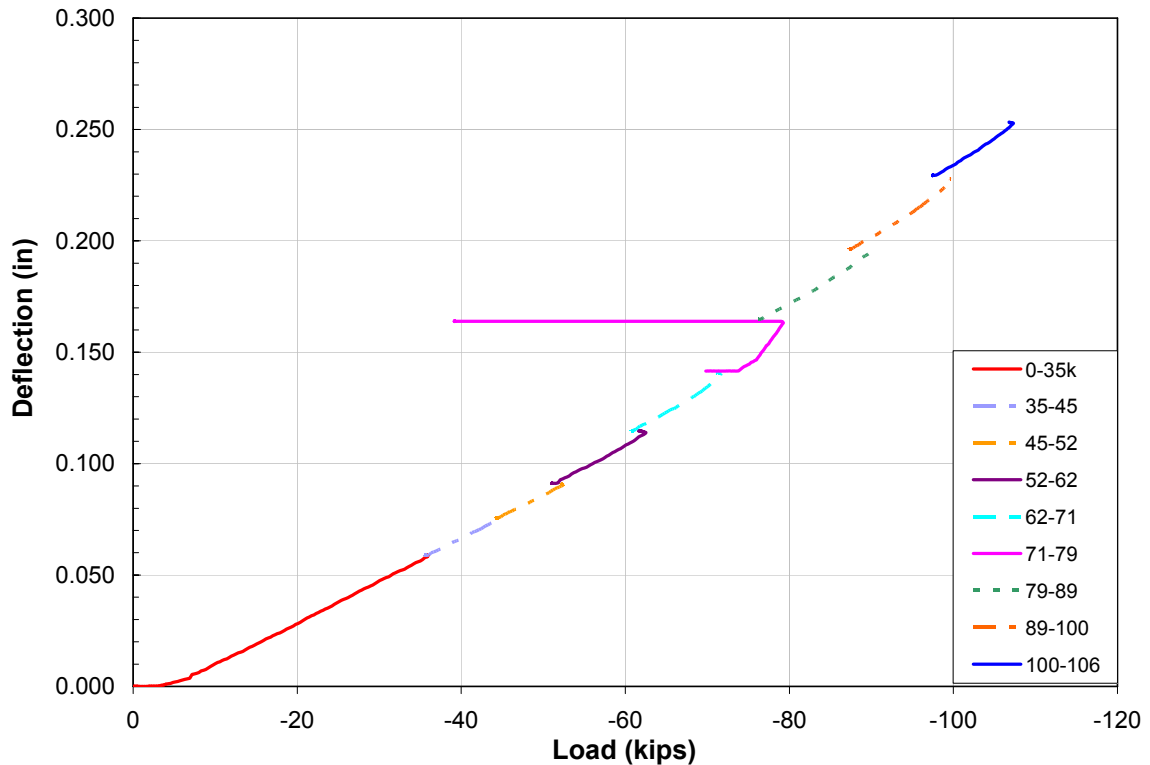
Figure 7-6: Fatigue Test Load Defection

change in rigidity. Mapping of deck cracking was done at 1 million, 1.5 million and 2 million cycles of load. Figures 7-10 and 7-11 contain crack maps at 1 million cycles. Figure 7-10 contains crack width data for the initial cracks from Figure 7-9. Figure 7-11 shows crack width information for additional cracks formed during the first 1 million cycles of load. From these maps, the largest crack widths occurred at the diaphragm edge, near the edge of the slab. Additional cracks had formed further out from the diaphragm center-line. Crack maps for 1.5 million loading cycles are shown in Figures 7-12 and 7-13. A comparison of the crack widths from 1.5 million to 1 million load cycles shows that there was virtually no change in crack widths over this interval. Likewise, Figures 7-14 and 7-15 contain crack maps at 2 million cycles of load. Comparing these results to previous crack maps resulted in little recognizable change. There were a few additional short cracks propagating inward from the edge of the deck, but the measured widths of existing cracks were unchanged.

Figure 7-7: Deck Crack Mapping

Figure 7-8: Mapping of Initial Cracks
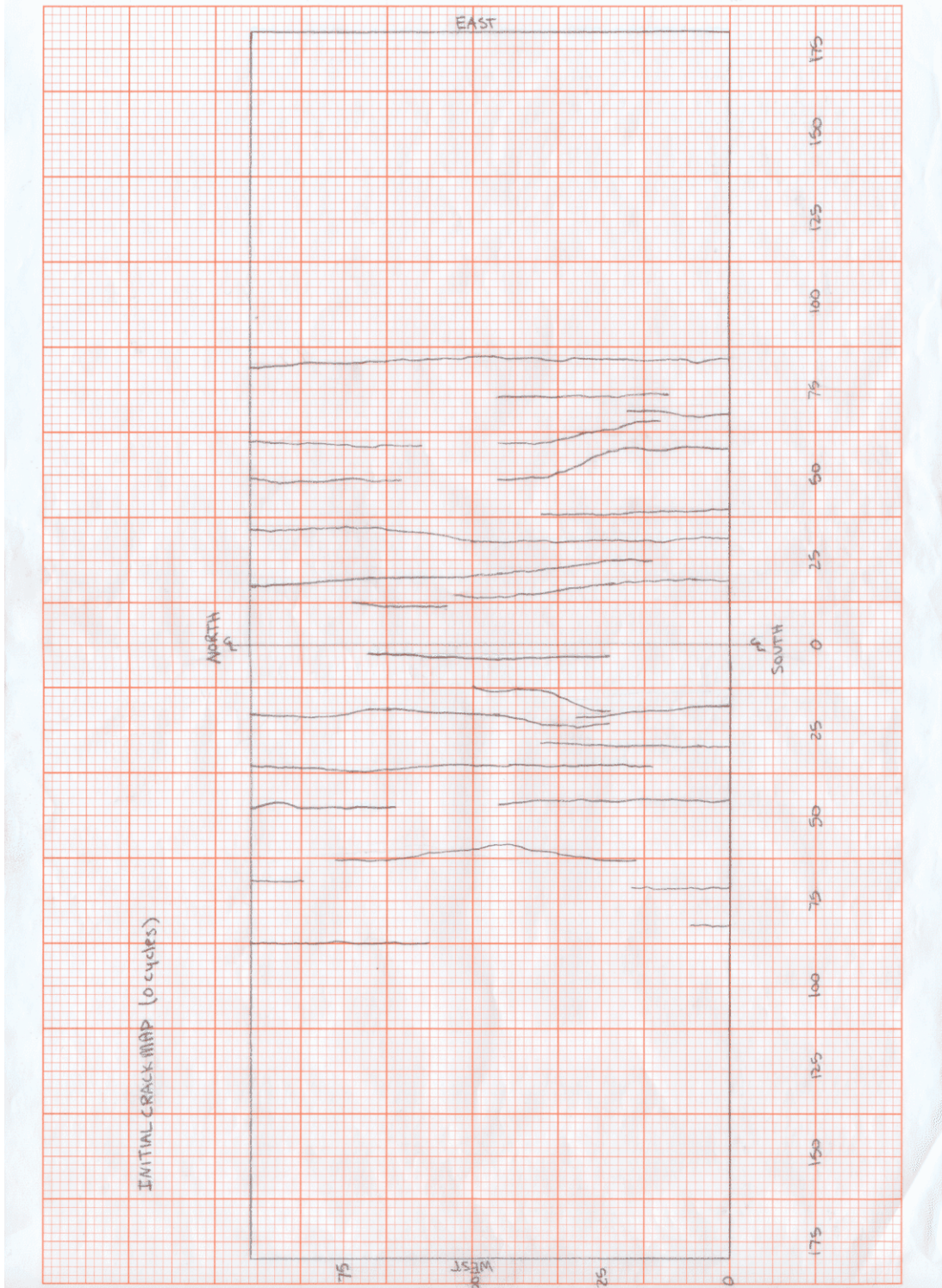
Figure 7-9: Initial Crack Map for 0 Cycles
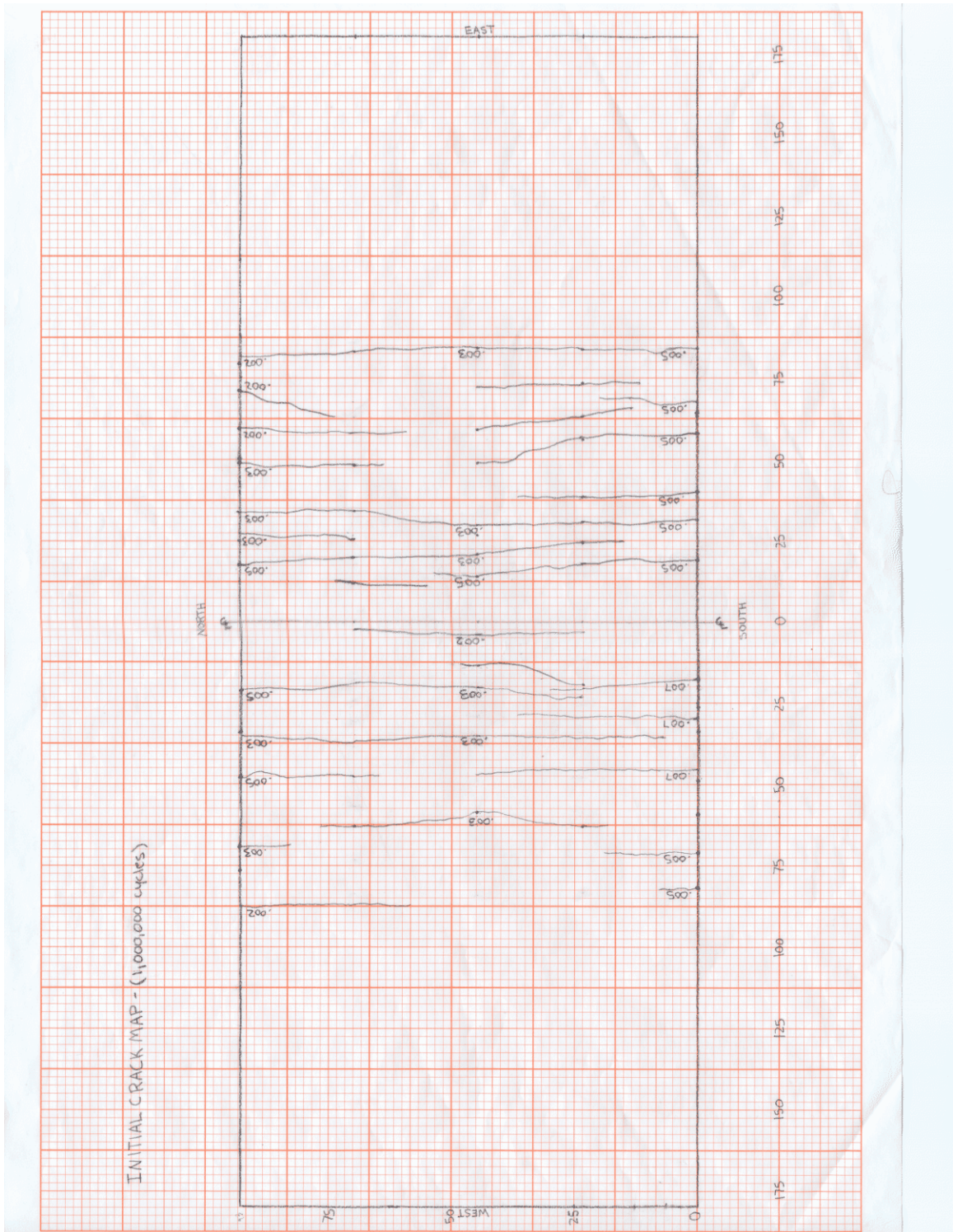
Figure 7-10: Map of Initial Cracks After 1 Million Cycles.
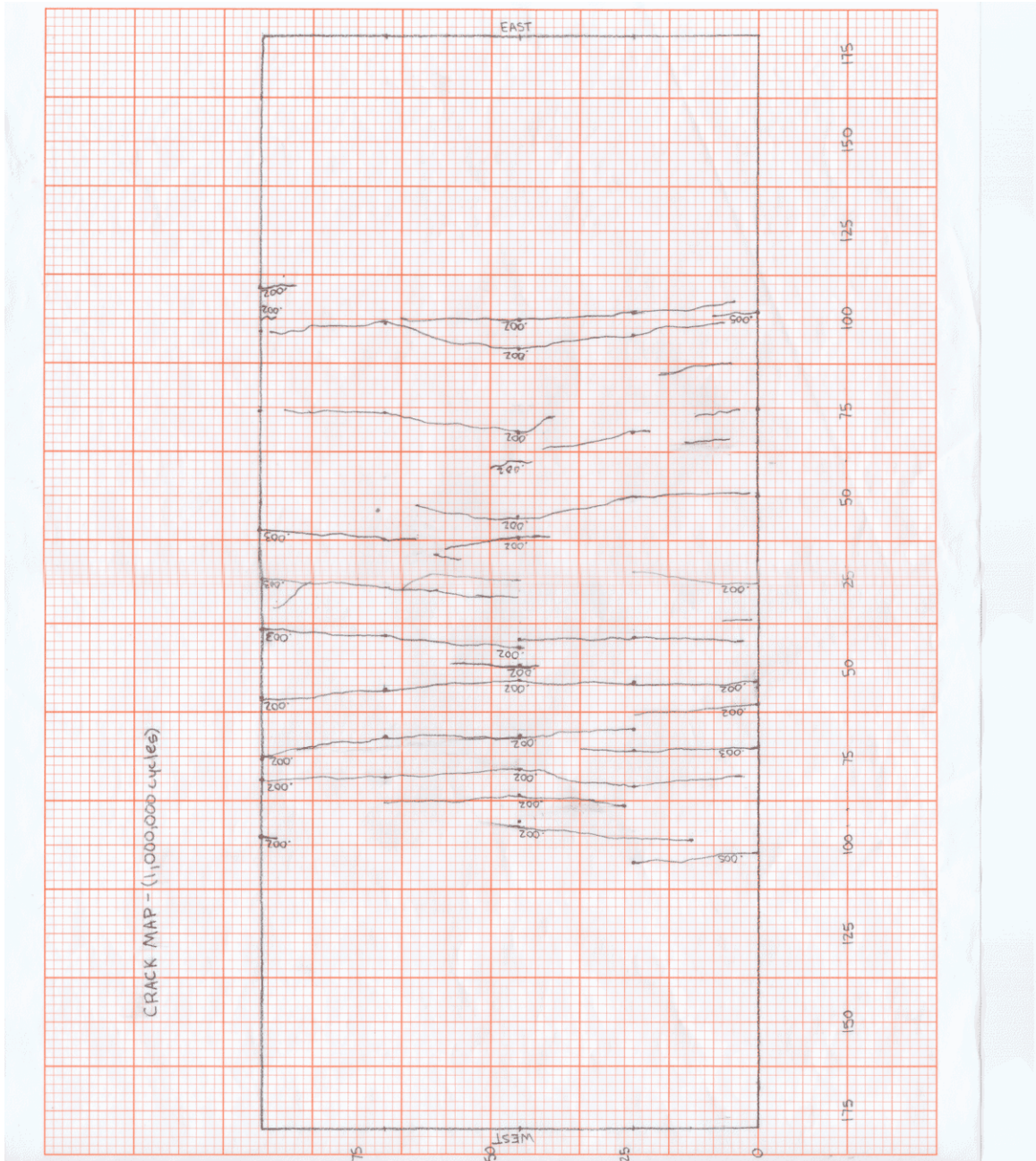
Figure 7-11: Map of Additional Cracks After 1 Million Cycles
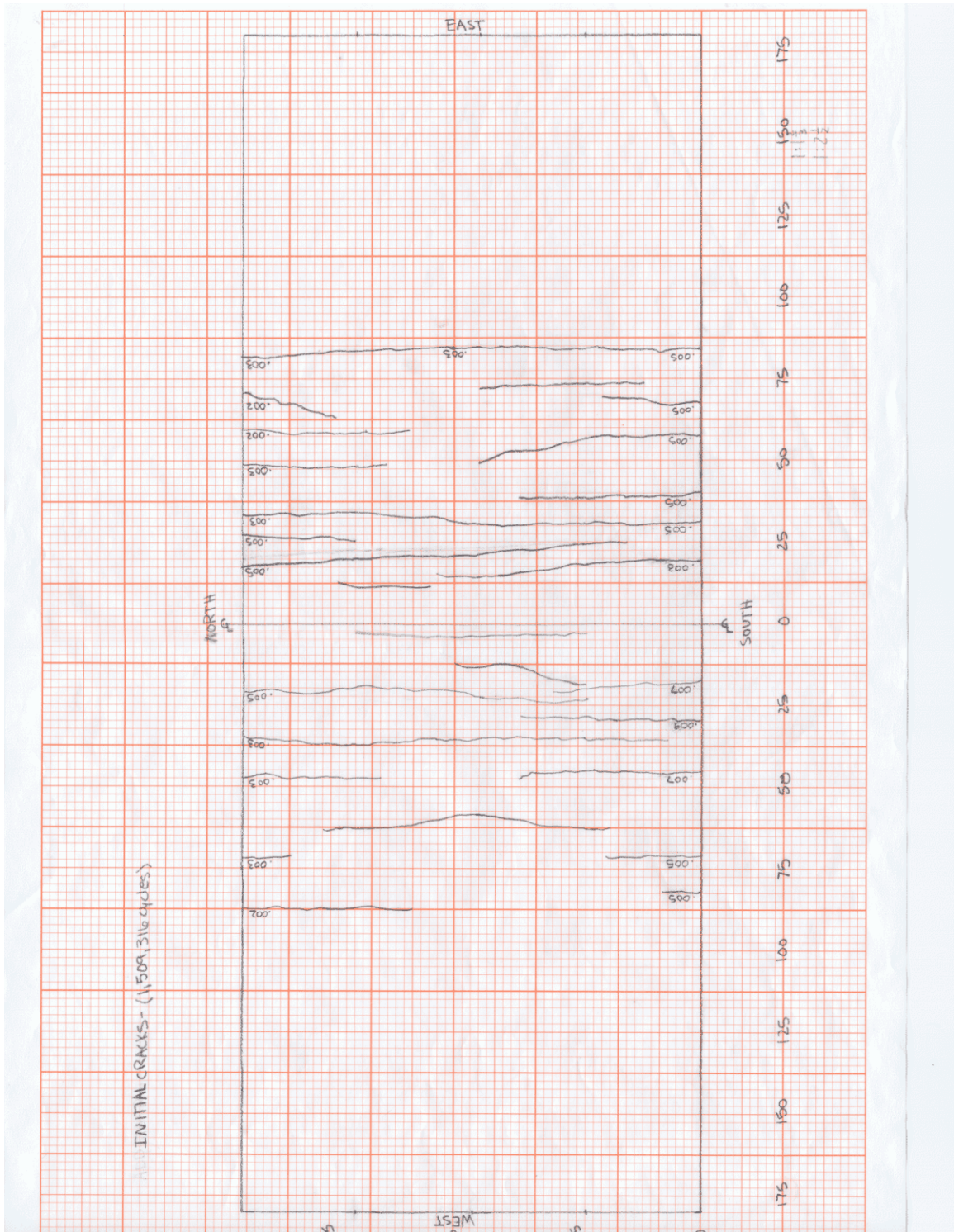
Figure 7-12: Map of Initial Cracks After 1.5 Million Cycles
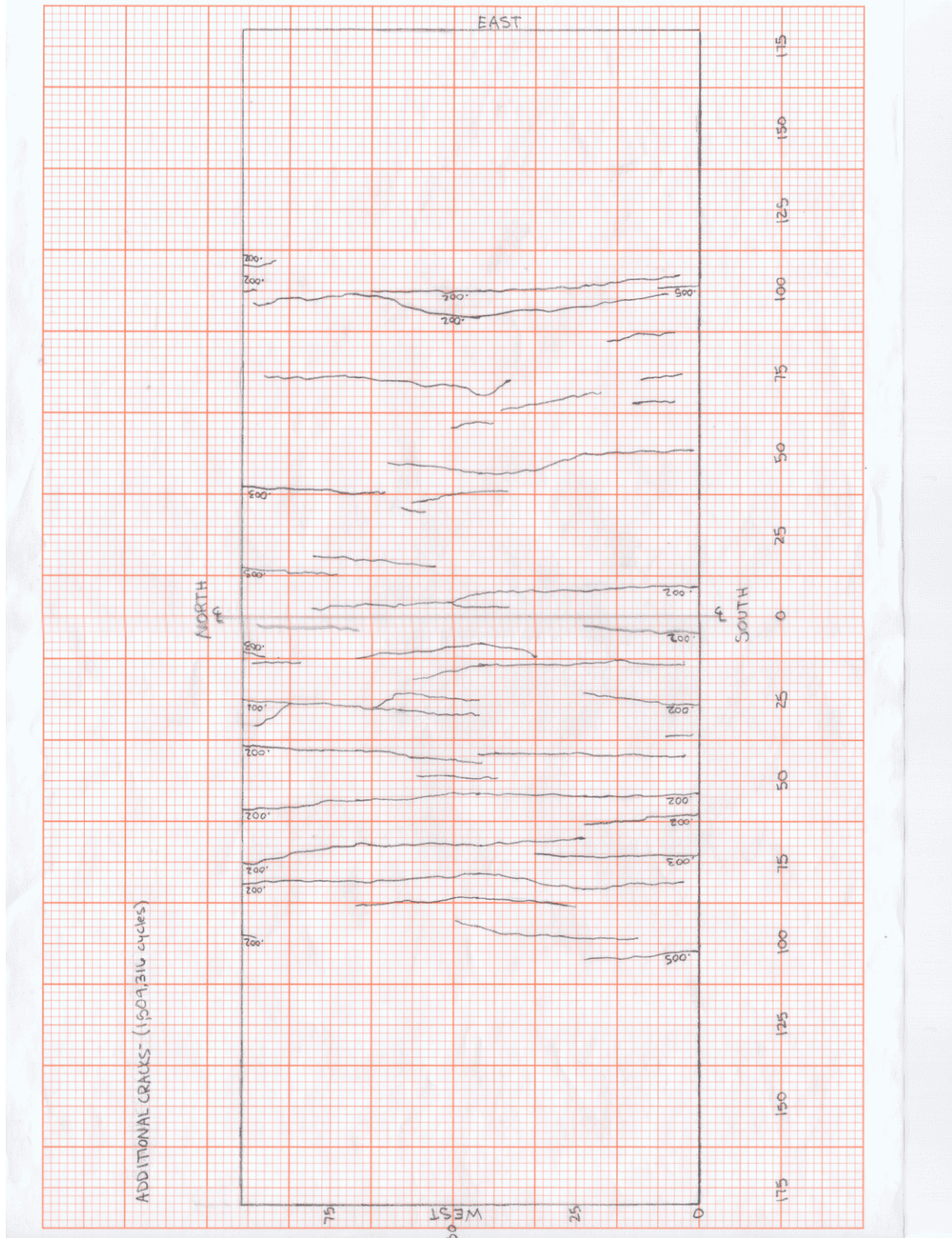
Figure 7-13: Map of Additional Cracks After 1.5 Million Cycles
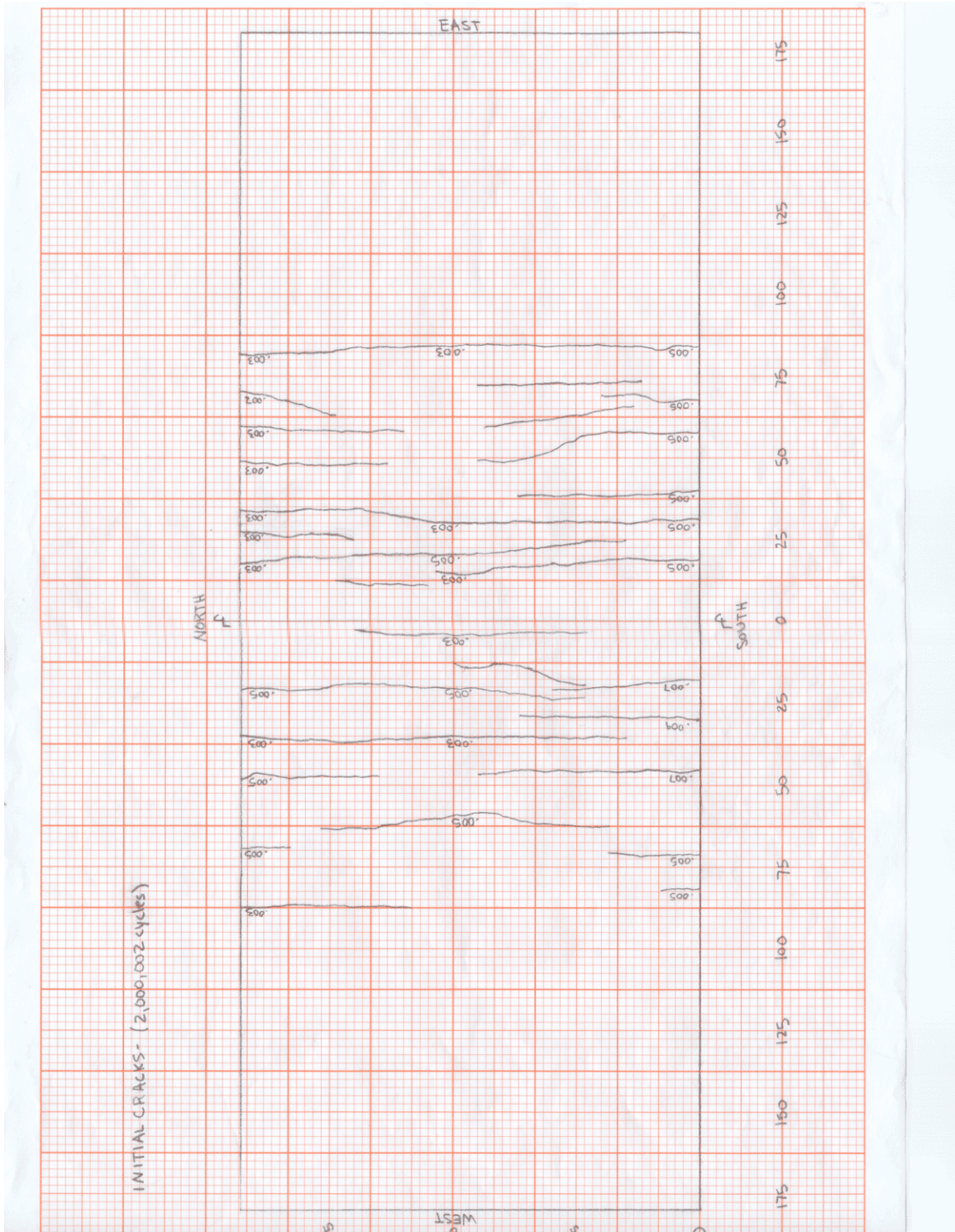
Figure 7-14: Map of Initial Cracks After 2 Million Cycles
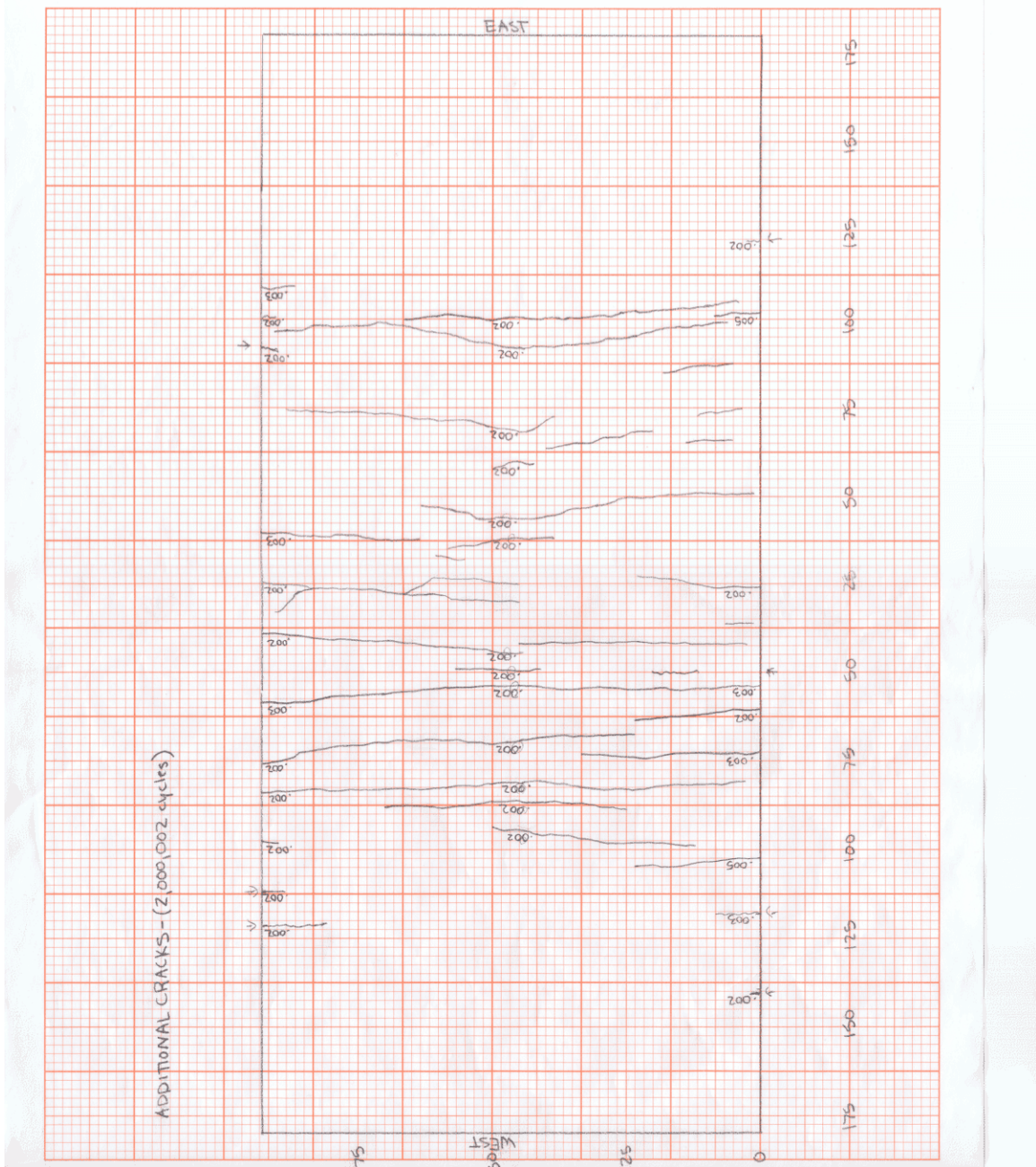
Figure 7-15: Map of Additional Cracks After 2 Million Cycles

During the fatigue portion of the experimental investigation, data sets were collected once daily. The loading frequency was set at 2 cycles per second, which resulted in data sets being collected at every 172,800 cycles of load. The daily sets were collected at peak static load, minimum static load, and continuously over an interval of 5 cycles at a loading rate of ½-cycle per second. Load-deflection plots for the specimen during the fatigue test are shown in Figures 7-16 and 7-17. These plots were generated from data collected during the 5 cycles of loading. The first plot contains loops at 0, 1, and 2 million cycles, in which little change in specimen stiffness is observed over the complete interval. The second plot contains loops at all cycle values where data was collected. The specimen did experience some reduction in stiffness. At approximately 7400 cycles, the maximum displacement was increased from 0.3083 to 0.3115 in. Referring again to Figure 7-16, the increase in displacement and the loss of specimen stiffness are evident between 0 and 1 million cycles. The initial load deflection plot has a greater slope than similar data at subsequent loading cycles. Likewise, there is virtually no change in specimen response throughout the remaining fatigue cycles

The embedment gage locations were specified as to provide a means for generating strain profiles across the depth of the diaphragm, these locations were labeled as Sections 1 through Section 6 (Figure 6-9 contains section locations). Figure 7-18 contains the strain distribution plot for Section 2. Similarly, Figures 7-19 and 7-20 contain information for Sections 3 and 4, respectively. In each of these plots, the strain distributions exhibited only slight variations over the 2 million cycle interval. A similar plot is shown in Figure 7-21, across the bottom of the diaphragm. Like the previous results have shown, some redistribution of stress occurred initially and virtually none throughout the remaining 2 million cycles.
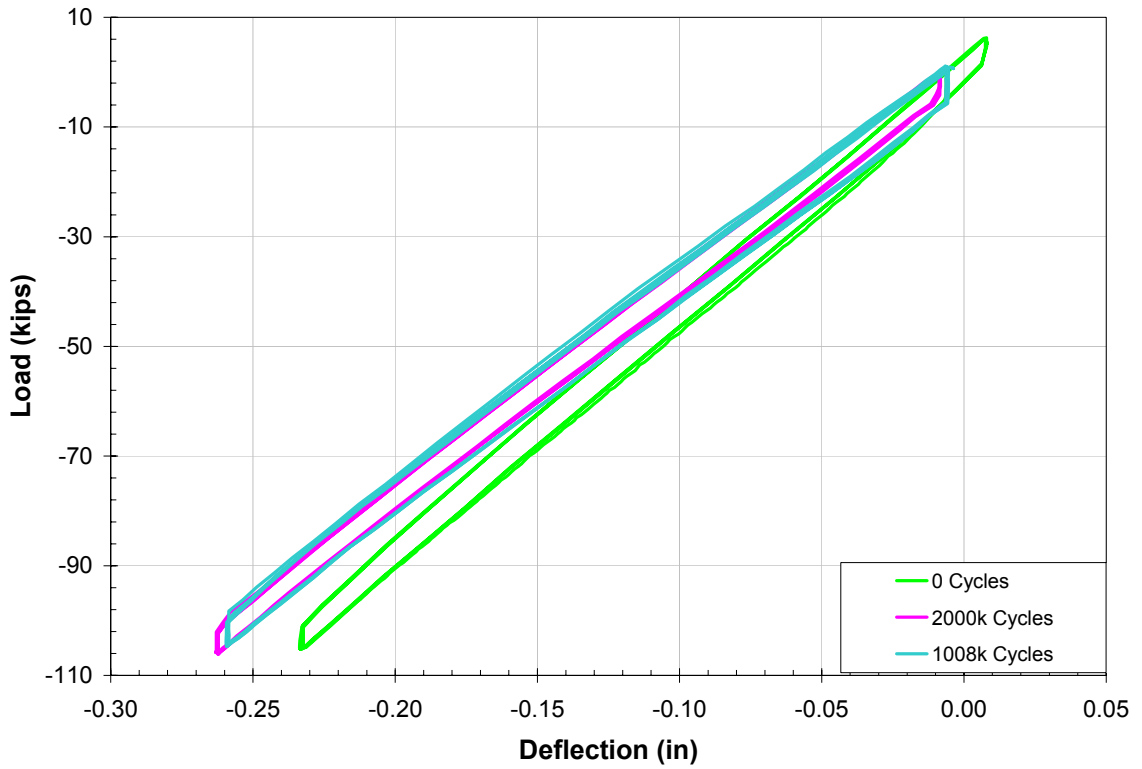
Figure 7-16: Cyclic Load Deflection Comparison
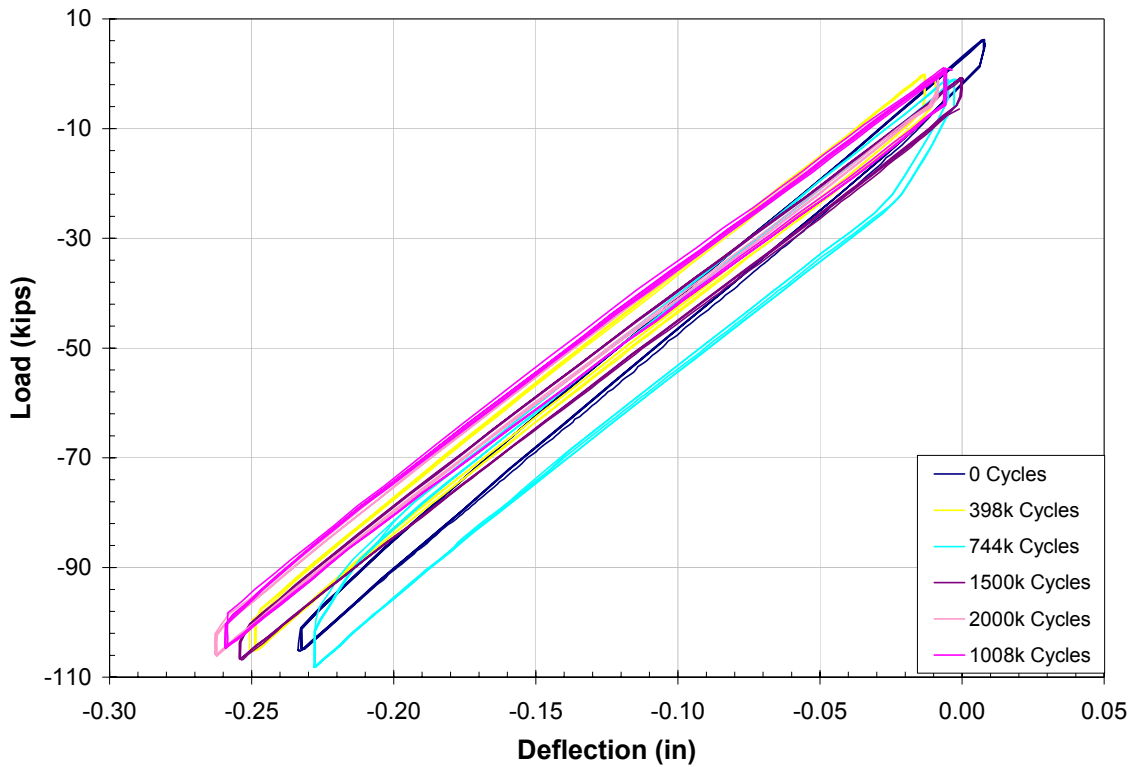
Figure 7-17: Cyclic Load Deflection Comparison
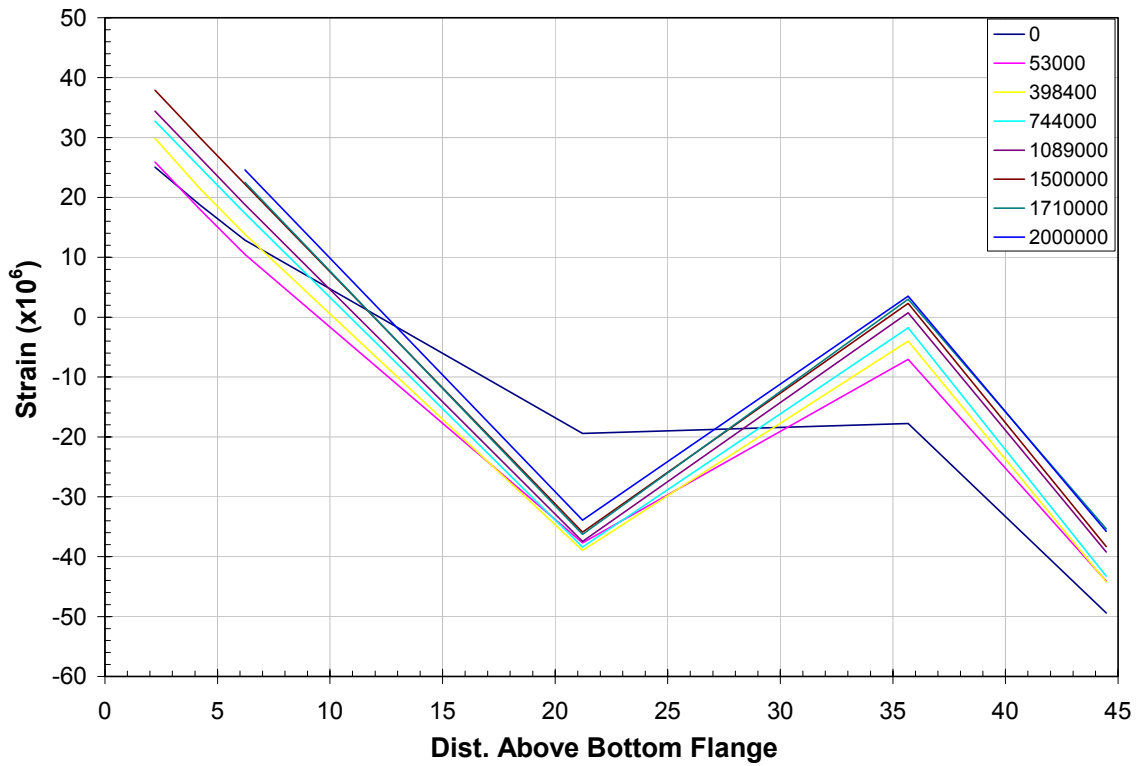
Figure 7-18: Strain Profile at Location 2
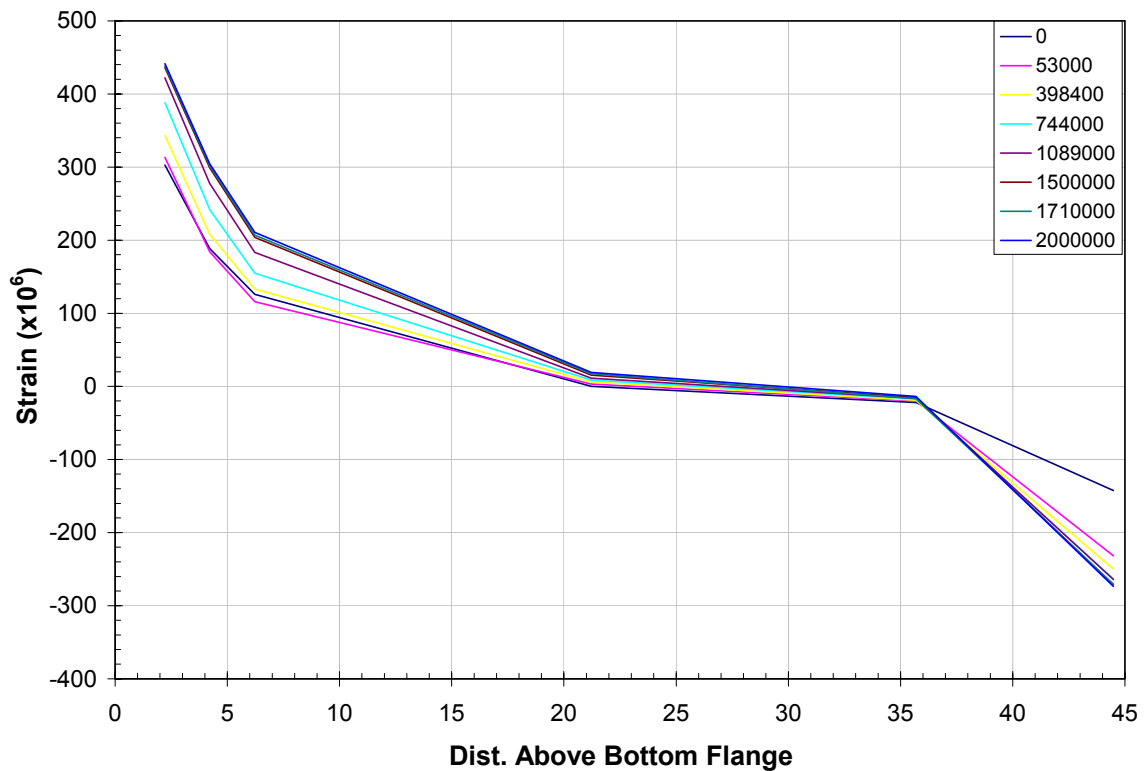
Figure 7-19: Strain Profile at Location 3
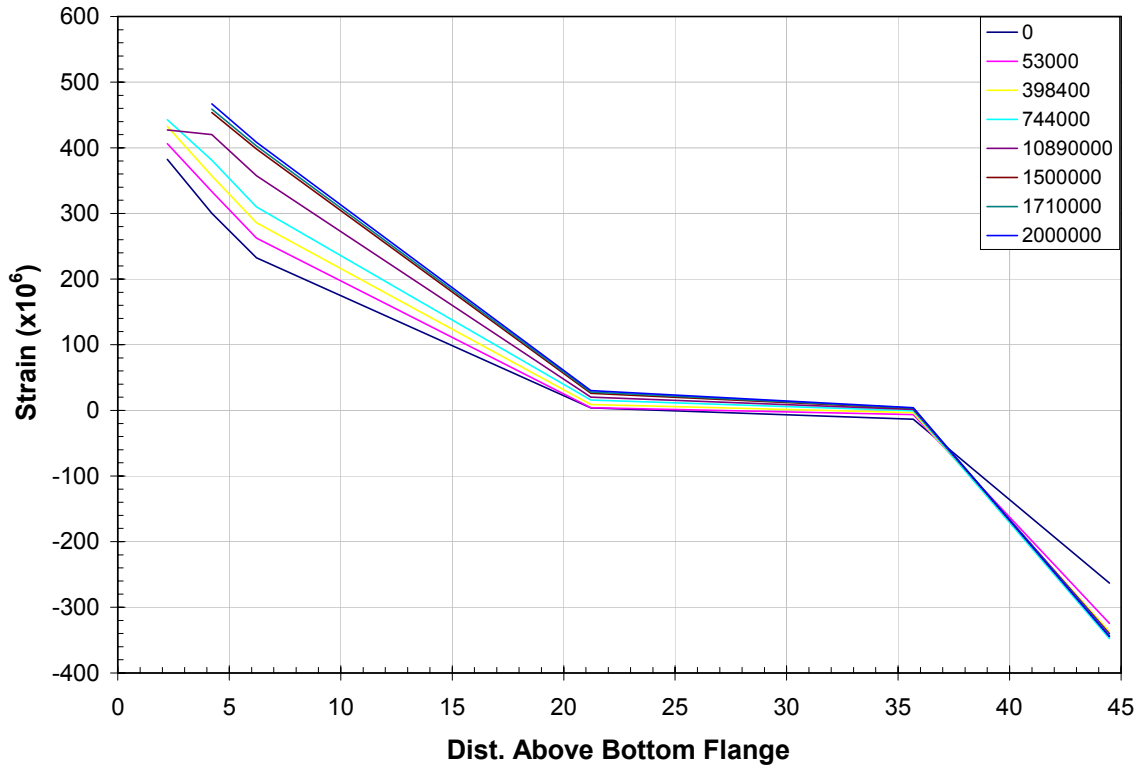
Figure 7-20: Strain Profile at Location 4
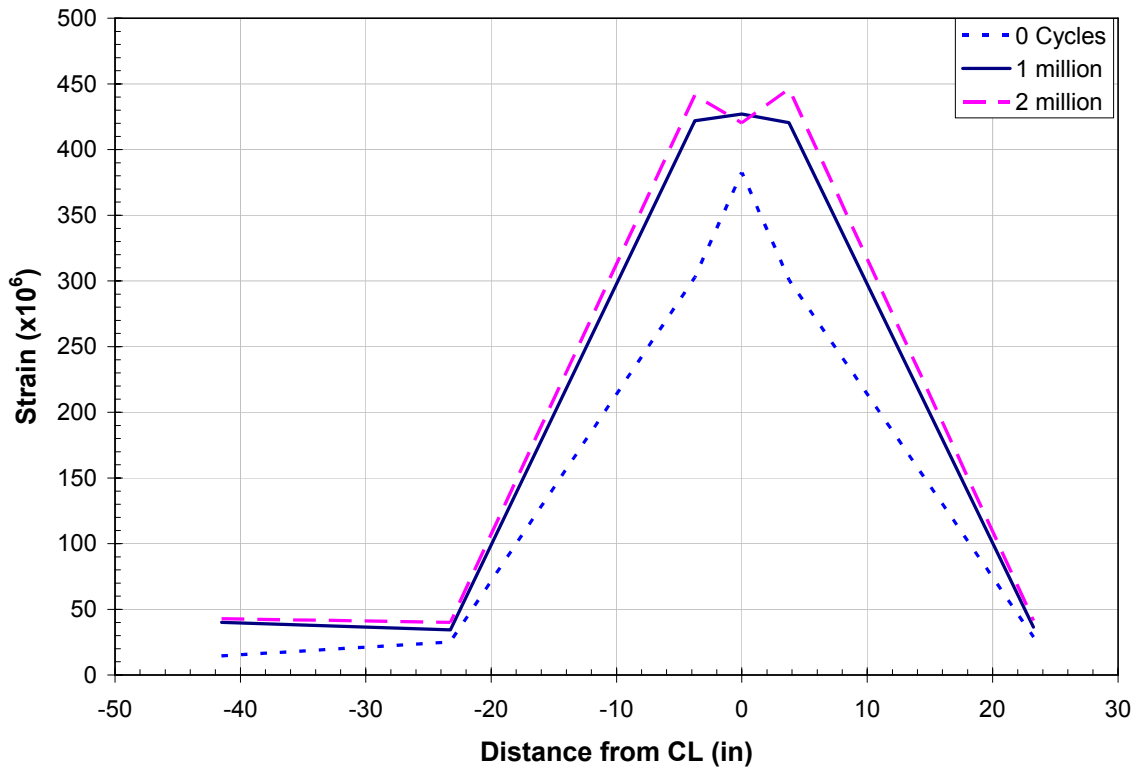
Figure 7-21: Horizontal Strain Distribution at Bottom of Diaphragm

The stress in the deck reinforcement was also monitored over the 2 million cycle interval. Figure 7-22 shows stress plots for 4 reinforcing bars in the deck; gages SG15 and SG22 were located near the outer most edge of the effective slab and gages SG18 and SG20 were located near the centerline. The tensile stress in the reinforcing steel varied only slightly over the 2 million cycles.
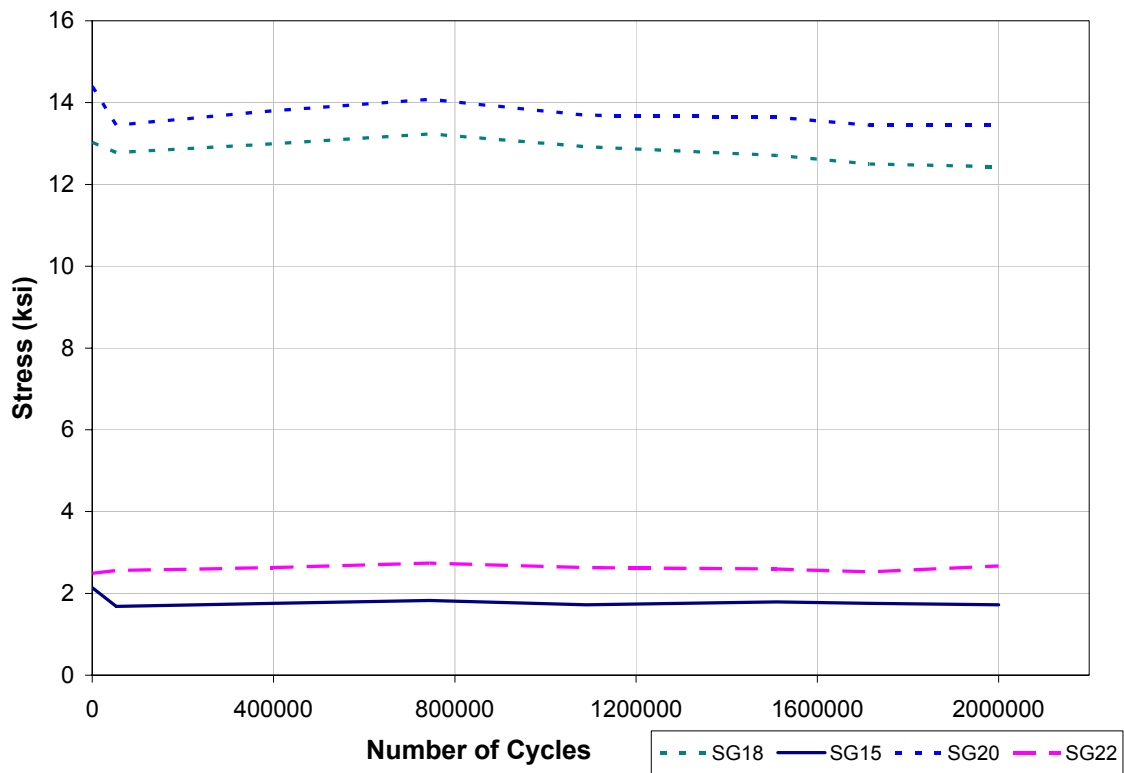
Figure 7-22: Reinforcement Stress Comparison

7.1.3 ULTIMATE STRENGTH TESTING

In this test, the load was to be applied incrementally until the specimen failed. At a load of 225 kips, the hydraulic pump used to load the west side of the specimen failed to apply additional load. The specimen was then unloaded and the defective pump removed. The test was restarted and at 255-kips load, the pump used to load the east side failed to increase load. The specimen was unloaded and this pump removed. The third attempt to apply failure load was successful. The load deflection curve for the successful loading is shown in Figure 7-23. From this curve it can be shown that inelastic behavior begins near a load of 350 kips or a moment of 4200 kp·ft. Investigation into experimental results show that the reinforcement near the girder centerline has reached yield at this load. The saw tooth appearance of the curve was caused by pauses for data collection, in which relaxation of the specimen occurs due to the onset of plastic flow.
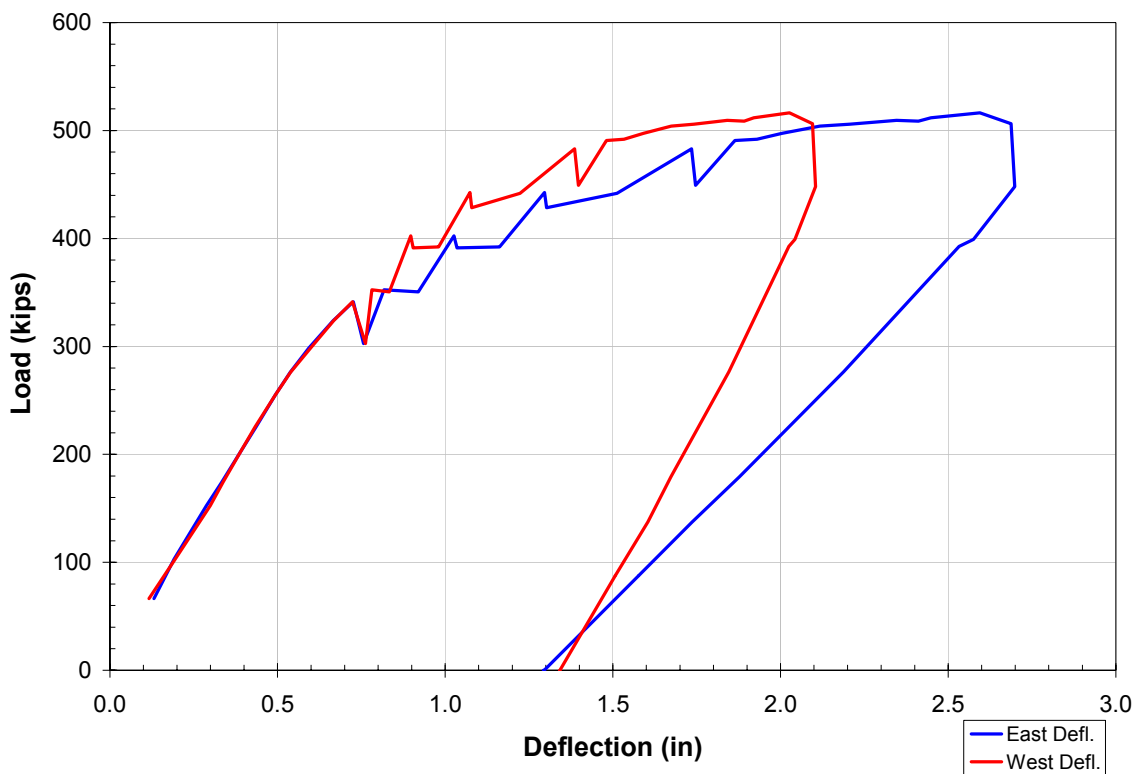
Figure 7-23: Ultimate Capacity Test Load Deflection Curve

Examining the stress in the deck reinforcement, bars located near the middle of the deck yielded first. As the middle bars yielded, load was shed to adjacent reinforcing steel as the load increased. Figure 7-24 shows the load shedding pattern from first yield to final condition. Similar trends were observed in stresses in the bottom flange, as shown in Figure 7-25. The solid line represents compressive stress outside the concrete diaphragm. Note the linear increase in stress up to stresses near 50 ksi. The dashed line indicates compressive stress near the pier centerline inside the diaphragm. Initially the slope is flatter than the solid line indicating the concrete is resisting a significant portion of the compressive force. Compressive stress in the concrete between the end bearing plates is shown in Figure 7-26. The stress in the concrete 1 in above the flange experiences a rapid increase at a load of about 275 kips. The maximum value of stress approaches 5 ksi. Recall from the linear elastic finite element results, a maximum value for Case 4 (Chapter 5) was 5.9 ksi.
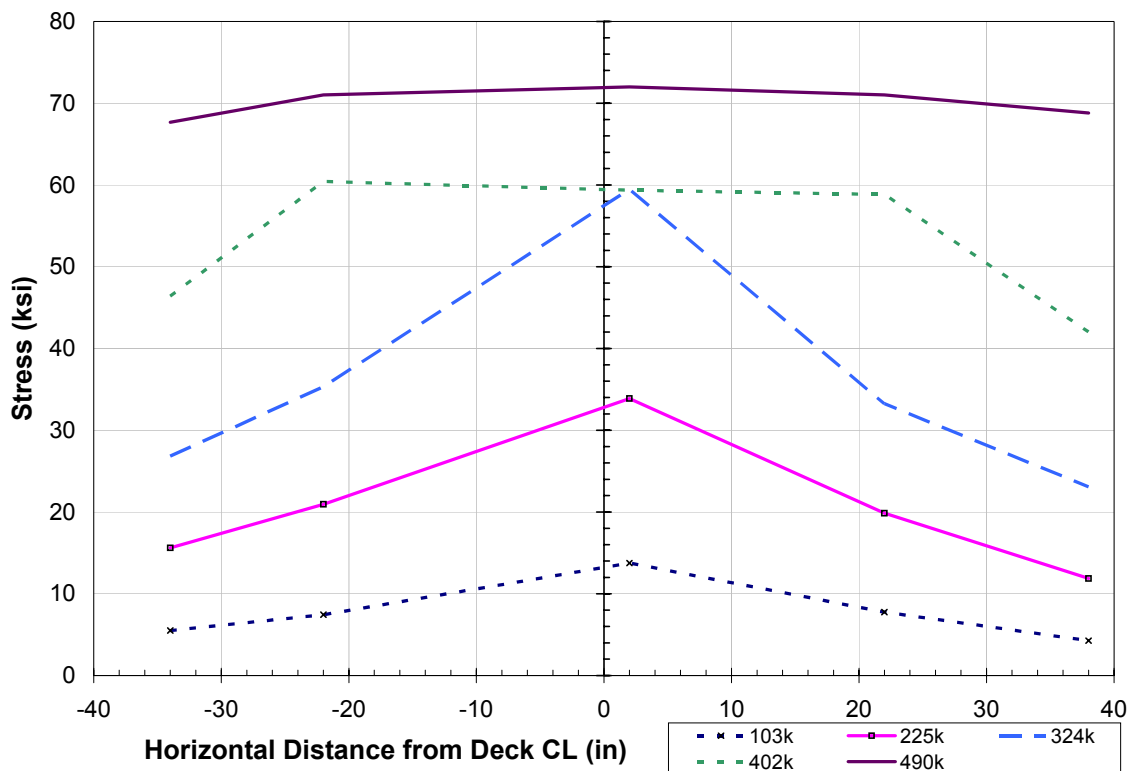
Figure 7-24: Horizontal Strain Distribution at Bottom of Diaphragm
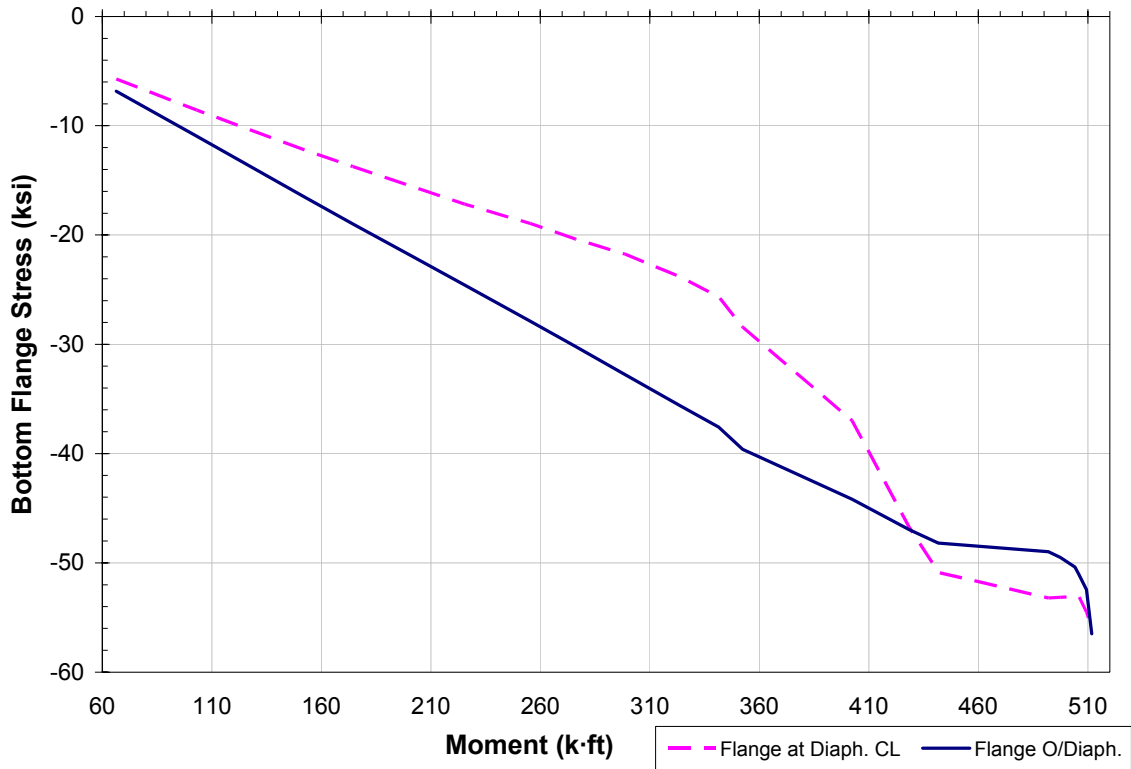
Figure 7-25: Bottom Flange Stresses at Ultimate Capacity
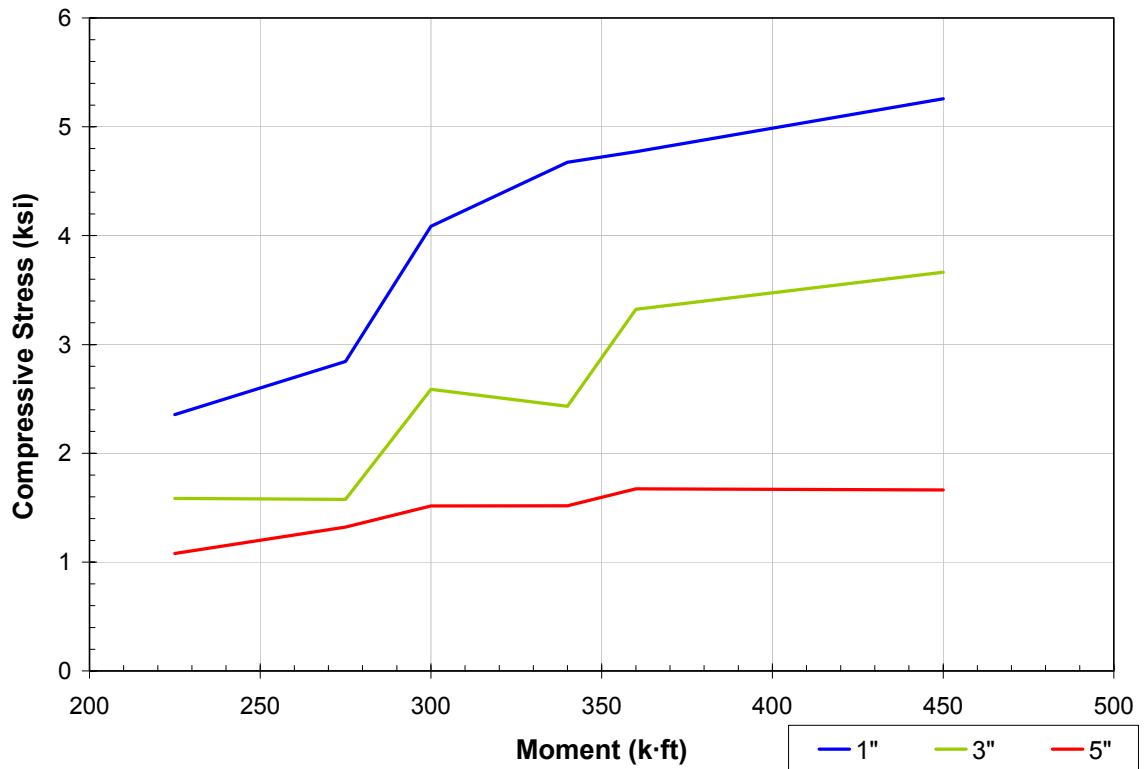
Figure 7-26: Concrete Compressive Stress Between End Bearing Plates

Results from moment curvature analysis are shown for the diaphragm centerline and outside the diaphragm. Using both the actual measurements and material properties obtained from the girders, a similar moment curvature investigation was conducted at both the support centerline and outside the diaphragm. The analysis at the diaphragm edge was performed neglecting the top flange of the wide-flange section, since the limited length of embedment allows for a limited number of shear connectors required to develop the tensile capacity of the flange. Similar analysis was performed using the actual material properties for the concrete and steel members. The results are shown in Figure 7-27 and 7-28. As these plots illustrate, the predicted and experimental trends are similar. At the diaphragm centerline, the experimental results exceed the predicted using the actual material properties. At the diaphragm edge, the experimental results closely resemble those obtained when the top flange is neglected.
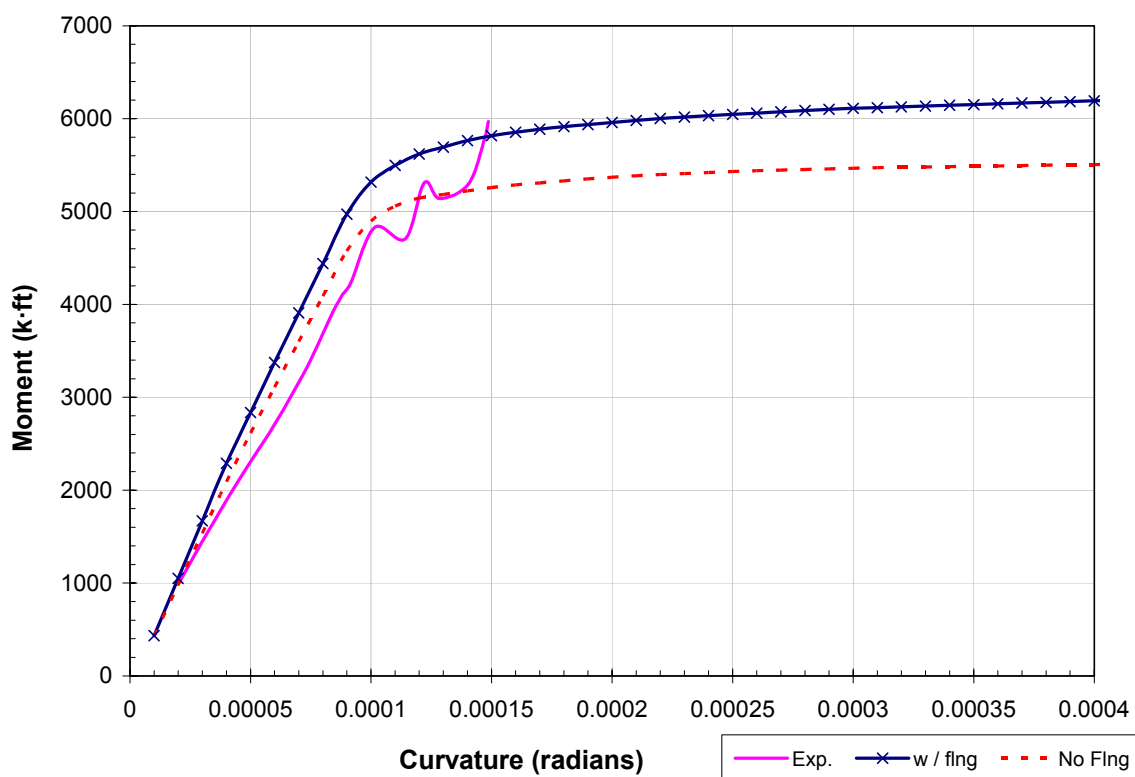
Figure 7-27: Moment Curvature at Support Centerline
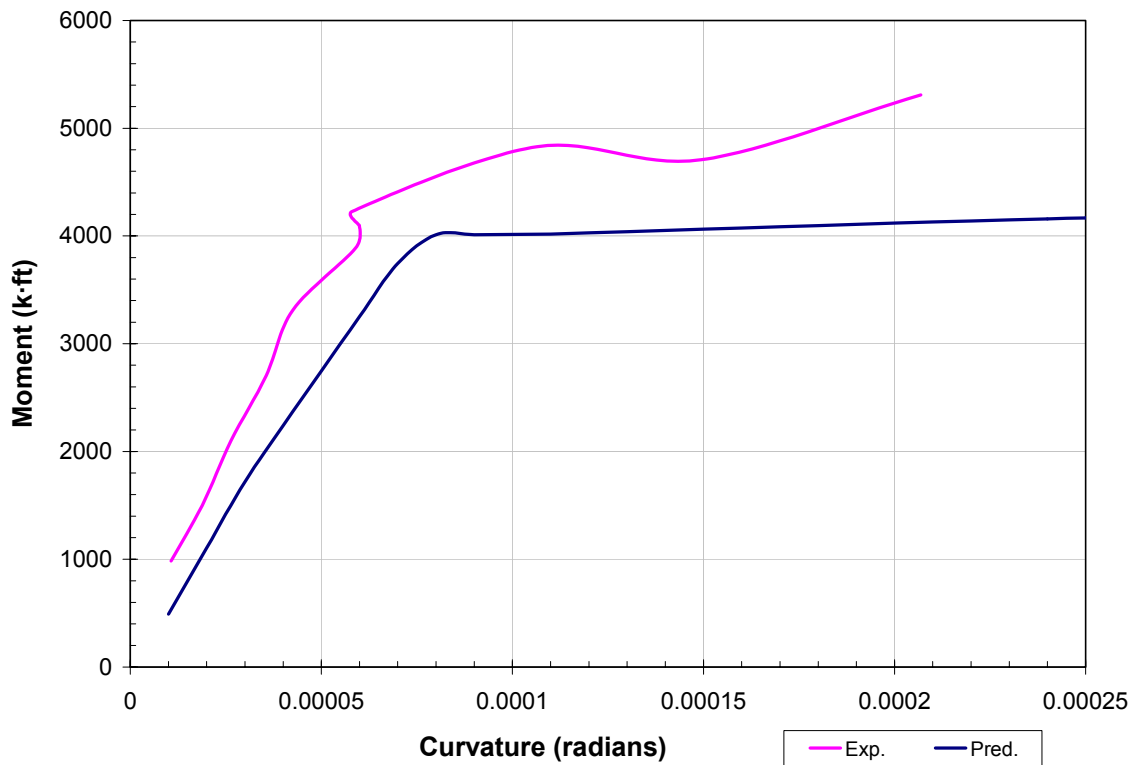
Figure 7-28: Moment Curvature Outside the Diaphragm

The system behaved well under ultimate strength loading. The specimen was subjected to significant displacement after the system had passed the elastic limit. Figures 7-29 and 7-30 show some of the large deformation effects.
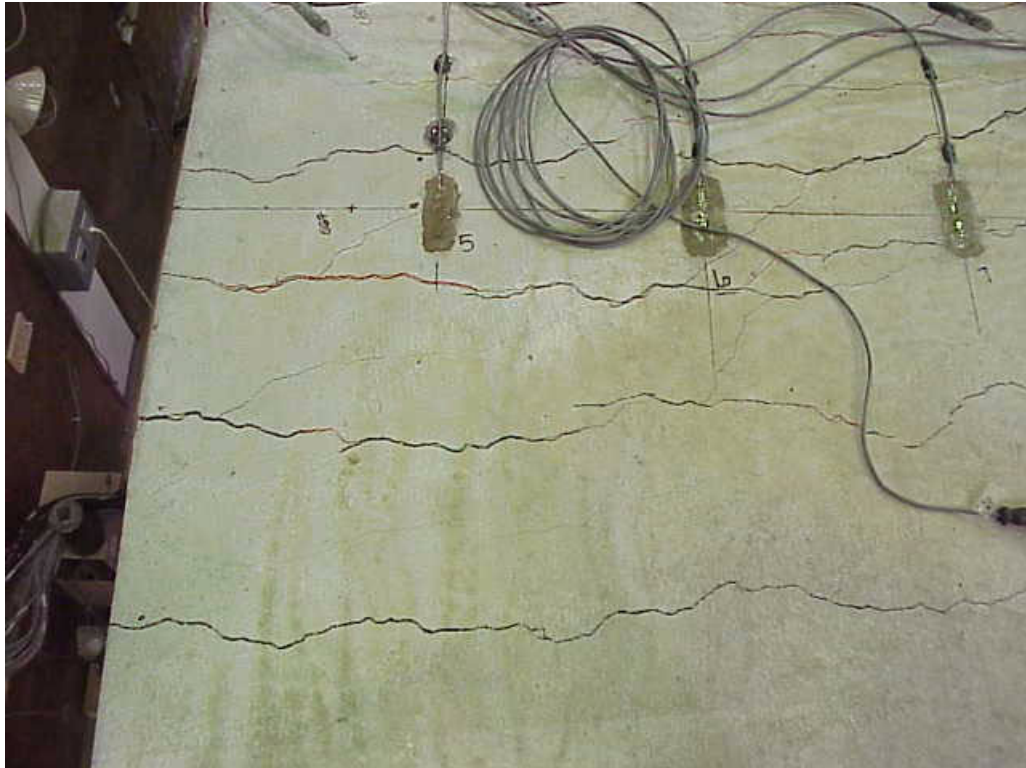
Figure 7-29: Deck Slab After Ultimate Loading
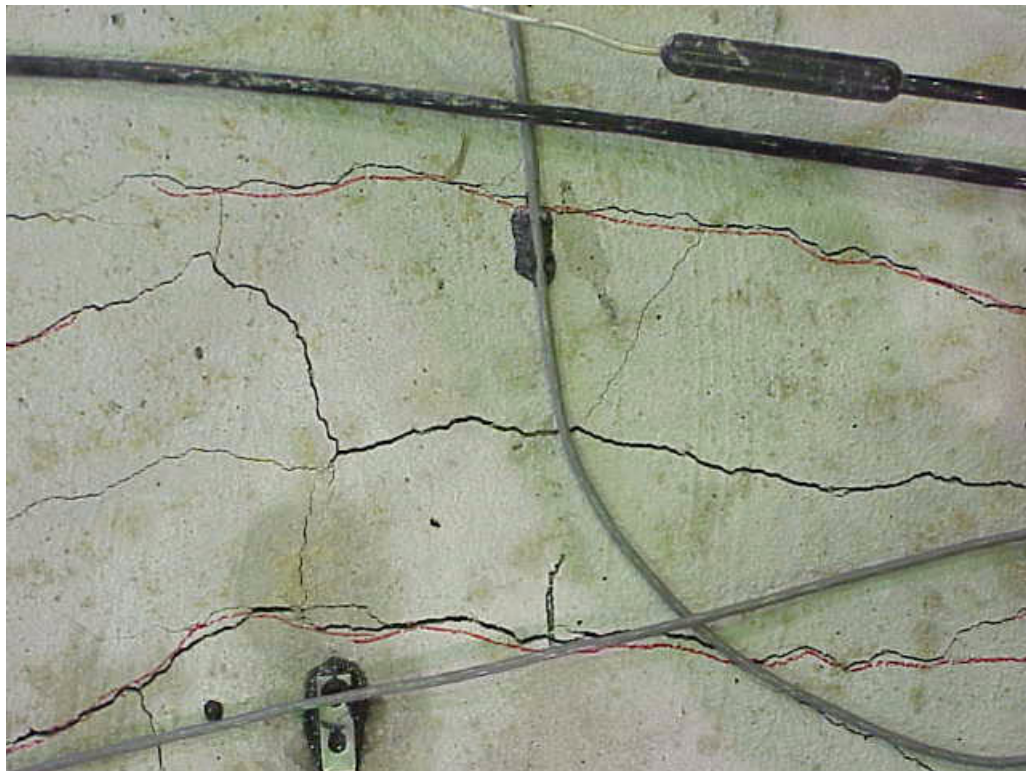
Figure 7-30: Large Deformation Effects

7.2 TEST SUMMARY

This research was conducted to investigate the performance of a steel bridge system which would behave as simply supported for non-composite dead loads and continuous for composite dead and live loads. From the experimental results several conclusions can be made:

1. No appreciable decrease in rigidity or increases in strains were evident in the system when subjected to heavy truck traffic over the design life of the structure. The was an initial reduction in specimen stiffness near 7400 cycles, however, the system behavior remained virtually unchanged over the remaining load cycles.

2. From the deck reinforcement stress plot, "failure" of the specimen was ultimately caused by yielding of the deck reinforcement. This ductile mode of failure is shown in the load deflection curve, during which the specimen was subjected to additional deflection, with only small decreases in stiffness. The plots showing stresses in the reinforcement provide insight into this mechanism, with load shedding to adjacent bars when additional moment was applied.

3. The magnitude of compressive stress in the concrete diaphragm was approximately 5 ksi. From the finite element analysis in Chapter 5, the maximum stress in the concrete was 5.9 ksi for the case with a continuous flange and end bearing plates. Since the location of this gage was 1 in. above the surface of the bottom flange, the experimental value would be larger near the flange surface.

4. The design of the test specimen was based on a Strength I limit state moment of 3911 kp·ft From the experimental results, first yield occurred near 4200 kp·ft The resulting over design of approximately 7% occurred. Further, using the actual material properties results in a moment capacity of 4330 kp·ft.

Summary and Conclusions

The use of steel girder bridges has declined since the introduction of more economical materials and methods of construction. Through a market analysis of several mid-western states, it was determined that spans 80 to 110 ft in length have accounted for the largest declines. Several factors can be attributed to the loss of economy in these medium to short span bridges. In a series of discussions with fabricators, designers, and contractors, the recommendation was to eliminate the bolted field splices and simplify the interior pier bearing details. The concept investigated consists of placing two simple span girders over the abutment and pier and casting the deck slab. At the pier location, the girder ends are cast in a concrete diaphragm. Compressive force from negative bending would be transferred through bearing of the steel section on the concrete diaphragm. The tensile force is carried by the reinforcing steel in the deck slab. The system then

becomes continuous only after the concrete has cured, thus providing continuity for live load and superimposed dead loads only.

Trial designs were carried out to compare the proposed concept to conventional design practice. On average, the proposed concept required 4 to 5% more steel than fully continuous design. Review of the trial designs prompted recommendations to focus on spans near 100 ft in length and to utilizing rolled I-shaped girders. The Military Road bridge in Omaha, NE was chosen as the model for the prototype bridge. The spans were 95 ft long, and the bridge had recently been reconstructed. Therefore, this bridge would provide up-to-date cost information for comparisons between the conventional construction and proposed systems.

Design of the continuity connection over the pier focused on the transfer of the large compressive force in the bottom flange to the concrete diaphragm without crushing the concrete. From the finite element analysis, stresses in the concrete diaphragm exceed far beyond the concrete compressive strength. Based on this analysis, a mechanism was required to transfer the compressive stress reducing the stress in the concrete. The connection detail selected consisted of extending the girder bottom flange through the diaphragm and providing end bearing plates flush with the end of the girder web and top flange. The extended bottom flanges would be partial penetration welded after placement.

8.1 CONCLUSIONS

8.1.1 ANALYSIS AND DESIGN

1. Considering a 2-span bridge with each span equal to 100 ft, the maximum negative moment at the interior support can be reduced by 35 percent when the girders are placed to act as simply supported for non-composite dead loads and continuous for composite dead and live loads. The corresponding increase to positive moment at mid-span is approximately 17 percent.

2. For the same 2-span bridge, the additional steel weight required to resist the larger positive moments is offset by a reduction in steel weight required in the negative flexure region. The combined effect correlates to 5 percent increase in total girder weight.

3. Results of the cost comparison for the Military Road bridge demonstrated material and girder fabrication cost savings of 4 to 8% over the conventional continuous girder design.

4. With this concept, the resulting dead load deflections are greater than the fully continuous counterpart. This characteristic reduces the applicability of this concept project utilizing phased construction.

5. From finite element analysis results, the compressive force in the bottom flange will produce stresses in the concrete diaphragm exceeding the compressive strength if no mechanism is provided to transfer the compressive force. The connection detail tested provides an economical and efficient means of transferring this force, and reducing the stress carried by the concrete.

8.1.2 EXPERIMENTAL INVESTIGATION

When the connection detail was subjected to 75 years of simulated truck traffic, the connection experienced no appreciable loss in rigidity.

The mode of failure of the connection detail was yielding of the tension reinforcement in the slab. Yielding of the reinforcement provides the mechanism for a ductile failure. The connection was subjected to significant displacement after the reinforcement had yielded without a noticeable decrease in load.

8.2 RECOMMENDATIONS FOR FURTHER RESEARCH

The performance of this connection detail was judged a success. The connection is durable, reliable, and inexpensive to fabricate. Further investigation into the simplification the connection detail is necessary. The level of concrete confinement of the diaphragm between the girders may prevent crushing if the end bearing plates were omitted.

Bibliography

[1] Dunker, K. F., and Rabbat, B. G., "Performance of Prestressed Concrete Highway Bridges in the United States - The First 40 Years," *PCI Journal*, Vol. 37, No. 3, May-June 1992, pp: 487-64.

[2] AASHTO, *LRFD Bridge Design Specifications, Second Edition (w/1999 interims)*, American Association of State Highway Transportation Officials, Washington D.C., 1998.

[3] Federal Highway Administration (FHWA), *Recording and Coding Guide for Structure Inventory and Appraisal of the Nation's Bridges*, Report No. FHWA-PD-96-001, December, 1995.

[4] Barker, R. M., and Puckett, J. A., *Design of Highway Bridges*, John Wiley and Sons, Inc., 1997.

[5] "QCONBRIDGE," Release 1.1, (1999), Washington Department of Transportation Bridges and Structures Office.

[6] Nebraska Department of Roads, *Bridge Office Policies and Procedures Manual (BOPP)*, Bridge Divison, Nebraska Department of Roads, 1996.

[7] Freyermuth, C. L., "Design of Continuous Highway Bridges with Precast, Prestressed Concrete Girders," *PCI Journal*, Vol. 14, No. 2, April 1969, pp. 14-39.

[8] ACI Committee 318, *Building Code Requirements for Structural Concrete (ACI 318-95) and Commentary (ACI318R-95)*, American Concrete Institute, Farmington Hills, MI, 1995.

[9] "SAP2000," Release 7.40, Computers and Structures, Inc., Berkeley, CA.

Additional Trial Designs A

Design calculations using the American Association of State Highway and Transportation Officials (AASHTO) Second Edition LRFD Bridge Design Specifications (1998) are presented.

A.1 95' SPAN (MILITARY ROAD GEOMETRY)

Design Assumptions

- span length = 95'

- W40 x 215 I-section girders

- number of girders = 4

- girder spacing = 8' 4"

- composite concrete slab

- slab depth = 7.5"

Calculation of Dead Loads

DC_1 Non-composite dead loads

> <u>Deck:</u>
> Interior girder, $(8"/12)*(8.333')*(0.15\,^k/_{ft}{}^3) = 0.833$ k/ft
> Exterior girder, $(8"/12)*(7.870')*(0.15\,^k/_{ft}{}^3) = 0.787$ k/ft

Total DC_1

	Interior Girder	Exterior Girder
Deck	0.833	0.787
Steel	0.235	0.235
Form-work	0.083	0.079
Total DC_1	**1.151** k/ft	**1.101** k/ft

DC_2 Long Term Composite Dead Load
> Assume the weight per unit length of the barrier is 536 lb/ft, and all girders carry the load equally.
> $DC_2 = (0.536 * 2) / 4 = \textbf{0.268}$ k/ft

DW Future Wearing Surface Load
> Assume equal distribution among all girders.
> $DW = (0.025 * 30) / 4 = \textbf{0.188}$ k/ft

Design Factors

$$\text{Ductility } \eta_D \quad 1.0$$
$$\text{Redundancy } \eta_R \quad 1.0$$
$$\text{Operational Importance } \eta_I \quad 1.0$$

$$\eta = \eta_D * \eta_R * \eta_I = \mathbf{1.0}$$

Bridge is subjected to HL93 loading, the distribution factors and shear / moment envelopes are generated using QconBridge®. The shear / moment envelopes are shown on the following pages, with the distribution factors and section properties preceding.

Note: The exterior girder controls the design for flexural design and the interior controls the design for shear, as is shown in the moment and shear envelopes.

Effective Flange Width

Interior Girder:

$$\tfrac{1}{4} * (\text{span} * 12^{in}/_{ft}) = \tfrac{1}{4} * (95' * 12^{in}/_{ft}) = 285"$$

$$12.0 * (t_s) + (b_f/2) \quad = 12.0 * (7.5) + (^{15.75}/_2) = \mathbf{98"} \qquad \text{(controls)}$$

$$\text{Spacing} \qquad = 100"$$

Exterior Girder:

$$\tfrac{1}{8} * (\text{span} * 12^{in}/_{ft}) = \tfrac{1}{8} * (95' * 12^{in}/_{ft}) = 143"$$

$$6.0 * (t_s) + (b_f/2) \quad = 6.0 * (7.5) + (^{15.75}/_2) = 53"$$

$$\text{Overhang} \qquad = \mathbf{44"} \qquad \text{(controls)}$$

$$b_{eff} = \tfrac{1}{2} * \text{controlling interior} + \text{controlling exterior}$$

$$= \tfrac{1}{2} * 98 + 44 = \mathbf{93"} \qquad \text{(governing } b_{eff})$$

Positive Flexure

Determining neutral axis (N.A.)

$$P_t = 50 * 15.75 * 1.22 = 960.75 \text{ kips}$$

$$P_c = 50 * 15.75 * 1.22 = 960.75 \text{ kips}$$

$$P_w = 50 * 36.54 * 0.65 = 1187.50 \text{ kips}$$

$$P_s = 0.85 * 4 * 93 * 7.5 = 2371.50 \text{ kips}$$

Case 1

$$P_t + P_w \geq P_c + P_s$$

$$2148.3 \ngeq 3332.25 \text{ kips}$$ <u>N.G.</u>

Case 2

$$P_t + P_w + P_c \geq P_s$$

$$3109.1 \geq 2371.50 \text{ kips}$$ <u>O.K.</u>

$$y_{bar} = \frac{t_c}{2}\left[\frac{P_w + P_t - P_s}{P_c} + 1\right]$$

$$y_{bar} = 0.387"$$

Measured from the top of the top flange.

Plastic Moment Capacity

$$M_p = \frac{P_c}{2t_c}\left[y^2{}_{bar} + \left(t_c - y_{bar}\right)^2\right] + \left[P_s d_s + P_w d_w + P_t d_t\right]$$

$$M_p = 5777 \text{ k*ft}$$

Strength Limit State

	Strength I	Strength IV
M_{DC1} = 1192	1490	1788
M_{DC2} = 169	211.3	253.5
M_{DW} = 119	178.5	178.5
M_{LL+IM} = 1797	<u>3144.8</u>	<u>N. A.</u>
	5024.5 k*ft (governs)	2220 k*ft

Ductility Requirement

$$\frac{D_p}{D'} \le 5$$

$$D' = \beta\left(\frac{d + t_s + t_h}{7.5}\right)$$

$$D' = 0.7 * (38.98 + 7.5) / 7.5 = 4.34$$

$$D_p = 7.5 + 0.387 = 7.887$$

$$D_p / D' = 1.82 < 5$$

Section Proportional Limits

$$0.1 \le \frac{I_{YC}}{I_Y} \le 0.9$$

$$I_{YC} = {}^1/_{12}(1.22)*(15.75)^2 = 397.2 \text{ in}^4$$

$$I_Y = 397.2 + 397.2 + 0.836 = 795.3 \text{ in}^4$$

$$I_{YC} / I_Y = 0.5 \qquad \underline{\text{O.K.}}$$

Web Slenderness

$$\frac{2D_{cp}}{t_w} \le 3.76\sqrt{\frac{E}{F_{yc}}} \qquad \underline{\text{O.K.}}$$

(N.A. in the top flange, $D_{cp} = 0$)

Compression Flange Slenderness

$$\frac{b_f}{2t_f} \le 0.382\sqrt{\frac{E}{F_{yc}}}$$

$$\frac{15.75}{2*1.22} = 6.45 \le 24.08 = \sqrt{\frac{29000}{50}} \qquad \underline{\text{O.K.}}$$

Compression Flange Bracing

O.K. (deck is braced continuously at strength limit state)

Positive Flexure Resistance

$$M_n = \frac{5M_p - 0.85M_y}{4} + \frac{0.85M_y - M_p}{4}\left(\frac{D_p}{D'}\right)$$

$$M_n = \frac{2(5820) - 0.85(4598)}{4} + \frac{0.85(4598) - 5820}{4}(1.82)$$

$1.3 * M_y = 5977$ k*ft

$M_n = 5428$ k*ft

5428 k*ft $\geq$ **5024.5** k*ft   O.K.

Negative Flexure

Determining neutral axis (N.A.)

P_t =   50 * 15.75 * 1.22   =   960.75 kips

P_c =   50 * 15.75 * 1.22   =   960.75 kips

P_w =   50 * 36.54 * 0.65   =   1187.55 kips

P_{rb} =   60 * 3.5 =   210 kips

P_{rt} =   60 * 4   =   240 kips

Case 1

$$P_c + P_w \geq P_t + P_{rb} + P_{rt}$$

$2148.3 \geq 1410.75$ kips   O.K.

$$y_{bar} = \frac{D}{2} * \left[\frac{P_c - P_t - P_{rt} - P_{rb}}{P_w} + 1 \right]$$

$y_{bar} = 11.35"$

Measured from the bottom of the top flange.

Plastic Moment Capacity

$$M_p = \frac{P_w}{2D} \left[y^2{}_{bar} + \left(D - y_{bar} \right)^2 \right] + \left[P_{rt}d_{rt} + P_{rb}d_{rb} + P_t d_t + P_c d_c \right]$$

$M_p = 4716$ k*ft

Strength Limit State

	Strength I	Strength IV
M_{DC1} = 0	0	0
M_{DC2} = 302	378	453
M_{DW} = 212	318	318
M_{LL+IM} = 1837	3214.75	N. A.
	3911 k*ft (governs)	771 k*ft

Section Proportional Limits

$$0.1 \le \frac{I_{YC}}{I_Y} \le 0.9$$

$I_{YC} = {}^1/_{12}(1.22)*(15.75)^3 = 397.2 \text{ in}^4$

$I_Y = 397.2 + 397.2 + .836 = 795.3 \text{ in}^4$

$I_{YC} / I_Y = 0.5$ O.K.

Web Slenderness

$$\frac{2D_{cp}}{t_w} \le 3.76\sqrt{\frac{E}{F_{yc}}}$$

$$\frac{2*25.19}{0.65} = 77.51 \le 90.55 = 3.76\sqrt{\frac{29000}{50}}$$

Ratio = 0.856

Compression Flange Slenderness

$$\frac{b_f}{2t_f} \le 0.382\sqrt{\frac{E}{F_{yc}}}$$

$$\frac{15.75}{2*1.22} = 6.45 \le 9.2 = \sqrt{\frac{29000}{50}}$$

Ratio = 0.70

Compression Flange Bracing

Assume adequate bracing

Negative Flexure Resistance

$$M_r = 4716 \text{ k*ft}$$

4716 k*ft $\geq$ **3911** k*ft   <u>O.K.</u>

<u>Live Load Deflection</u>

$$\Delta_{all} = {}^L/_{800} = 1.425"$$

$$\Delta_{anl} = 1.417"$$ <u>O.K.</u>

<u>Permanent Deflection</u>

$$f_{all} = 47.5 \text{ ksi}$$

<u>Positive</u>	<u>Tension</u>	<u>Compression</u>
M_{DC1}	${}^{1192(12)}/_{838.7} = 17.06$	${}^{1192(12)}/_{838.7} = 17.06$
M_{DC2}	${}^{169(12)}/_{1015.2} = 2.00$	${}^{169(12)}/_{2332.4} = 0.87$
M_{DW}	${}^{119(12)}/_{1015.2} = 1.41$	${}^{119(12)}/_{2332.4} = 0.61$
M_{LL+IM}	${}^{1797(12)1.3}/_{1103.6} = \underline{25.40}$	${}^{1797(12)1.3}/_{6537.0} = \underline{4.29}$
	45.86 ksi	22.83 ksi <u>O.K.</u>

Negative	Tension	Compression
M_{DC1}	$^{0(12)}/_{838.7} = 0$	$^{0(12)}/_{838.7} = 0$
M_{DC2}	$^{302(12)}/_{1744.3} = 2.08$	$^{302(12)}/_{977.0} = 3.71$
M_{DW}	$^{212(12)}/_{1744.3} = 1.46$	$^{212(12)}/_{977.0} = 2.60$
M_{LL+IM}	$^{1837(12)1.3}/_{1744.3} = \underline{16.42}$	$^{1837(12)1.3}/_{977.0} = \underline{29.33}$
	19.97 ksi	35.65 ksi O.K.

Live Load Deflection

$$\Delta_{all} = {}^{L}/_{800} = 1.425"$$

$$\Delta_{anl} = 1.417" \qquad \text{O.K.}$$

Shear Resistance

V_{DC1} = 52 kips   * 1.25 =   65 kips

V_{DC2} = 10 kips   * 1.25 =   13 kips

V_{DW} = 7 kips   * 1.50 =   11 kips

V_{LL+IM} = 7 kips   * 1.75 =   <u>167 kips</u>

At Strength Limit State $\mathbf{V_u}$ =   **256** kips

Shear Resistance V_n of Unstiffened Web

V_n = 0.58*36.54*0.65*50

   = 689 kips

V_r = 1.0 * 689 = 689 kips   <u>OK</u>

Deck Design

Use empirical deck design, check conditions;

1. Supporting components are made of steel.

2. Deck is fully cast in place and water cured.

3. Deck has uniform thickness, except at haunches.

4. Effective length / design depth is less than 18 and greater than 6.

5. Core depth is greater than 4 inches.

6. Effective length is less than 13.5 ft.

7. Minimum slab depth is greater than 7 inches.

8. Minimum overhang is greater than 5 times the depth.

9. Deck 28 day f'c is greater than or equal to 4 ksi.

10. Deck is to be composite.

From Nebraska Department of Roads Bridge Office Policies and Practice (BOPP)

Manual.

Transverse:

Top: #4 bars @ 12" spacing

Bottom: #5 bars @ 12" spacing

Longitudinal:

Minimum area of longitudinal reinforcement per inch of slab width.

$$\text{Area}_{min} = 7.5 * 0.01 = 0.075 \; ^{in2}/_{in}$$

$$\text{Top: } A_{reinf} = ^2/_3 * (0.075) = 0.05 \; ^{in2}/_{in}$$

Use #5 bars @ 12" spacing

$$A_{reinf} = 0.31/12 * (2) = 0.052 > 0.05 \; ^{in2}/_{in}$$

Bottom: $A_{reinf} = \frac{1}{3} * (0.075) = 0.025$ $^{in2}/_{in}$

Use #4 bars @ 12" spacing

$A_{reinf} = 0.20/12 * (2) = 0.033 > 0.025$ $^{in2}/_{in}$

Additional Reinforcement Required to Resist Strength I Design Moment.

$M_u = 3911$ k*ft $\qquad\qquad b_f = 15.75$ inches

$d = 41.51$ inches $\qquad\qquad f'c = 4.0$ ksi

Summing moments about the centroid of the bottom flange.

$\Sigma M_o = 0, 0 = A_s(f_s)(d) - C_c(a/2) - M_u$ $\qquad\qquad$ <u>i</u>

$\Sigma F_h = 0, 0 = A_s(f_s) - 0.85(f'c)a(b_f) - A'_s(f'_s)$ $\qquad\qquad$ <u>ii</u>

Assume tension steel yields,

$0 = A_s(2490.6) - 53.55a(a/2) - 46932$

$A_s(f_s) = 53.55a + 960.75$

$a = (60\ A_s - 960.75) / 53.55$

Sub <u>i</u> - <u>ii</u> $\qquad A_s(2490.6) = 53.55[(60\ A_s - 960.75) / 53.55]^2 + 46932$

$A_s(2490.6) = 33.61\ A_s^2 - 1076.47\ A_s + 8618.49 + 46932$

$33.61\ A_s^2 - 3567.07\ A_s + 55550.49 = 0$

$A_s = $ **18.96 in²**

Check assumptions;

$$C_c - C_s = T$$

$$0.85(f'c)a(b_f) + 960.75 = 18.96(f_s)$$

$$0.85(f'c)a(b_f) = 176.85$$

$$a = 3.3 \text{ inches}$$

$$C = 3.3 \text{ / beta} = 3.885"$$ OK

$$f_{sa} = \frac{Z}{(d_c A)^{1/3}} \leq 0.6 f_y$$ Assume Z = 130 k/in (severe exposure)

$$d_c = 2 + 0.5 + 0.5 = 3"$$

$$A = 2(3) *94 = 564 \text{ in}^2$$

$$f_{sa} = \frac{130}{11.916} = 10.9 \leq 36 = 0.6*60$$ OK

Top Layer:

   Use 2 - #8 bars between adjacent #5 bars

   $$8 * 0.31 = 2.48 \text{ in}^2$$

   $$14 * 0.79 = 11.06 \text{ in}^2$$

Bottom Layer:

   Use 1 - #7 bar between adjacent #4 bars

   $$8 * 0.2 = 1.6 \text{ in}^2$$

   $$7 * 0.6 = 4.2 \text{ in}^2$$

$$A_s = 2.48 + 11.06 + 1.6 + 4.2 = 19.34 \text{ in}^2 > 18.96 \text{ in}^2$$ OK

Shear Connectors

Fatigue:

I (steel and rebar) = 24410 in^4

pitch:

$$p = \frac{nZ_r I}{V_{sr} Q}$$

Use 5" by 3/4" diameter studs

n = 3, 3 per row

$Z_r = \alpha d^2 \geq 5.5 d^2 / \alpha$

$\alpha = 34.5 - 4.28 * Log(N)$

For N = 2,000,000 cycles

$\alpha = 7.53$

$Z_r = 4.23 \geq 1.55$

Q = 12.67*(14.02+(7.5-2))+(6.33*(14.02+2)) = 1078.4 in^4

$p = 287.2 / V_{sr}$

Calculation of V_{sr}

F = M / S_{bottom}

13 = M / 977

M = 1058 k*ft   (applied at 12' from centerline)

$M = V_{sr} * L$

$V_{sr} = 88$ kips

since shear is constant in the cantilever specimen

$p = 287.2 / 88 = 3.26 \leq 4.5 = 6(.875)$

Use 4.5" spacing

Strength:

$$Q_s = \phi_{sc} Q_n$$
$$where \phi_{sc} = 0.85$$
$$Q_n = 0.5 A_s \sqrt{f'_c E_c} \leq A_{sc} F_u$$

$A_{sc} = 0.44$ in^2 $E_c = 3605$ ksi

$F_u = 60$ ksi $f'_c = 4$ ksi

$Qn = 0.5 * (0.44)(4 * (3605))^{0.5} = 26.4$ kips

$A_{sc}F_u = 0.44 * (60) = 26.4$ kips

$Q_r = 0.85 * (26.4) = 22.5$ kips

$V_h = 19 * (60) = 1140$ kips

$n = 1140 / 22.4 = 51$ studs for each region

$p = (24 * 12) / (51 / 3) = 16.9" < 24"$ O.K.

Fatigue Governs at 4.5" pitch.

Longitudinal Reinforcement

$$f_f = 21 - 0.33 f_{min} + 8\left(\frac{r}{h}\right)$$

$$f_{min} = \frac{(302 + 212)*12*(14.02 + 5.5)}{24410} = 4.93 ksi$$

f_f = 21 - 0.33 * (4.93) + 0.8 * (0.3) = 21.77 ksi

$$\gamma(\Delta f) = \frac{0.75(469)(12)(14.02 + 5.5)}{24410} = 3.38 ksi$$

3.38 ≤ 21.77 ksi   O.K.

Bearing Stiffeners

V_u at the interior pier section = 297 kips

If V_u > 0.75 * ϕ_b * V_n bearing stiffeners are required

Where ϕ_b = 1.0

$V_n = V_p$ = 0.58 * (F_{yw}) * D * (t_w)

= 0.58(50)36.54(0.65) = 689 kips

$\phi_b V_n$ = 0.75(1.0)689 = 517

297 < 517 kips

Stiffeners not required

Strength Moments

Position	DC₁	DC₂	DW	LL + IM M+	LL + IM M-	1.25 DC₁	1.25 DC₂	1.5 DW	Factored DL	1.75(LL+IM) M+	1.75(LL+IM) M-	Factored & Distributed Strength 1 ν	M+	M-
0	0	0	0	0	0	0	0	0	0	0	0	1	0	0
9.5	447	79	55	784	-102	559	99	83	740	1372	-179	1	2112	561
19	795	133	93	1330	-204	994	166	140	1299	2328	-357	1	3627	942
28.5	1043	163	115	1653	-306	1304	204	173	1680	2894	-536	1	4574	1144
38	1192	169	119	1797	-408	1490	211	179	1880	3145	-715	1	5026	1165
47.5	1242	151	106	1763	-511	1553	189	159	1900	3086	-894	1	4986	1007
57	1192	109	76	1576	-613	1490	136	114	1741	2758	-1072	1	4499	668
66.5	1043	42	30	1221	-715	1304	53	45	1402	2137	-1251	1	3539	151
76	795	-48	-34	727	-966	994	-60	-51	883	1272	-1690	1	2154	-808
85.5	447	-163	-115	265	-1170	559	-204	-173	183	463	-2048	1	646	-1865
95	0	-302	-212	0	-1837	0	-378	-318	-696	0	-3215	1	-696	-3911

Fatigue Load Combination

Position	Fatigue Truck Moments (IM+1.15) M+	M-	Unfactored & Distributed Fatigue Moments D.F.	M+	M-	Govern. Factored & Distributed Fatigue Moments L.F.	M+	M-
0	0	0		0	0		0	0
9.5	521	-66	0.709	369	-47	0.75	277	-35
19	860	-132	0.709	610	-94	0.75	457	-70
28.5	1070	-199	0.709	759	-141	0.75	569	-106
38	1131	-265	0.709	802	-188	0.75	601	-141
47.5	1090	-331	0.709	773	-235	0.75	580	-176
57	1007	-397	0.709	714	-281	0.75	535	-211
66.5	792	-464	0.709	562	-329	0.75	421	-247
76	469	-530	0.709	333	-376	0.75	249	-282
85.5	185	-596	0.709	131	-423	0.75	98	-317
95	0	-662	0.709	0	-469	0.75	0	-352

Shear Calculations

IM*(Vehicle Shears) + Lane Load

Position	Design Truck V+	V-	Design Tandem V+	V-	Govern. Shears V+	V-	Unfactored & Distributed Shears D.F.	V+	V-
0	112	-13	91	-10	112	-13	0.849	95	-11
9.5	94	-13	77	-11	94	-13	0.849	80	-11
19	78	-19	64	-20	78	-20	0.849	66	-17
28.5	62	-31	52	-30	62	-31	0.849	53	-26
38	48	-45	41	-40	48	-45	0.849	41	-38
47.5	36	-60	31	-51	36	-60	0.849	31	-51
57	24	-74	22	-61	24	-74	0.849	20	-63
66.5	15	-89	14	-72	15	-89	0.849	13	-76
76	8	-103	8	-83	8	-103	0.849	7	-87
85.5	3	-116	3	-93	3	-116	0.849	3	-98
95	0	-129	0	-103	0	-129	0.849	0	-110

Total Factored Shears for Strength 1 Load Combination

Position	DC₁	DC₂	DW	Distributed. LL + IM V+	V-	1.25 DC₁	1.25 DC₂	1.5 DW	Factored DL	V+	1.75*(LL + IM) V-	v	Factored & Distributed Strength Shears V+	V-
0	55	10	7	95	-11	68	13	11	91	166	-19	1	258	72
9.5	44	7	5	80	-11	55	9	8	71	140	-19	1	211	52
19	33	4	3	66	-17	41	5	5	51	116	-30	1	166	21
28.5	22	2	1	53	-26	27	3	2	31	92	-46	1	123	-15
38	11	-0.6	-0.4	41	-38	14	-1	-1	12	71	-67	1	84	-55
47.5	0	-3	-2	31	-51	0	-4	-3	-7	53	-89	1	47	-96
57	-11	-6	-4	20	-63	-14	-8	-6	-27	36	-110	1	8	-137
66.5	-22	-8	-6	13	-76	-27	-10	-9	-46	22	-132	1	-24	-179
76	-33	-10	-8	7	-87	-41	-13	-12	-66	12	-153	1	-54	-219
85.5	-44	-13	-9	3	-98	-55	-16	-14	-84	4	-172	1	-80	-257
95	-55	-16	-11	0	-110	-68	-20	-17	-105	0	-192	1	-105	-297

Fatigue Shear Loading Combination

Position	IM*(Fatigue Truck Shears) & Lane Load			Govern. Unfactored & Distributed Shears			Govern. Factored & Distributed Shears		
	V+	V-	D.F.	V+	V-	L.F.	V+	V-	
0	65	-7	0.71	46	-5	0.75	35	-4	
9.5	55	-7	0.71	39	-5	0.75	29	-4	
19	45	-10	0.71	32	-7	0.75	24	-5	
28.5	36	-16	0.71	26	-11	0.75	19	-9	
38	28	-22	0.71	20	-16	0.75	15	-12	
47.5	20	-32	0.71	14	-23	0.75	11	-17	
57	13	-41	0.71	9	-29	0.75	7	-22	
66.5	9	-50	0.71	6	-35	0.75	5	-27	
76	5	-58	0.71	4	-41	0.75	3	-31	
85.5	2	-66	0.71	1	-47	0.75	1	-35	
95	0	-72	0.71	0	-51	0.75	0	-38	

A.2 100' Span (military Road Geometry)

Design Assumptions

- span length = 100'
- W40 x 249 I-section girders
- number of girders = 4
- girder spacing = 8' 4"
- composite concrete slab
- slab depth = 7.5"

Calculation of Dead Loads

DC_1 Non-composite dead loads

Deck:

Interior girder, $(8"/12)*(8.333')*(0.15\,^k/_{ft}{}^3) = 0.833$ k/ft
Exterior girder, $(8"/12)*(7.870')*(0.15\,^k/_{ft}{}^3) = 0.787$ k/ft

Total DC_1

	Interior Girder	Exterior Girder
Deck	0.833	0.787
Steel	0.260	0.260
Form-work	0.083	0.079
Total DC_1	**1.176** k/ft	**1.126** k/ft

DC_2 Long Term Composite Dead Load

Assume the weight per unit length of the barrier is 536 lb/ft, and all girders carry the load equally.

$$DC_2 = (0.536 * 2) / 4 = \mathbf{0.268} \text{ k/ft}$$

DW Future Wearing Surface Load

Assume equal distribution among all girders.

$$DW = (0.025 * 30) / 4 = \mathbf{0.188} \text{ k/ft}$$

Design Factors

$$\text{Ductility } \eta_D \quad 1.0$$
$$\text{Redundancy } \eta_R \quad 1.0$$
$$\text{Operational Importance } \eta_I \quad 1.0$$

$$\eta = \eta_D * \eta_R * \eta_I = \textbf{1.0}$$

Bridge is subjected to HL93 loading, the distribution factors and shear / moment envelopes are generated using QconBridge®. The shear / moment envelopes are shown on the following pages, with the distribution factors and section properties preceding.

Note: The exterior girder controls the design for flexural design and the interior controls the design for shear, as is shown in the moment and shear envelopes.

Effective Flange Width

Interior Girder:

$$\tfrac{1}{4} * (\text{span} * 12^{in}/_{ft}) = \tfrac{1}{4} * (100' * 12^{in}/_{ft}) = 300"$$

$$12.0 * (t_s) + (b_f/_2) = 12.0 * (7.5) + (^{15.75}/_2) = \textbf{98"} \qquad \text{(controls)}$$

$$\text{Spacing} \qquad = 100"$$

Exterior Girder:

$$\tfrac{1}{8} * (\text{span} * 12^{in}/_{ft}) = \tfrac{1}{8} * (100' * 12^{in}/_{ft}) = 150"$$

$$6.0 * (t_s) + (b_f/_2) = 6.0 * (7.5) + (^{15.75}/_2) = 53"$$

$$\text{Overhang} \qquad = \textbf{44"} \qquad \text{(controls)}$$

$$b_{eff} = \tfrac{1}{2} * \text{controlling interior} + \text{controlling exterior}$$

$$= \tfrac{1}{2} * 98 + 44 = \textbf{93"} \qquad \text{(governing } b_{eff})$$

<u>Positive Flexure</u>

Determining neutral axis (N.A.)

$$P_t \ = \ 50 * 15.75 * 1.42 \ = \ 1118.3 \text{ kips}$$

$$P_c \ = \ 50 * 15.75 * 1.42 \ = \ 1118.3 \text{ kips}$$

$$P_w \ = \ 50 * 36.54 * 0.75 \ = \ 1370.3 \text{ kips}$$

$$P_s \ = \ 0.85 * 4 * 93 * 7.5 \ = \ 2496.0 \text{ kips}$$

Case 1

$$P_t + P_w \ \geq \ P_c + P_s$$

2488.6 ≱ 3614.3 kips   N.G.

Case 2

$$P_t + P_w + \ P_c \geq P_s$$

3606.9 ≥ 2496. kips   O.K.

$$y_{bar} \ = \ \frac{t_c}{2}\left[\frac{P_w + P_t - P_s}{P_c} + 1\right]$$

$$y_{bar} = 0.705"$$

Measured from the top of the top flange.

Plastic Moment Capacity

$$M_p \ = \ \frac{P_c}{2t_c}\left[y^2_{bar} + \left(t_c - y_{bar}\right)^2\right] + \left[P_s d_s + P_w d_w + P_t d_t\right]$$

$$M_p = 6665 \text{ k*ft}$$

Strength Limit State

	Strength I	Strength IV
M_{DC1} = 1351	1689	2027
M_{DC2} = 188	235	282
M_{DW} = 132	198	198
M_{LL+IM} = 1932	<u>3381</u>	<u>N. A.</u>
	5503 k*ft (governs)	2507 k*ft

Ductility Requirement

$$\frac{D_p}{D'} \le 5$$

$$D' = \beta \left(\frac{d + t_s + t_h}{7.5} \right)$$

D' = 0.7 * (39.38 + 7.5) / 7.5 = 4.375

D_p = 7.5 + 0.705 = 8.205"

D_p / D' = 1.88 < 5

Section Proportional Limits

$$0.1 \le \frac{I_{YC}}{I_Y} \le 0.9$$

$$I_{YC} = {}^{1}/_{12}(1.42)*(15.75)^3 = 462.3 \text{ in}^4$$

$$I_Y = 462.3 + 462.3 + 1.3 = 925.9 \text{ in}^4$$

$$I_{YC} / I_Y = 0.5 \qquad\qquad \text{O.K.}$$

Web Slenderness

$$2D_{cp}\Big/t_w \le 3.76\sqrt{E\Big/F_{yc}}$$

$$D_{cp} = 0 \text{ (Plastic N.A. is in slab)}$$

Compression Flange Slenderness

$$b_f\Big/2t_f \le 0.382\sqrt{E\Big/F_{yc}}$$

$$15.75\Big/2*1.42 = 5.55 \le 9.2 = \sqrt{29000\Big/50}$$

Compression Flange Bracing

O.K.   (braced continuously at strength limit state)

Positive Flexure Resistance

$$M_n = \frac{5M_p - 0.85M_y}{4} + \frac{0.85M_y - M_p}{4}\left(\frac{D_p}{D'}\right)$$

$$M_n = \frac{2(6665) - 0.85(5307)}{4} + \frac{0.85(5307) - 6665}{4}(1.88)$$

$$1.3 * M_y = 6899 \text{ k*ft}$$

$$M_n = 6194 \text{ k*ft}$$

6194 k*ft $\geq$ **5503** k*ft   <u>O.K.</u>

Negative Flexure

   Determining neutral axis (N.A.)

$$P_t \quad = \quad 50 * 15.75 * 1.42 \quad = \quad 1118.3 \text{ kips}$$

$$P_c \quad = \quad 50 * 15.75 * 1.42 \quad = \quad 1118.3 \text{ kips}$$

$$P_w \quad = \quad 50 * 36.54 * 0.75 \quad = \quad 1370.3 \text{ kips}$$

$$P_{rb} \quad = \quad 60 * 3.5 = \quad 210 \text{ kips}$$

$$P_{rt} \quad = \quad 60 * 4 \quad = \quad 240 \text{ kips}$$

   Case 1

$$P_c + P_w \quad \geq P_t + P_{rb} + P_{rt}$$

   2488.6 $\geq$ 1568.3 kips   O.K.

$$y_{bar} = \frac{D}{2} * \left[\frac{P_c - P_t - P_{rt} - P_{rb}}{P_w} + 1 \right]$$

$$y_{bar} = 12.27"$$

   Measured from the bottom of the top flange.

Plastic Moment Capacity

$$M_p = \frac{P_w}{2D}\left[y^2_{bar} + \left(D - y_{bar}\right)^2\right] + \left[P_{rt}d_{rt} + P_{rb}d_{rb} + P_t d_t + P_c d_c\right]$$

$$M_p = 5395 \text{ k*ft}$$

Strength Limit State

	Strength I	Strength IV
$M_{DC1} = 0$	0	0
$M_{DC2} = 335$	418.75	502.5
$M_{DW} = 235$	352.5	352.5
$M_{LL+IM} = 1970$	<u>3447.5</u>	<u>N. A.</u>
	4219 k*ft (governs)	855 k*ft

Section Proportional Limits

$$0.1 \le \frac{I_{YC}}{I_Y} \le 0.9$$

$$I_{YC} = {}^1/_{12}(1.42)*(15.75)^3 = 462.3 \text{ in}^4$$

$$I_Y = 462.3 + 462.3 + 1.3 = 925.9 \text{ in}^4$$

$$I_{YC} / I_Y = 0.5 \qquad\qquad \text{O.K.}$$

Web Slenderness

$$\frac{2D_{cp}}{t_w} \le 3.76\sqrt{\frac{E}{F_{yc}}}$$

$$\frac{2*24.27}{0.75} = 64.72 \le 90.55 = 3.76\sqrt{\frac{29000}{50}}$$

Ratio = 0.71

Compression Flange Slenderness

$$\frac{b_f}{2t_f} \le 0.382\sqrt{\frac{E}{F_{yc}}}$$

$$\frac{15.75}{2*1.42} = 5.55 \le 9.2 = \sqrt{\frac{29000}{50}}$$

Ratio = 0.60

Compression Flange Bracing

Assume adequate bracing

Negative Flexure Resistance

$$M_r = 5395 \text{ k*ft}$$

5395 k*ft $\ge$ **4219** k*ft   <u>O.K.</u>

Permanent Deflection

$$f_{all} = 47.5 \text{ ksi}$$

Positive	Tension	Compression
M_{DC1}	$^{1351(12)}/_{973.6} = 16.65$	$^{1351(12)}/_{973.6} = 16.65$
M_{DC2}	$^{188(12)}/_{1166.8} = 1.93$	$^{188(12)}/_{2450.0} = 0.92$
M_{DW}	$^{132(12)}/_{1166.8} = 1.36$	$^{132(12)}/_{2450.0} = 0.65$
M_{LL+IM}	$^{1932(12)1.3}/_{1273.7} = \underline{23.66}$	$^{1932(12)1.3}/_{6373} = \underline{4.29}$
	43.61 ksi	22.95 ksi O.K.

Negative	Tension	Compression
M_{DC1}	$^{0(12)}/_{973.6} = 0$	$^{0(12)}/_{973.6} = 0$
M_{DC2}	$^{335(12)}/_{1306.8} = 3.08$	$^{335(12)}/_{1045} = 3.85$
M_{DW}	$^{235(12)}/_{1306.8} = 2.16$	$^{235(12)}/_{1045} = 2.70$
M_{LL+IM}	$^{1970(12)1.3}/_{1306.8} = \underline{23.52}$	$^{1970(12)1.3}/_{1045} = \underline{29.41}$
	28.75 ksi	35.95 ksi O.K.

Live Load Deflection

$$\Delta_{all} = {}^{L}/_{800} = 1.5"$$

$$\Delta_{anl} = 1.439" \qquad \qquad \underline{O.K.}$$

Shear Resistance

Positive

V_{DC1} = 56 kips   * 1.25 =   70 kips

V_{DC2} = 10 kips   * 1.25 =   13 kips

V_{DW} = 7 kips   * 1.50 =   11 kips

V_{LL+IM} = 97 kips   * 1.75 =   <u>170 kips</u>

At Strength Limit State V_u = **263** kips

Shear Resistance V_n of Unstiffened Web

V_n = 0.58 * 36.54 * 0.75 * 50

    = 857 kips

V_r = 1.0 * 857 = 857 kips

         857 > 263 kips   <u>OK</u>

Negative

V_{DC1} = 56 kips   * 1.25 =   70 kips

V_{DC2} = 17 kips   * 1.25 =   21 kips

V_{DW} = 12 kips   * 1.50 =   18 kips

V_{LL+IM} = 111 kips   * 1.75 =   <u>194 kips</u>

At Strength Limit State V_u = **304** kips

Shear Resistance V_n of Unstiffened Web

$$V_n = 0.58 * 36.54 * 0.75 * 50$$

$$= 857 \text{ kips}$$

$$V_r = 1.0 * 857 = 857 \text{ kips}$$

857 > 304 kips   O.K.

Strength 1 Moments

Position	DC₁	DC₂	DW	LL + IM M+	LL + IM M-	1.25 DC₁	1.25 DC₂	1.5 DW	Factored DL	1.75(LL+IM) M+	1.75(LL+IM) M-	ν	Factored & Distributed Strength 1 M+	M-
0	0	0	0	0	0	0	0	0	0	0	0		0	0
10	507	87	61	841	-110	633	109	92	834	1471	-192	1	2305	642
20	901	147	103	1428	-219	1126	184	155	1464	2499	-383	1	3963	1082
30	1182	181	127	1778	-328	1478	226	191	1895	3111	-575	1	5006	1320
40	1351	188	132	1932	-438	1689	235	198	2122	3381	-767	1	5503	1355
50	1408	168	118	1896	-548	1759	210	177	2146	3318	-959	1	5464	1187
60	1351	121	85	1694	-657	1689	151	128	1968	2965	-1150	1	4933	818
70	1182	47	33	1313	-767	1478	59	50	1586	2298	-1342	1	3884	244
80	901	-54	-38	783	-1039	1126	-68	-57	1002	1370	-1818	1	2372	-817
90	507	-181	-127	283	-1262	633	-226	-191	217	494	-2209	1	711	-1992
100	0	-335	-235	0	-1970	0	-419	-353	-771	0	-3448	1	-771	-4219

Fatigue Load Combination

Position	Fatigue Truck Moments (IM*1.15) M+	M-	Unfactored & Distributed Fatigue Moments D.F.	M+	M-	Govern. Factored & Distributed Fatigue Moments L.F.	M+	M-
0	0	0		0	0		0	0
10	557	-71	0.709	395	-50	0.75	296	-38
20	921	-141	0.709	653	-100	0.75	490	-75
30	1148	-212	0.709	814	-150	0.75	610	-113
40	1215	-283	0.709	861	-201	0.75	646	-150
50	1173	-353	0.709	832	-250	0.75	624	-188
60	1080	-424	0.709	766	-301	0.75	574	-225
70	849	-495	0.709	602	-351	0.75	451	-263
80	505	-565	0.709	358	-401	0.75	269	-300
90	197	-636	0.709	140	-451	0.75	105	-338
100	0	-707	0.709	0	-501	0.75	0	-376

Shear Calculations

IM*(Vehicle Shears) + Lane Load

Position	Design Truck V+	Design Truck V-	Design Tandem V+	Design Tandem V-	Govern. Shears V+	Govern. Shears V-	D.F.	Unfactored & Distributed Shears V+	Unfactored & Distributed Shears V-
0	114	-13	92	-10	114	-13	0.849	97	-11
10	96	-13	78	-11	96	-13	0.849	82	-11
20	79	-19	65	-20	79	-20	0.849	67	-17
30	64	-32	52	-30	64	-32	0.849	54	-27
40	49	-47	41	-41	49	-47	0.849	42	-40
50	36	-61	31	-51	36	-61	0.849	31	-52
60	25	-76	22	-62	25	-76	0.849	21	-65
70	15	-90	15	-73	15	-90	0.849	13	-76
80	8	-105	8	-84	8	-105	0.849	7	-89
90	3	-118	3	-95	3	-118	0.849	3	-100
100	0	-131	0	-105	0	-131	0.849	0	-111

Total Factored Shears for Strength 1 Load Combination

Position	DC_1	DC_2	DW	Distributed. LL + IM V+	Distributed. LL + IM V-	1.25 DC_1	1.25 DC_2	1.5 DW	Factored DL	1.75*(LL + IM) V+	1.75*(LL + IM) V-	γ	Factored & Distributed Strength Shears V+	Factored & Distributed Strength Shears V-
0	59	10	7	97	-11	74	13	11	97	169	-19	1	266	77
10	47	7	5	82	-11	59	9	8	75	143	-19	1	218	56
20	35	5	3	67	-17	44	6	5	55	117	-30	1	172	25
30	24	2	1	54	-27	29	3	2	33	95	-48	1	128	-14
40	12	-0.7	-0.5	42	-40	15	-1	-1	13	73	-70	1	86	-57
50	0	-3	-2	31	-52	0	-4	-3	-7	53	-91	1	47	-97
60	-12	-6	-4	21	-65	-15	-8	-6	-28	37	-113	1	9	-141
70	-24	-9	-6	13	-76	-29	-11	-9	-50	22	-134	1	-27	-183
80	-35	-11	-8	7	-89	-44	-14	-12	-70	12	-156	1	-58	-226
90	-47	-14	-10	3	-100	-59	-18	-15	-91	4	-175	1	-87	-267
100	-59	-17	-12	0	-111	-74	-21	-18	-113	0	-195	1	-113	-307

A.3 105' SPAN (MILITARY ROAD GEOMETRY)

Design Assumptions

- span length = 105'
- W40 x 277 I-section girders
- number of girders = 4
- girder spacing = 8' 4"
- composite concrete slab
- slab depth = 7.5"

Calculation of Dead Loads

DC_1 Non-composite dead loads

    <u>Deck:</u>

    Interior girder, $(8"/12)*(8.333')*(0.15\,^k/_{ft}^3) = 0.833$ k/ft

    Exterior girder, $(8"/12)*(7.870')*(0.15\,^k/_{ft}^3) = 0.787$ k/ft

Total DC_1

	Interior Girder	Exterior Girder
Deck	0.833	0.787
Steel	0.300	0.300
Form-work	<u>0.083</u>	<u>0.079</u>
Total DC_1	**1.216** k/ft	**1.166** k/ft

DC_2 Long Term Composite Dead Load

    Assume the weight per unit length of the barrier is 536 lb/ft, and all girders carry the load equally.

        $DC_2 = (0.536 * 2) / 4 = $ **0.268** k/ft

DW Future Wearing Surface Load

    Assume equal distribution among all girders.

        $DW = (0.025 * 30) / 4 = $ **0.188** k/ft

Design Factors

$$\text{Ductility } \eta_D \quad 1.0$$
$$\text{Redundancy } \eta_R \quad 1.0$$
$$\text{Operational Importance } \eta_I \quad 1.0$$

$$\eta = \eta_D * \eta_R * \eta_I = \mathbf{1.0}$$

Bridge is subjected to HL93 loading, the distribution factors and shear / moment envelopes are generated using QconBridge®. The shear / moment envelopes are shown on the following pages, with the distribution factors and section properties preceding.

Note: The exterior girder controls the design for flexural design and the interior controls the design for shear, as is shown in the moment and shear envelopes.

<u>Effective Flange Width</u>

Interior Girder:

$$\tfrac{1}{4} * (\text{span} * 12^{in}/_{ft}) = \tfrac{1}{4} * (105' * 12^{in}/_{ft}) = 315"$$

$$12.0 * (t_s) + (b_f/_2) = 12.0 * (7.5) + (^{15.75}/_2) = \mathbf{98"} \qquad \text{(controls)}$$

$$\text{Spacing} \qquad = 100"$$

Exterior Girder:

$$\tfrac{1}{8} * (\text{span} * 12^{in}/_{ft}) = \tfrac{1}{8} * (105' * 12^{in}/_{ft}) = 158"$$

$$6.0 * (t_s) + (b_f/_2) = 6.0 * (7.5) + (^{15.75}/_2) = 53"$$

$$\text{Overhang} \qquad = \mathbf{44"} \qquad \text{(controls)}$$

$$b_{eff} = \tfrac{1}{2} * \text{controlling interior} + \text{controlling exterior}$$

$$= \tfrac{1}{2} * 98 + 44 = \mathbf{93"} \qquad \text{(governing } b_{eff})$$

Positive Flexure

Determining neutral axis (N.A.)

$$P_t = 50 * 15.75 * 1.575 = 1247 \text{ kips}$$

$$P_c = 50 * 15.75 * 1.575 = 1247 \text{ kips}$$

$$P_w = 50 * 36.54 * 0.83 = 1516 \text{ kips}$$

$$P_s = 0.85 * 4 * 93 * 7.5 = 2497 \text{ kips}$$

Case 1

$$P_t + P_w \geq P_c + P_s$$

2763 $\ngeq$ 3744 kips   N.G.

Case 2

$$P_t + P_w + P_c \geq P_s$$

4010 ≥ 2497 kips   O.K.

$$y_{bar} = \frac{t_c}{2}\left[\frac{P_w + P_t - P_s}{P_c} + 1\right]$$

$$y_{bar} = 0.956"$$

Measured from the top of the top flange.

Plastic Moment Capacity

$$M_p = \frac{P_c}{2t_c}\left[y^2_{bar} + \left(t_c - y_{bar}\right)^2\right] + \left[P_s d_s + P_w d_w + P_t d_t\right]$$

$$M_p = 7351 \text{ k*ft}$$

Strength Limit State

	Strength I	Strength IV
M_{DC1} = 1543	1929	2315
M_{DC2} = 207	259	311
M_{DW} = 190	285	285
M_{LL+IM} = 2070	<u>3623</u>	<u>N. A.</u>
	6095 k*ft (governs)	2910 k*ft

Ductility Requirement

$$\frac{D_p}{D'} \leq 5$$

$$D' = \beta\left(\frac{d + t_s + t_h}{7.5}\right)$$

D' = 0.7 * (39.69 + 7.5) / 7.5 = 4.404

D_p = 7.5 + 0.956 = 8.456"

D_p / D' = 1.92 < 5

Section Proportional Limits

$$0.1 \leq \frac{I_{YC}}{I_Y} \leq 0.9$$

$$I_{YC} = \frac{1}{12}(1.575)*(15.75)^3 = 512.8 \text{ in}^4$$

$$I_Y = 512.8 + 512.8 + 1.7 = 1027 \text{ in}^4$$

$$I_{YC} / I_Y = 0.5 \qquad\qquad \text{O.K.}$$

Web Slenderness

$$\frac{2D_{cp}}{t_w} \leq 3.76\sqrt{\frac{E}{F_{yc}}}$$

$D_{cp} = 0$ (Plastic N.A. is in slab)

Compression Flange Slenderness

$$\frac{b_f}{2t_f} \leq 0.382\sqrt{\frac{E}{F_{yc}}}$$

$$\frac{15.75}{2*1.575} = 5.0 \leq 9.2 = \sqrt{\frac{29000}{50}}$$

Compression Flange Bracing

O.K.   (braced continuously at strength limit state)

Positive Flexure Resistance

$$M_n = \frac{5M_p - 0.85M_y}{4} + \frac{0.85M_y - M_p}{4}\left(\frac{D_p}{D'}\right)$$

$$M_n = \frac{2(7351) - 0.85(5877)}{4} + \frac{0.85(5877) - 7351}{4}(1.92)$$

1.3 * M_y = 7640 k*ft

M_n = 6809 k*ft

6809 k*ft $\geq$ **6028** k*ft   O.K.

Negative Flexure

Determining neutral axis (N.A.)

P_t =   50 * 15.75 * 1.575   =   1247 kips

P_c =   50 * 15.75 * 1.575   =   1247 kips

P_w =   50 * 36.54 * 0.83   =   1516 kips

P_{rb} =   60 * 3.5 =   210 kips

P_{rt} =   60 * 4   =   240 kips

Case 1

$P_c + P_w \geq P_t + P_{rb} + P_{rt}$

2763 $\geq$ 1697 kips   O.K.

$$y_{bar} = \frac{D}{2} * \left[\frac{P_c - P_t - P_{rt} - P_{rb}}{P_w} + 1 \right]$$

$$y_{bar} = 12.85"$$

Measured from the bottom of the top flange.

Plastic Moment Capacity

$$M_p = \frac{P_w}{2D} \left[y^2_{bar} + \left(D - y_{bar} \right)^2 \right] + \left[P_{rt} d_{rt} + P_{rb} d_{rb} + P_t d_t + P_c d_c \right]$$

$$M_p = 5949 \text{ k*ft}$$

Strength Limit State

	Strength I	Strength IV
$M_{DC1} = 0$	0	0
$M_{DC2} = 369$	461	554
$M_{DW} = 339$	509	509
$M_{LL+IM} = 2106$	<u>3686</u>	<u>N. A.</u>
	4656 k*ft (governs)	1063 k*ft

Section Proportional Limits

$$0.1 \le \frac{I_{YC}}{I_Y} \le 0.9$$

$$I_{YC} = \frac{1}{12} * (1.575)*(15.75)^3 = 512.8 \text{ in}^4$$

$$I_Y = 512.8 + 512.8 + 1.7 = 1028 \text{ in}^4$$

$$I_{YC} / I_Y = 0.5 \qquad\qquad \text{O.K.}$$

Web Slenderness

$$\frac{2D_{cp}}{t_w} \leq 3.76\sqrt{\frac{E}{F_{yc}}}$$

$$\frac{2*23.7}{0.83} = 57.1 \leq 90.55 = 3.76\sqrt{\frac{29000}{50}}$$

Ratio = 0.63

Compression Flange Slenderness

$$\frac{b_f}{2t_f} \leq 0.382\sqrt{\frac{E}{F_{yc}}}$$

$$\frac{15.75}{2*1.575} = 5.0 \leq 9.2 = \sqrt{\frac{29000}{50}}$$

Ratio = 0.54

Compression Flange Bracing

Assume adequate bracing

Negative Flexure Resistance

$$M_r = 5949 \text{ k*ft}$$

5949 k*ft $\geq$ **4656** k*ft $\qquad\qquad$ <u>O.K.</u>

Permanent Deflection

$$f_{all} = 47.5 \text{ ksi}$$

Positive	Tension	Compression
M_{DC1}	$^{1543(12)}/_{1083.1} = 17.09$	$^{1543(12)}/_{1083.1} = 17.09$
M_{DC2}	$^{207(12)}/_{1288.7} = 1.93$	$^{207(12)}/_{2549.9} = 0.97$
M_{DW}	$^{190(12)}/_{1288.7} = 1.77$	$^{190(12)}/_{2549.9} = 0.89$
M_{LL+IM}	$^{2070(12)1.3}/_{1410.6} = \underline{22.89}$	$^{2070(12)1.3}/_{6315.3} = \underline{5.11}$
	43.68 ksi	24.06 ksi O.K.

Negative	Tension	Compression
M_{DC1}	$^{0(12)}/_{1083.1} = 0$	$^{0(12)}/_{1083.1} = 0$
M_{DC2}	$^{369(12)}/_{1156.8} = 3.13$	$^{369(12)}/_{1416} = 3.83$
M_{DW}	$^{339(12)}/_{1156.8} = 2.87$	$^{339(12)}/_{1416} = 3.52$
M_{LL+IM}	$^{2106(12)1.3}/_{1156.8} = \underline{23.19}$	$^{2106(12)1.3}/_{1416} = \underline{28.4}$
	29.19 ksi	35.75 ksi O.K.

Live Load Deflection

$$\Delta_{all} = {^L}/_{800} = 1.575"$$

$$\Delta_{anl} = 1.556" \qquad\qquad\qquad \underline{O.K.}$$

Shear Resistance

Positive

V_{DC1} = 62 kips   * 1.25 =   78 kips

V_{DC2} = 11 kips   * 1.25 =   14 kips

V_{DW} = 10 kips   * 1.50 =   15 kips

V_{LL+IM} = 99 kips   * 1.75 =   173 kips

At Strength Limit State V_u =   **280** kips

Shear Resistance V_n of Unstiffened Web

V_n = 0.58 * 36.54 * 0.83 * 50

    = 955 kips

V_r = 1.0 * 955 = 955 kips

955 > 280 kips   OK

Negative

V_{DC1} = 62 kips   * 1.25 =   78 kips

V_{DC2} = 18 kips   * 1.25 =   23 kips

V_{DW} = 16 kips   * 1.50 =   24 kips

V_{LL+IM} = 113 kips   * 1.75 =   198 kips

At Strength Limit State V_u =   **323** kips

Shear Resistance V_n of Unstiffened Web

V_n = 0.58 * 36.54 * 0.83 * 50

    = 955 kips

V_r = 1.0 * 955 = 955 kips

955 > 323 kips   O.K.

Strength 1 Moments

Position	DC₁	DC₂	DW	LL + IM M+	LL + IM M-	1.25 DC₁	1.25 DC₂	1.5 DW	Factored DL	1.75(LL+IM) M+	1.75(LL+IM) M-	Factored & Distributed Strength 1 v	M+	M-
0	0	0	0	0	0	0	0	0	0	0	0	1	0	0
10.5	559	96	88	898	-117	698	120	132	950	1571	-204	1	2521	746
21	993	163	149	1528	-234	1241	204	224	1669	2673	-410	1	4342	1259
31.5	1303	199	183	1904	-351	1629	249	275	2153	3331	-615	1	5484	1538
42	1490	207	190	2070	-469	1862	259	285	2406	3622	-821	1	6028	1585
52.5	1552	185	170	2032	-585	1940	231	255	2426	3556	-1025	1	5982	1401
63	1490	133	122	1814	-703	1862	166	183	2211	3175	-1230	1	5386	981
73.5	1303	52	47	1407	-820	1629	65	71	1765	2462	-1436	1	4227	329
84	993	-59	-54	839	-1113	1241	-74	-81	1087	1468	-1948	1	2555	-861
94.5	559	-199	-183	300	-1354	698	-249	-275	175	526	-2369	1	701	-2194
105	0	-369	-339	0	-2106	0	-461	-509	-970	0	-3686	1	-970	-4656

Fatigue Load Combination

Position	Fatigue Truck Moments (IM+1.15) M+	M-	Unfactored & Distributed Fatigue Moments D.F.	M+	M-	Govern. Factored & Distributed Fatigue Moments L.F.	M+	M-
0	0	0	0.709	0	0	0.75	0	0
10.5	629	-79	0.709	446	-56	0.75	334	-42
21	1044	-158	0.709	740	-112	0.75	555	-84
31.5	1303	-237	0.709	924	-168	0.75	693	-126
42	1383	-317	0.709	981	-225	0.75	735	-169
52.5	1339	-396	0.709	949	-281	0.75	712	-211
63	1227	-475	0.709	870	-337	0.75	652	-253
73.5	964	-555	0.709	683	-393	0.75	513	-295
84	579	-634	0.709	411	-450	0.75	308	-337
94.5	219	-713	0.709	155	-506	0.75	116	-379
105	0	-799	0.709	0	-566	0.75	0	-425

Shear Calculations

IM*(Vehicle Shears) + Lane Load

Position	Design Truck V+	Design Truck V-	Design Tandem V+	Design Tandem V-	Govern. Shears V+	Govern. Shears V-	Unfactored & Distributed Shears D.F.	V+	V-
0	116	-13	94	-10	116	-13	0.849	98	-11
10.5	98	-14	79	-11	98	-14	0.849	83	-12
21	80	-20	66	-21	80	-21	0.849	68	-18
31.5	65	-33	53	-31	65	-33	0.849	55	-28
42	50	-48	42	-41	50	-48	0.849	42	-41
52.5	37	-62	32	-52	37	-62	0.849	31	-53
63	26	-77	23	-63	26	-77	0.849	22	-65
73.5	16	-92	15	-74	16	-92	0.849	14	-78
84	8	-106	8	-86	8	-106	0.849	7	-90
94.5	3	-109	3	-88	3	-109	0.849	3	-93
105	0	-133	0	-107	0	-133	0.849	0	-113

Total Factored Shears for Strength 1 Load Combination

Position	DC₁	DC₂	DW	Distributed. LL + IM V+	Distributed. LL + IM V-	1.25 DC₁	1.25 DC₂	1.5 DW	Factored DL	Factored V+	1.75*(LL + IM) V-	v	Factored & Distributed Strength Shears V+	V-
0	62	11	10	98	-11	77	14	15	106	172	-19	1	278	87
10.5	49	8	7	83	-12	62	10	11	82	146	-21	1	228	61
21	37	5	5	68	-18	46	6	8	60	119	-31	1	179	29
31.5	25	2	2	55	-28	31	3	3	36	97	-49	1	133	-13
42	12	-0.7	-0.6	42	-41	15	-1	-1	14	74	-71	1	88	-58
52.5	0	-4	-3	31	-53	0	-5	-5	-10	55	-92	1	45	-102
63	-12	-6	-6	22	-65	-15	-8	-9	-32	39	-114	1	7	-146
73.5	-25	-9	-8	14	-78	-31	-11	-12	-54	24	-137	1	-30	-191
84	-37	-12	-11	7	-90	-46	-15	-17	-78	12	-157	1	-66	-235
94.5	-49	-15	-14	3	-93	-62	-19	-21	-101	4	-162	1	-97	-263
105	-62	-18	-16	0	-113	-77	-23	-24	-124	0	-198	1	-124	-321

A.4 90' SPAN (INITIAL DESIGN GEOMETRY)

Design Assumptions

- span length = 90'

- I girders with appro. 36" web and F_y = 50 ksi

- number of girders = 4

- girder spacing = 10'

- composite concrete slab with f'$_c$ = 4 ksi

- slab thickness = 8"

Designs for this geometry were completed for continuous dead and live, and simply

supported for dead loads, as welded plate girders and using a rolled shape as simply

supported.

Note: Optimization of the design is in terms of total steel area of the cross section, and

only the strength limit state is considered in the design.

Calculation of Dead Loads

DC_1 Non-composite dead loads

Deck:
Interior girder, $(8.5"/12)*(10')*(0.15\,^k/_{ft}{}^3) = 1.063$ k/ft
Exterior girder, $(8.5"/12)*(8.5')*(0.15\,^k/_{ft}{}^3) = 0.903$ k/ft

Total DC_1

	Interior Girder	Exterior Girder
Deck	1.063	0.903
Concrete Haunch	0.033	0.033
Steel	0.170	0.170
Form-work	0.135	0.079
Total DC_1	**1.401** k/ft	**1.185** k/ft

DC_2 Long Term Composite Dead Load

> Assume the weight per unit length of the barrier is 536 lb/ft, and all girders carry the load equally.
>
> $$DC_2 = (0.536 * 2) / 4 = \mathbf{0.268} \text{ k/ft}$$

DW Future Wearing Surface Load

> Assume equal distribution among all girders.
>
> $$DW = (0.025 * 34) / 4 = \mathbf{0.213} \text{ k/ft}$$

Design Factors

$$
\begin{array}{rl}
\text{Ductility } \eta_D & 1.0 \\
\text{Redundancy } \eta_R & 1.0 \\
\text{Operational Importance } \eta_I & 1.0 \\
\end{array}
$$

$$\eta = \eta_D * \eta_R * \eta_I = \mathbf{1.0}$$

Bridge is subjected to HL93 loading, the distribution factors and shear / moment envelopes are generated using QconBridge®. The shear / moment envelopes are shown on the following pages, with the distribution factors and section properties preceding.

Note: The exterior girder controls the design for flexural design and the interior controls the design for shear, as is shown in the moment and shear envelopes.

Effective Flange Width

> Interior Girder:
>
> $$\tfrac{1}{4} * (\text{span} * 12^{in}/_{ft}) = \tfrac{1}{4} * (90' * 12^{in}/_{ft}) = 285"$$
>
> $$12.0 * (t_s) + (b_f/_2) = 12.0 * (8.0) + (^{12}/_2) = \mathbf{102"} \qquad \text{(controls)}$$
>
> $$\text{Spacing} = 120"$$

Exterior Girder:

$$\frac{1}{8} * (\text{span} * 12^{in}/_{ft}) = \frac{1}{8} * (90' * 12^{in}/_{ft}) = 135"$$

$$6.0 * (t_s) + (b_f/_2) \quad = \; 6.0 * (8.0) + (^{12}/_2) = 54"$$

$$\text{Overhang} \qquad = \textbf{42"} \qquad\qquad\qquad\qquad \text{(controls)}$$

$b_{eff} = \frac{1}{2} *$ controlling interior + controlling exterior

$$= \frac{1}{2} * 102 + 42 = \textbf{93"} \qquad\qquad\qquad \text{(governing} \;\; b_{eff})$$

Positive Flexure

Determining neutral axis (N.A.)

$$P_t \; = \; 50 * 15 * 1.25 \; = \; 843.8 \text{ kips}$$

$$P_c \; = \; 50 * 13.5 * 0.875 \; = \; 525 \text{ kips}$$

$$P_w \; = \; 50 * 36 * 0.50 \; = \; 900 \text{ kips}$$

$$P_s \; = \; 0.85 * 4 * 93 * 8 \; = \; 2543 \text{ kips}$$

Case 1

$$P_t + P_w \; \geq \; P_c + P_s$$

$$1743.8 \ngeq 3068 \text{ kips} \qquad\qquad\qquad\qquad \text{N.G.}$$

Case 2

$$P_t + P_w + \; P_c \geq P_s$$

$$2268.8 \ngeq 2556.8 \text{ kips} \qquad\qquad\qquad\qquad \text{N.G.}$$

Neutral axis lies within the slab.

$$y_{bar} \; = \; t_s \left[\frac{P_w + P_t + P_c}{P_s} \right]$$

$$y_{bar} = 7.14"$$

Measured from the top of the slab.

Plastic Moment Capacity

$$M_p = \frac{y^2{}_{bar} P_s}{2t_s} + \left[P_c d_c + P_w d_w + P_t d_t \right]$$

$$M_p = 7092 \text{ k*ft}$$

Strength Limit State

	Strength I	Strength IV
M_{DC1} = 878	1097	1317
M_{DC2} = 152	190	228
M_{DW} = 121	182	182
M_{LL+IM} = 1692	<u>2961</u>	<u>N. A.</u>
	4430 k*ft (governs)	1727 k*ft

Ductility Requirement

$$\frac{D_p}{D'} \leq 5$$

$$D' = \beta \left(\frac{d + t_s + t_h}{7.5} \right)$$

D' = 0.7 * (38 + 8.0) / 7.5 = 4.29

D_p = 7.14

D_p / D' = 1.66 < 5   O.K.

Section Proportional Limits

$$0.1 \leq \frac{I_{YC}}{I_Y} \leq 0.9$$

$I_{YC} = {}^1/_{12}(.875)*(12)^2 = 126 \text{ in}^4$

$I_Y = 126 + 316.4 + 0.375 = 442.8 \text{ in}^4$

I_{YC} / I_Y = 0.28   O.K.

Web Slenderness

$$\frac{2D_{cp}}{t_w} \leq 3.76\sqrt{\frac{E}{F_{yc}}}$$

Plastic neutral axis is in slab, web slenderness is satisfied.

Nominal Flexure Resistance

For D' < D_p <5D'

$$M_n = \frac{5M_p - 0.85M_y}{4} + \frac{0.85M_y - M_p}{4}\left(\frac{D_p}{D'}\right)$$

M_y = 3886 k*ft

M_n = 4700 k*ft

4430 < 4700 k*ft   O.K.

Shear Resistance

Each section requires stiffeners to meet the shear requirements.

Constructibility

Web Slenderness

$$\frac{2D_c}{t_w} \leq 6.77\sqrt{E/f_c}$$

82.55 < 178.81   O.K.

Compression Flange Slenderness

$$\frac{b_f}{2t_f} \leq 1.38\sqrt{\frac{E}{f_c\sqrt{\frac{2D_c}{t_w}}}}$$

6.86 < 12.09   O.K.

Compression Flange Bracing

Bracing requirements were assumed to be satisfied.

Negative Flexure Region

Plastic Moment Capacity

$$D_{cp} = \frac{D}{2A_wF_{yw}}\left(F_{yt}A_t + F_{yw}A_w + F_{yr}A_r - F_{yc}A_c\right)$$

D_{cp} = 20.63 in

$P_c = F_{yc}b_ct_c = 50 * 1.125 * 15 = 843.75$ kips

$P_w = F_{yw}Dt_w = 50 * 0.5 * 36 = 900$ kips

$P_t = F_{yt}b_tt_t = 50 * 0.875 * 12 = 525$ kips

$P_{rb} = F_{yrb}A_{rb} = 60 * 4 = 240$ kips

$P_{rt} = F_{yrt}A_{rt} = 60 * 6 = 360$ kips

$$P_c + P_w \geq P_t + P_{rb} + P_{rt}$$

1743.8 > 1125 kips

$$y_{bar} = \left(\frac{D}{2}\right)\left[\frac{P_c - P_t - P_{rt} - P_{rb}}{P_w} + 1\right]$$

y_{bar} = 15.38 in

Y_{bar} is measured from bottom of top flange.

$$M_p = \frac{P_w}{2D}\left[y^2{}_{bar} + \left(D - y_{bar}\right)^2\right] + \left[P_{rt}d_{rt} + P_{rb}d_{rb} + P_t d_t + P_c d_c\right]$$

$$M_p = 3940 \text{ k*ft}$$

Strength Limit State

Unfactored Moments	Strength I
$M_{DC1} = 0$ k*ft	0
$M_{DC2} = 271$ k*ft	339
$M_{DW} = 216$ k*ft	324
$M_{LL+IM} = 1735$ k*ft	3036
	3699 k*ft

Web Slenderness

$$\frac{2D_c}{t_w} \le 3.76\sqrt{\frac{E}{F_{yc}}}$$

82.5 < 90.55   O.K.

Compression-Flange Slenderness

$$\frac{b_f}{2t_f} \le 0.382\sqrt{\frac{E}{F_{yc}}}$$

6.67 < 9.2   O.K.

Compression Flange Bracing

Is assumed to be adequate for these designs.

Sectional Properties

$$0.1 \leq \frac{I_{YC}}{I_Y} \leq 0.9$$

$I_{yc}/I_y = 0.71$ O.K.

Nominal Flexure Resistance

$$M_n = 3940 \text{ k*ft}$$

3699 < 3940 k*ft   O.K.

Permanent Deflection

$f_{all} = 47.5$ ksi

Positive	Tension	Compression
M_{DC1}	$^{878(12)}/_{668} = 15.77$	$^{878(12)}/_{512} = 20.58$
M_{DC2}	$^{152(12)}/_{864} = 2.11$	$^{152(12)}/_{2086} = 0.87$
M_{DW}	$^{121(12)}/_{864} = 1.68$	$^{121(12)}/_{2086} = 0.70$
M_{LL+IM}	$^{1692(12)1.3}/_{933} = \underline{28.3}$	$^{1692(12)1.3}/_{7241} = \underline{3.64}$
	47.87ksi	25.79 ksi <u>O.K.</u>

Negative	Tension	Compression
M_{DC1}	$^{0(12)}/_{668} = 0$	$^{0(12)}/_{512} = 0$
M_{DC2}	$^{271(12)}/_{752} = 4.32$	$^{271(12)}/_{840} = 3.87$
M_{DW}	$^{216(12)}/_{752} = 3.44$	$^{216(12)}/_{840} = 3.09$
M_{LL+IM}	$^{1735(12)1.3}/_{752} = \underline{35.97}$	$^{1735(12)1.3}/_{840} = \underline{32.22}$
	43.74 ksi	39.17 ksi $\quad$ <u>O.K.</u>

Intermediate stiffeners are necessary with this section to meet the shear requirements.

These designs were completed for comparison purposes only, therefore the fatigue limit

state was not investigated.

The shear / moment envelopes for the controlling girder are shown on the following

pages.

Strength 1 Moments

Position	DC_1	DC_2	DW	LL + IM M+	LL + IM M-	1.25 DC_1	1.25 DC_2	1.5 DW	Factored 1.75(LL+IM) DL	M+	M-	Factored & Distributed Strength 1 v	M+	M-
0	0	0	0	0	0	0	0	0	0	0	0	1	0	0
9	329	71	56	740	-97	411	89	84	584	1296	-170	1	1880	415
18	585	119	95	1255	-193	731	149	143	1023	2196	-338	1	3219	685
27	768	147	116	1558	-290	960	184	174	1318	2726	-507	1	4044	811
36	878	152	121	1692	-386	1097	190	182	1469	2961	-675	1	4430	794
45	914	136	108	1660	-483	1143	170	162	1475	2905	-845	1	4380	630
54	878	98	78	1484	-580	1097	123	117	1337	2598	-1014	1	3934	322
63	768	38	30	1149	-676	960	48	45	1053	2010	-1182	1	3063	-130
72	585	-43	-35	683	-908	731	-54	-53	625	1196	-1589	1	1821	-964
81	329	-147	-116	252	-1098	411	-184	-174	54	441	-1921	1	494	-1867
90	0	-271	-216	0	-1735	0	-339	-324	-663	0	-3037	1	-663	-3699

Fatigue Load Combination

Position	Fatigue Truck Moments (IM+1.15) M+	M-	Unfactored & Distributed Fatigue Moments D.F.	M+	M-	Govern. Factored & Distributed Fatigue Moments L.F.	M+	M-
0	0	0	0.708	0	0	0.75	0	0
9	485	-62	0.708	343	-44	0.75	258	-33
18	799	-123	0.708	566	-87	0.75	424	-65
27	994	-185	0.708	704	-131	0.75	528	-98
36	1048	-247	0.708	742	-175	0.75	556	-131
45	1007	-309	0.708	713	-219	0.75	535	-164
54	935	-370	0.708	662	-262	0.75	496	-196
63	736	-432	0.708	521	-306	0.75	391	-229
72	434	-494	0.708	307	-350	0.75	230	-262
81	174	-556	0.708	123	-394	0.75	92	-295
90	0	-617	0.708	0	-437	0.75	0	-328

A.5 90' SPAN (ROLLED SECTION DESIGN)

Calculation of Dead Loads

DC_1 Non-composite dead loads

Deck:

Interior girder, $(8.5"/12)*(10')*(0.15\,^k/_{ft}{}^3) = 1.063$ k/ft

Exterior girder, $(8.5"/12)*(8.5')*(0.15\,^k/_{ft}{}^3) = 0.903$ k/ft

Total DC_1

	Interior Girder	Exterior Girder
Deck	1.063	0.903
Concrete Haunch	0.033	0.033
Steel	0.170	0.170
Form-work	0.135	0.079
Total DC_1	**1.401** k/ft	**1.185** k/ft

DC_2 Long Term Composite Dead Load

Assume the weight per unit length of the barrier is 536 lb/ft, and all girders carry the load equally.

$$DC_2 = (0.536 * 2) / 4 = \textbf{0.268} \text{ k/ft}$$

DW Future Wearing Surface Load

Assume equal distribution among all girders.

$$DW = (0.025 * 34) / 4 = \textbf{0.213} \text{ k/ft}$$

Design Factors

Ductility η_D	1.0
Redundancy η_R	1.0
Operational Importance η_I	1.0

$$\eta = \eta_D * \eta_R * \eta_I = \textbf{1.0}$$

Bridge is subjected to HL93 loading, the distribution factors and shear / moment

envelopes are generated using QconBridge®. The shear / moment envelopes are shown

on the following pages, with the distribution factors and section properties preceding.

Note: The exterior girder controls the design for flexural design and the interior controls the design for shear, as is shown in the moment and shear envelopes.

Effective Flange Width

Interior Girder:

$$\tfrac{1}{4} * (\text{span} * 12^{in}/_{ft}) = \tfrac{1}{4} * (90' * 12^{in}/_{ft}) = 285"$$

$$12.0 * (t_s) + (b_f/_2) = 12.0 * (8.0) + (^{15.75}/_2) = \mathbf{104"} \qquad \text{(controls)}$$

$$\text{Spacing} = 120"$$

Exterior Girder:

$$\tfrac{1}{8} * (\text{span} * 12^{in}/_{ft}) = \tfrac{1}{8} * (90' * 12^{in}/_{ft}) = 135"$$

$$6.0 * (t_s) + (b_f/_2) = 6.0 * (8.0) + (^{15.75}/_2) = 56"$$

$$\text{Overhang} = \mathbf{42"} \qquad \text{(controls)}$$

$$b_{eff} = \tfrac{1}{2} * \text{controlling interior} + \text{controlling exterior}$$

$$= \tfrac{1}{2} * 104 + 42 = \mathbf{94"} \qquad \text{(governing } b_{eff})$$

Positive Flexure

Determining neutral axis (N.A.)

$$P_t = 50 * 15.75 * 1.065 = 838.7 \text{ kips}$$
$$P_c = 50 * 15.75 * 1.065 = 838.7 \text{ kips}$$
$$P_w = 50 * 36.54 * 0.65 = 1187.6 \text{ kips}$$
$$P_s = 0.85 * 4 * 94 * 8 = 2556.8 \text{ kips}$$

Case 1

$$P_t + P_w \geq P_c + P_s$$
$$2026.3 \ngeq 3395.5 \text{ kips} \qquad \text{N.G.}$$

Case 2

$$P_t + P_w + P_c \geq P_s$$

$2865 \geq 2556.8$ kips   O.K.

Neutral axis lies within the top flange.

$$y_{bar} = \left(\frac{t_c}{2}\right)\left[\frac{P_w + P_t - P_s}{P_c} + 1\right]$$

$y_{bar} = 0.204"$

Measured down from the top of the top flange.

Plastic Moment Capacity

$$M_p = \left(\frac{P_c}{2t_c}\right) * \left[y^2_{bar} + \left(t_c - y_{bar}\right)^2 + \left(P_s d_s + P_w d_w + P d_t\right)\right]$$

$M_p = 5461$ k*ft

Strength Limit State

	Strength I	Strength IV
M_{DC1} = 878	1097	1317
M_{DC2} = 152	190	228
M_{DW} = 121	182	182
M_{LL+IM} = 1692	<u>2961</u>	<u>N. A.</u>
	4430 k*ft (governs)	1727 k*ft

Ductility Requirement

$$\frac{D_p}{D'} \leq 5$$

$$D' = \beta\left(\frac{d + t_s + t_h}{7.5}\right)$$

D' = 0.7 * (38.67 + 8.0) / 7.5 = 4.36

D_p = 8.19

D_p / D' = 1.88 < 5   O.K.

Section Proportional Limits

$$0.1 \leq \frac{I_{YC}}{I_Y} \leq 0.9$$

$$I_{YC} = \frac{1}{12}(1.065)*(15.75)^2 = 347 \text{ in}^4$$
$$I_Y = 126 + 316.4 + 0.836 = 694 \text{ in}^4$$
$$I_{YC} / I_Y = 0.50 \qquad \text{O.K.}$$

Web Slenderness

$$\left. 2D_{cp} \middle/ t_w \right. \leq 3.76\sqrt{\frac{E}{F_{yc}}}$$

Plastic neutral axis is in top flange, web slenderness is satisfied.

Nominal Flexure Resistance

For D' < D$_p$ <5D'

$$M_n = \frac{5M_p - 0.85M_y}{4} + \frac{0.85M_y - M_p}{4}\left(\frac{D_p}{D'}\right)$$

M$_y$ = 3886 k*ft

M$_n$ = 4700 k*ft

5042 < 4700 k*ft O.K.

Shear Resistance

Each section requires stiffeners to meet the shear requirements.

Constructibility

Web Slenderness

$$\frac{2D_c}{t_w} \leq 6.77\sqrt{\frac{E}{f_c}}$$

$$56.22 < 216.45 \qquad\qquad\qquad \text{O.K.}$$

Compression Flange Slenderness

$$\frac{b_f}{2t_f} \leq 1.38\sqrt{\frac{E}{f_c\sqrt{\frac{2D_c}{t_w}}}}$$

$$7.39 < 16.11 \qquad\qquad\qquad \text{O.K.}$$

Compression Flange Bracing

Bracing requirements were assumed to be satisfied.

Negative Flexure Region

Plastic Moment Capacity

$$D_{cp} = \frac{D}{2A_w F_{yw}}\left(F_{yt}A_t + F_{yw}A_w + F_{yr}A_r - F_{yc}A_c\right)$$

$$D_{cp} = 25.19 \text{ in}$$

$P_c = F_{yc}b_c t_c = 50*1.125*15 = 838.7$ kips

$P_w = F_{yw}Dt_w = 50*0.5*36 = 1188$ kips

$Pt = F_{yt}b_t t_t = 50*0.875*12 = 838.7$ kips

$P_{rb} = F_{yrb}A_{rb} = 60*4 = 240$ kips

$P_{rt} = F_{yrt}A_{rt} = 60*6 = 360$ kips

$$P_c + P_w \geq P_t + P_{rb} + P_{rt}$$

2026.7 > 1438.7 kips

$$y_{bar} = \left(\frac{D}{2}\right)\left[\frac{P_c - P_t - P_{rt} - P_{rb}}{P_w} + 1\right]$$

y_{bar} = 11.35 in

Y_{bar} is measured from bottom of top flange.

$$M_p = \frac{P_w}{2D}\left[y^2_{bar} + \left(D - y_{bar}\right)^2\right] + \left[P_{rt}d_{rt} + P_{rb}d_{rb} + P_td_t + P_cd_c\right]$$

M_p = 4320 k*ft

Strength Limit State

Unfactored Moments	Strength I
M_{DC1} = 0 k*ft	0
M_{DC2} = 271 k*ft	339
M_{DW} = 216 k*ft	324
$\underline{M_{LL+IM}}$= 1735 k*ft	3036
	3699 k*ft

Web Slenderness

$$\frac{2D_c}{t_w} \leq 3.76\sqrt{\frac{E}{F_{yc}}}$$

77.5 < 90.55   O.K.

Compression-Flange Slenderness

$$\frac{b_f}{2t_f} \leq 0.382\sqrt{\frac{E}{F_{yc}}}$$

$7.39 < 9.2$ O.K.

Compression Flange Bracing

Is assumed to be adequate for these designs.

Sectional Properties

$$0.1 \leq \frac{I_{YC}}{I_Y} \leq 0.9$$

$I_{yc}/I_y = 0.50$ O.K.

Nominal Flexure Resistance

$$M_n = 4320 \text{ k*ft}$$

$3699 < 4320$ k*ft   O.K.

This section satisfies the strength limit state for flexure.

These designs were completed for comparison purposes only, therefore the fatigue limit state was not investigated.

A.6 130' SPAN - 48" WEB (INITIAL DESIGN GEOMETRY)

Design Assumptions

- span length = 130'

- I girders with appro. 48" web and F_y = 50 ksi

- number of girders = 4

- girder spacing = 10'

- composite concrete slab with f'_c = 4 ksi

- slab thickness = 8"

This superstructure geometry was designed using the traditional continuous support and the proposed support condition.

Note: Optimization of the design is in terms of total steel area of the cross section, and only the strength limit state is considered in the design.

Continuous Dead and Live Loads

Calculation of Dead Loads

DC_1 Non-composite dead loads

Deck:
Interior girder, (8.5"/12)*(10')*(0.15 $^k/_{ft}{}^3$) = 1.063 k/ft
Exterior girder, (8.5"/12)*(8.5')*(0.15 $^k/_{ft}{}^3$) = 0.903 k/ft

Total DC$_1$

	Interior Girder	Exterior Girder
Deck	1.063	0.903
Concrete Haunch	0.033	0.033
Steel	0.300	0.300
Form-work	0.135	0.079
Total DC$_1$	**1.531** k/ft	**1.315** k/ft

DC$_2$ Long Term Composite Dead Load

Assume the weight per unit length of the barrier is 536 lb/ft, and all girders carry the load equally.

$$DC_2 = (0.536 * 2) / 4 = \textbf{0.268} \text{ k/ft}$$

DW Future Wearing Surface Load

Assume equal distribution among all girders.

$$DW = (0.025 * 34) / 4 = \textbf{0.213} \text{ k/ft}$$

Design Factors

Ductility η_D	1.0
Redundancy η_R	1.0
Operational Importance η_I	1.0

$$\eta = \eta_D * \eta_R * \eta_I = \textbf{1.0}$$

Bridge is subjected to HL93 loading, the distribution factors and shear / moment envelopes are generated using QconBridge®. The shear / moment envelopes are shown on the following pages, with the distribution factors and section properties preceding.

Note: The exterior girder controls the design for flexural design and the interior controls the design for shear, as is shown in the moment and shear envelopes.

Effective Flange Width

Interior Girder:

$\frac{1}{4}$ * (span * $12^{in}/_{ft}$) = $\frac{1}{4}$ * (130' * $12^{in}/_{ft}$) = 390"

12.0 * (t_s) + ($b_f/_2$) = 12.0 * (8.0) + ($^{14}/_2$) = **103"**   (controls)

Spacing   = 120"

Exterior Girder:

$\frac{1}{8}$ * (span * $12^{in}/_{ft}$) = $\frac{1}{8}$ * (130' * $12^{in}/_{ft}$) = 195"

6.0 * (t_s) + ($b_f/_2$)   = 6.0 * (8.0) + ($^{14}/_2$) = 55"

Overhang   = **42"**   (controls)

b_{eff} = $_{1/2}$ * controlling interior + controlling exterior

= $_{1/2}$ * 103 + 42 = **94"**   (governing b_{eff})

Positive Flexure

Determining neutral axis (N.A.)

P_t = 50 * 1.5 * 21 = 1575 kips

P_c = 50 * 1.375 * 14 = 962.5 kips

P_w = 50 * 48 * 0.375 = 900 kips

P_s = 0.85 * 4 * 94 * 8 = 2556.8 kips

Case 1

$P_t + P_w \geq P_c + P_s$

2475 $\ngeq$ 3519 kips   N.G.

Case 2

$P_t + P_w + P_c \geq P_s$

3437 $\geq$ 2556.8 kips   O.K.

Neutral axis lies within the top flange.

$$y_{bar} = \left(\frac{t_c}{2}\right)\left[\frac{P_w + P_t - P_s}{P_c} + 1\right]$$

$$y_{bar} = 0.454"$$

Measured down from the top of the top flange.

Plastic Moment Capacity

$$M_p = \left(\frac{P_c}{2t_c}\right) * \left[y^2{}_{bar} + \left(t_c - y_{bar}\right)^2 + \left(P_s d_s + P_w d_w + P d_t\right)\right]$$

$$M_p = 9459 \ k*ft$$

Strength Limit State

	Strength I	Strength IV
M_{DC1} = 2780	3475	4170
M_{DC2} = 289	361	434
M_{DW} = 230	345	345
M_{LL+IM} = 2755	<u>4821</u>	<u>N. A.</u>
	9003 k*ft (governs)	4949 k*ft

Ductility Requirement

$$\frac{D_p}{D'} \le 5$$

$$D' = \beta\left(\frac{d + t_s + t_h}{7.5}\right)$$

D' = 0.7 * (50.875 + 8.0) / 7.5 = 5.5

D_p = 8.47

D_p / D' = 1.54 < 5   O.K.

Section Proportional Limits

$$0.1 \leq \frac{I_{YC}}{I_Y} \leq 0.9$$

$$I_{YC} = \frac{1}{12}(1.375)*(14)^2 = 314 \text{ in}^4$$
$$I_Y = 314 + 1157 + 0.211 = 1472 \text{ in}^4$$
$$I_{YC} / I_Y = 0.21 \qquad\qquad \text{O.K.}$$

Web Slenderness

$$\frac{2D_{cp}}{t_w} \leq 3.76 \sqrt{\frac{E}{F_{yc}}}$$

Plastic neutral axis is in top flange, web slenderness is satisfied.

Nominal Flexure Resistance

For D' < D$_p$ <5D'

$$M_n = \frac{5M_p - 0.85M_y}{4} + \frac{0.85M_y - M_p}{4}\left(\frac{D_p}{D'}\right)$$

M$_y$ = 8056 k*ft

M$_n$ = 9107 k*ft

9003 < 9107 k*ft O.K.

Shear Resistance

Each section requires stiffeners to meet the shear requirements.

Constructibility

Web Slenderness

$$\frac{2D_c}{t_w} \le 6.77\sqrt{\frac{E}{f_c}}$$

$$151.6 < 184.5 \qquad\qquad \text{O.K.}$$

Compression Flange Slenderness

$$\frac{b_f}{2t_f} \le 1.38\sqrt{\frac{E}{f_c\sqrt{\frac{2D_c}{t_w}}}}$$

$$5.09 < 10.72 \qquad\qquad \text{O.K.}$$

Compression Flange Bracing

Bracing requirements were assumed to be satisfied.

Negative Flexure Region

Plastic Moment Capacity

$$D_{cp} = \frac{D}{2A_wF_{yw}}\left(F_{yt}A_t + F_{yw}A_w + F_{yr}A_r - F_{yc}A_c\right)$$

$$D_{cp} = 33.6 \text{ in}$$

$P_c = F_{yc}b_ct_c = 50 * 2 * 22 = 2200 \text{ kips}$

$P_w = F_{yw}Dt_w = 50 * 0.4375 * 48 = 1200\text{kips}$

$P_t = F_{yt}b_tt_t = 50 * 2 * 22 = 2200 \text{ kips}$

$P_{rb} = F_{yrb}A_{rb} = 60 * 3 = 180 \text{ kips}$

$P_{rt} = F_{yrt}A_{rt} = 60 * 5 = 300 \text{ kips}$

$$P_c + P_w \geq P_t + P_{rb} + P_{rt}$$

$$3400 > 2680 \text{ kips} \qquad \text{O.K.}$$

$$y_{bar} = \left(\frac{D}{2}\right)\left[\frac{P_c - P_t - P_{rt} - P_{rb}}{P_w} + 1\right]$$

$$y_{bar} = 14.4 \text{ in}$$

Y_{bar} is measured from bottom of top flange.

$$M_p = \frac{P_w}{2D}\left[y^2_{bar} + \left(D - y_{bar}\right)^2\right] + \left[P_{rt}d_{rt} + P_{rb}d_{rb} + P_t d_t + P_c d_c\right]$$

$$M_p = 11376 \text{ k*ft}$$

Strength Limit State

Unfactored Moments	Strength I
M_{DC1} = 3257 k*ft	4071
M_{DC2} = 638 k*ft	798
M_{DW} = 506 k*ft	759
$\underline{M_{LL+IM}}$ = 3252 k*ft	5692
	11320 k*ft

Web Slenderness

$$\frac{2D_c}{t_w} \leq 3.76\sqrt{\frac{E}{F_{yc}}}$$

$$134.4 < 90.55 \qquad \text{N.G.}$$

$$\text{Ratio} = 1.5 > 0.75$$

Compression-Flange Slenderness

$$\frac{b_f}{2t_f} \le 0.382\sqrt{\frac{E}{F_{yc}}}$$

$$5.5 < 9.2 \qquad\qquad \text{O.K.}$$

$$\text{Ratio} = 0.60$$

Since web slenderness is not satisfied, the section is non compact.

Compression Flange Bracing

Is assumed to be adequate for these designs.

Sectional Properties

$$0.1 \le \frac{I_{YC}}{I_Y} \le 0.9$$

$$I_{yc}/I_y = 0.50 \qquad\qquad \text{O.K.}$$

Nominal Flexure Resistance

$$M_n = 11376 \text{ k*ft}$$

$$\mathbf{11319 < 11376} \text{ k*ft} \qquad\qquad \text{O.K.}$$

This section satisfies the strength limit state for flexure.

These designs were completed for comparison purposes only, therefore the fatigue limit state was not investigated.

Moment Summary

Position	DC₁	DC₂	DW	LL + IM M+	LL + IM M-	1.25 DC₁	1.25 DC₂	1.5 DW	Factored DL	1.75(LL+IM) M+	1.75(LL+IM) M-	Factored & Dist. Strength 1 γ	M+	M-
0	0	0	0	0	0	0	0	0	0	0	0	1	0	0
13	717	140	111	1207	-181	896	175	167	1238	2112	-316	1	3349	921
26	1202	235	187	2049	-362	1503	294	281	2077	3586	-634	1	5663	1442
39	1455	285	226	2550	-543	1819	356	339	2514	4463	-951	1	6977	1563
52	1477	289	230	2755	-725	1846	361	345	2553	4821	-1269	1	7374	1284
65	1267	248	197	2683	-906	1584	310	296	2189	4696	-1585	1	6885	604
78	826	161	128	2365	-1086	1033	201	192	1426	4139	-1901	1	5564	-476
91	153	30	24	1807	-1268	191	38	36	265	3162	-2219	1	3427	-1954
104	-752	-147	-117	1059	-1727	-940	-184	-176	-1299	1853	-3023	1	554	-4322
117	-1889	-369	-294	386	-2151	-2361	-461	-441	-3264	675	-3765	1	-2588	-7028
130	-3257	-638	-506	0	-3252	-4071	-798	-759	-5628	0	-5692	1	-5628	-11319

Fatigue Load Combination

Position	Fatigue Truck Moments (IM+1.15) M+	M-	Unfactored & Distributed Fatigue Moments D.F.	M+	M-	Govern. Factored & Distributed Fatigue Moments L.F.	M+	M-
0	0	0	0.708	0	0	0.75	0	0
13	766	-110	0.708	542	-78	0.75	407	-58
26	1269	-219	0.708	898	-155	0.75	674	-116
39	1578	-329	0.708	1117	-233	0.75	838	-175
52	1669	-438	0.708	1182	-310	0.75	886	-233
65	1608	-548	0.708	1138	-388	0.75	854	-291
78	1446	-658	0.708	1024	-466	0.75	768	-349
91	1120	-767	0.708	793	-543	0.75	595	-407
104	669	-877	0.708	474	-621	0.75	355	-466
117	257	-986	0.708	182	-698	0.75	136	-524
130	0	-1095	0.708	0	-775	0.75	0	-581

Shear Summary

IM*(Vehicle Shears) + Lane Load

Position	Design Truck V+	Design Truck V-	Design Tandem V+	Design Tandem V-	Govern. Shears V+	Govern. Shears V-	D.F.	Unfactored & Distributed Shears V+	V-
0	124	-16	100	-13	124	-16	0.865	107	-14
13	104	-17	84	-14	104	-17	0.865	90	-15
26	85	-24	69	-24	85	-24	0.865	74	-21
39	68	-39	55	-34	68	-39	0.865	59	-34
52	52	-54	43	-46	52	-54	0.865	45	-47
65	38	-70	32	-58	38	-70	0.865	33	-61
78	27	-86	23	-70	27	-86	0.865	23	-74
91	17	-101	15	-82	17	-101	0.865	15	-87
104	9	-117	8	-94	9	-117	0.865	8	-101
117	3	-132	3	-106	3	-132	0.865	3	-114
130	0	-146	0	-118	0	-146	0.865	0	-126

Total Factored Shears for Strength 1 Load Combination

Position	DC₁	DC₂	DW	Distributed. LL + IM V+	V-	1.25 DC₁	1.25 DC₂	1.5 DW	Factored DL	Factored V+	1.75*(LL + IM) V-	ν	Factored & Distributed Strength Shears V+	V-
0	64	13	10	107	-14	80	16	15	111	188	-24	1	284	83
13	46	9	7	90	-15	58	11	11	79	157	-26	1	225	51
26	28	6	4	74	-21	35	8	6	49	129	-36	1	168	12
39	11	2	2	59	-34	14	3	3	19	103	-59	1	116	-38
52	-7	-1	-1	45	-47	-9	-1	-2	-12	79	-82	1	64	-89
65	-25	-5	-4	33	-61	-31	-6	-6	-44	58	-106	1	13	-142
78	-43	-8	-7	23	-74	-54	-10	-11	-74	41	-130	1	-32	-194
91	-61	-12	-9	15	-87	-76	-15	-14	-105	26	-153	1	-75	-245
104	-79	-15	-12	8	-101	-99	-19	-18	-136	14	-177	1	-116	-297
117	-96	-19	-15	3	-114	-120	-24	-23	-166	5	-200	1	-154	-348
130	-114	-22	-18	0	-126	-143	-28	-27	-197	0	-221	1	-187	-397